1. Introduction

Acidic aerosols have drawn much attention of the investigators and technologists in the areas of atmospheric environment and public health. Previous studies have confirmed that the aerosols are the important influential factor, and have negative effect on human health. Human exposures to acidic aerosols in ambient air can cause inevitably respiratory irritants, pulmonary disease and asthma. Acidic aerosol comes mainly from the heterogeneous or homogeneous reactions of primary air pollutants such as SO_2 and NOx. The major emission sources of SO_2 are the combustion of coal and fuel of industrial plants. The major sources of NOx are fossil-fuel combustion for industrial process, power plant and automobile emissions. Many researches (McMurry , 2000; Asif *et al.*, 1999; Fang *et al.*, 1999; Wyers, 1997; Alfred, 1995) have investigated the composition and concentration of acidic aerosol, the sulfate, nitrate and ammonium were proved to be the major inorganic component of acidic aerosol. It is hard to expect the concentration of these second air pollutants because of their long range transport and their formation dependence on some unstable factor such as temperature and relative humidity. The constitution of aerosols is highly related to the types and numbers of emission sources in the monitoring area, and each area is a special case. Understanding of the acidic component distribution is helpful to take the correct treatment to acidic aerosols and the results of this study will be able to provide an air quality referential data to relative government.

In Taiwan, there are limited studies on the characteristics of acidic species in the ambient air. ADS and Universal sampler were used to measure the acidic

gas such as SO_2, HNO_3, HNO_2, HCl, and acidic compositions on particulates such as SO_4^{2-}, NO_3^-, NO_2^-, and Cl^-. The basic chemical species is an important media to neutralize the acidic chemical species in the ambient air. Therefore, the basic chemical species such as NH_3, NH_4^+, Na^+, K^+, Mg^{2+} and Ca^{2+} were also be measured in this study. The metal elements Na and Ca also provide an indication of the source of aerosols.

There were two sampling sites in this study. One site was set on an overbridge which come across the Chung-Chi Road (CCROB site), this site could be characterizes as a traffic site. Another site was set on the roof of a building of an eight floored building in the Hung-Kuang Institute of Technology (HKIT site), this site could be characterized as a non-traffic site. The data measured in these two characterized sampling sites could reveal the different chemical composition in the gaseous phase and particulate phase in traffic site and non-traffic site. The distance between two sites are about 900m, and the atmosphere samples were taken from June 1999 to January 2000. The main purpose of this study are as follows:

1. To measure the concentration of gaseous chemical species SO_2, HNO_3, HNO_2, HCl, NH_3 and particulate chemical species SO_4^{2-}, NO_3^-, NO_2^-, Cl^-, Na^+, K^+, Mg^{2+} and Ca^{2+} in traffic site and non-traffic site.
2. To compare the concentrations of the gaseous and particulate chemical species in summer and winter time, and the sampling time before and after the school opening.
3. To compare the ratios of species concentrations in fine and coarse particles.
4. To find the relationship between the concentrations of chemical species in the ambient air and the meteorological factors.

2. Literature Review

2.1 Sources

2.1.1 Source of particulate

Aerosols is defined as a suspension of liquid or solid particles in the air. In general, the characteristics of size distributions and chemical compositions of airborne aerosols would be different due to various formation mechanisms : 1) dispersion and 2) condensation. The aerosols produced by dispersion mechanism is almost always within the 2.5 to 1,000 μm diameter size range. This aerosol will be referred to as the coarse particle mode. Condensation aerosol is almost always of submicron size, with the major fraction of mass between 0.01 to 1 μm diameter. This aerosol will be referred to as the submicron aerosol or the fine particle mode aerosol. However, an ambient aerosol will normally have a bimodal distribution because both dispersion and condensation aerosols will present at the same time. Particle size distribution is one of the major parameters determining the transport and removal of pollutants in the atmosphere. Therefore, the size distributions of acidic aerosols would be useful for determining the fate of aerosols (Ronald *et al.*, 1998).

The particle matters suspended in the ambient air probably come from natural or anthropogenic sources. Several types of naturally emitted aerosol exist in the atmosphere, (1) sea-salt aerosol, (2) mineral aerosol (dust particles), and (3) sulfate aerosol from volcano eruptions. These aerosols play important roles in the atmosphere. For example, they scatter and absorb solar and terrestrial radiation (Chul *et al.*, 1999). Marine aerosols are among the most abundant and

important of the atmospheric aerosol components. Their vast and robust sources are the breaking waves of the world's entire sea surface and coastal surf zones. Their sink is the sea, also the continents. Along the coast they imprint the marine environment through affecting soil chemistry, weathering and vegetation. Being the most important source for condensation nuclei, essential for precipitation, they are vitally important for all activities on the continents (Mats, 2000).

According to the aerosols' retention time in the atmosphere, aerosols can be divided into two type : newborn aerosols and aging aerosols. Because of the different retention time, the two types aerosols have different surface conditions and chemical composition, which affect the morbific ability of aerosols (Wang *et al.*, 1999).

Aside from naturally occurring sources, particles are also generated by many anthropogenic processes, especially for fine and ultra-fine particles. Earlier work in Birmingham has shown that the atmospheric aerosol in the PM_{10} size range is normally dominated by particles from three sources. These sources are as follows: (1) Primary fine particle emissions from industrial and combustion sources, in practice predominantly road traffic. (2) Secondary aerosol, mostly ammonium sulfate and ammonium nitrate. This is mainly long-range transported and shows relatively weak spatial gradients; and (3) Wind-blown soil and resuspended street dust present largely in the coarse (2.5-10μm) particle fraction (Harrison *et al.*, 1999). Industrial activity and motorized traffic play an important role in the formation of particles, both directly and indirectly through the formation of secondary aerosols. (Fang *et al.*, 1999) It is estimated that about 30% of PM_{10} emissions in California USA are associated with traffic activity on paved roads (Venkatram, 1999). Motor vehicle emissions are considered to be the main source of fine particles in ambient urban

air of cities which are not directly influenced by industrial emissions (Lidia *et al.*, 1999). Motor vehicles are considered as one of the major contributors to air pollution. Though proportionate contribution to pollution varies with types of vehicles. Surveys in various fields indicated that in urban areas suspended particulate matter originated mainly from diesel-powered vehicles (Funasaka *et al.*, 1998).

A previous study indicated that the major contributors of PM_{10} aerosol mass in Brisbane include : soil/road side dust (25% by mass), motor vehicle exhausts (13%, not including the secondary products), sea salt (12%), Ca-rich and Ti-rich compounds (11%, from cement works and mineral processing industries), and biomass burning (7%). Elemental carbon and secondary products contribute to around 15% of the aerosol mass on average (4% elemental carbon, 6% ammonium sulfate and 4% organic; nitrate was not measured.) (Chan *et al.*, 1999). Alan's study (Alan *et al.*, 1995) used CMB (Chemical Mass Balance) to estimate the source of PM_{10} in Bulhead City, Arizona. Relative annual average contribution were 79.5, 16.7, 3.5, 0.1, and 0.1 % for geological material, motor vehicle emissions, secondary sulfate, coal-fired power plant emissions, and secondary ammonium sulfate or nitrate, respectively.

Aerosols can be classified as primary and secondary pollutants based on their sources. Primary aerosols are mainly emitted in particulate forms directly from sources. Secondary aerosols consist of particles produced in the atmosphere that are mainly submicron size formed from heterogeneous or homogeneous chemical reactions. Sulfate is a typical secondary pollutant, many studies have proved that sulfur dioxide may be converted to sulfate by oxidation-hydrolysis mechanism (Alfred, 1995). The production of fine (sub 2.5μm) sulfate by liquid transformation in clouds is an example of a process that

involves gas-to-particle mass transfer of species including water, sulfur dioxide, and oxidants (McMurry, 2000). Aerosol number concentrations and mass densities may increase by the sulfate produced. The aerosol scatters solar radiation and the number of cloud condensation nuclei (CCN) will be increased (Charles *et al.*, 1999).

2.1.2 Sources of SOx, NOx and NH_3

The primary inorganic air pollutants that form acidic aerosols are SO_2 and NOx. The SO_2 is produced by stationary-source combustion of coal and fuel of industrial plants. The major source of NOx are fossil-fuel combustion for industrial process, electricity and automobile emissions that are responsible for approximately half of these emissions. Gaseous HNO_3 can also be formed from indoor combustion of gas for cooking and heating (Chan *et al.*, 1993). Gaseous HCl comes mainly from combustion processes but also form reaction of nitric acid with sea salt (Spengler, 1990). The concentration of NH_3 is generally affected by local source, both from point source (farm facilities, manure stores) and intermittent emission events, such as manure spreading on fields (Burkhardt, 1998; Chan *et al.*, 1993). The atmospheric nitrogen, especially ammonia (NH_3) and ammonium (NH_4^+) compounds, have the significant potential of environmental impact. Atmospheric nitrogen compounds have many sources, both are anthropogenic and natural. They are transported by and transformed in the atmosphere before depositing onto sensitive ecosystems (Ronald *et al.*, 1998). Biomass burning, soils and plants, volcanoes, and dimethyl sulfide emissions from the oceans together account for 67 million tons of SO_2 every year on Earth. Combustion process are almost exclusively responsible for pollution by gaseous sulfur compounds. Coal burning and industrial smelting are

estimated to bring approximately 80 million t of SO_2 into the atmosphere every year on Earth (Malderen *et al.*, 1996).

2.1.3. Sources of metal elements

Base-cations such as calcium (Ca^{2+}), potassium (K^+) and magnesium (Mg^{2+}) are important plant nutrients. Their associated anions (mainly oxides, hydroxides, carbonates or silicates) may reduce the acidity of air precipitation and they increase soil base saturation. Base-cations mainly derive from mechanical erosion and wind mobilisation of soil particles, volcanic eruptions, forest fires, biological mobilisation, or from fuel combustion, wood or peat combustion and from industrial processes. Major primary anthropogenic source of mineral dust are power production, cement-, ferrous- or other industries. Of these, the cement industry is the largest source for Ca (Tψseth *et al.*, 1999). The presence of $CaSO_4$ particles in the atmosphere is not unusual and has been linked to several different sources. Continental $CaCO_3$ can react with SO_2 or H_2SO_4 and results in $CaSO_4$. $CaCO_3$ can be resulted from erosion and transport of Ca minerals, from worldwide dispersion of desert soil dust, or as a by-product of the iron and steel industry (Malderen *et al.*, 1996). The marine aerosols which transferred from marine to continental area by the monsoon are considered to be the major source of Na.

7

2.2 Harm of acidic particulate and gaseous species in the ambient air

Atmospheric aerosols affect the global climate through changing radiation budget of the Earth-atmosphere system by scattering and absorbing of solar radiation. The effect depends on the total amount in the atmosphere and the

optical properties, in particular absorptivity, of the aerosols. The aerosol also affect the climate by changing the cloud albedo due to increasing cloud droplet concentration, because water-soluble particles such as sulfate, nitrate or sea salt are easy to become cloud condensation nuclei (Sachio *et al.*, 1998).

Visibility, so-called the "visual range", can be used as an index of atmospheric turbidity. Concentrations of aerosols and inorganic salts in the atmosphere are highly related to "visibility" of ambient air (Rou *et al.*, 1999). The aerosols suspended in the air can scatter or absorb sunlight. Their physical and chemical conditions directly affect the visibility of atmosphere (Yuang *et al.*, 1999).

Particle matters with aerodynamic diameters less than 10 μm (PM_{10}), especially the fine particle fraction of PM_{10} (particle matter with aerodynamic diameter less than 2.5μm, $PM_{2.5}$), have been found to be associated with urban health problems such as increases in daily mortality (Fang *et al.*, 1999). Recent reports assessed by government and documented in the literature on epidemiology have indicated that particulate matter (PM) is believed to be causally associated with serious public health risks. The health risks are thought to be associated mainly with PM of aerodynamic particle size of 10μm or smaller. (Janssen *et al.*, 1999) Epidemiological studies that have examined air pollutant concentrations in relation to health statistics conclude that elevated fine particulate matter concentrations are associated with increased mortality and morbidity. (Lara *et al.*, 1998) Schwartz's study indicated that the 15 % increment of average $PM_{2.5}$ concentration is highly related to the 1.5 % increment of daily mortality (Schwartz *et al.*, 1996). The particles with size smaller than 10 μm can easily enter human respiratory channel. For fine or ultrafine particles, it is easy to accumulate on the surface of lung alveoli and

possibly penetrate the alveoli cells to reach the circulation of blood (Gau *et al.*, 1999). A majority of lung diseases are caused by inhaled particles such as viruses, bacteria, pollen, particles in cigarette smoke, and in occupational or environmental pollutants (toxic or radioactive aerosols). Inhaled particles may land on the surface of the lung's airspaces (Schürch *et al.*, 1999). Most particles larger than 10mm are removed in the mouth or nose prior to entering the body. Ten to 60% of the particles with aerodynamic diameters less than 10μm that pass the trachea may deposit in the lung where they might cause harm. The lung deposition is bimodal, peaking at 20% for about 3μm particles and at 60% for about 0.03μm particles. High deposition in the nasal airway may be related to upper respiratory diseases such as rhinitis, allergy, and sinus infections. When dry (but soluble) particles enter the human body where the relative humidity exceeds 99%, they grow substantially in particle diameter. Particle deposition in the lung will increase for soluble particle originally in the 0.5 to 1 μm size range, as they enlarge by taking on liquid water. Soluble particles within the droplet mode may cause greater pulmonary aggravation than insoluble particles (Chow, 1995).

Acid deposition acidifies the surface water, damages the forest, and deteriorates ancient monuments by dry and wet pathways. These detrimental effects have caused the phenomenon of acid precipitation to receive special attention and become one of the most important global problems. In the 1980s concern about ecological and health effects of atmospheric acidity has resulted in numerous air quality (Hoek *et al.*, 1996). Many studies have indicated that the input of nutrients and micronutrients from the atmosphere can impact biogeochemical cycles and biological productivity in coastal and open ocean surface waters (Tindale *et al.*, 1999). The acidic deposition can break the

memorial gradually. It is known that an important process which contributes to the damage of artworks is dry depositions of acid species (Katsanos *et al.*, 1999). The natural acidity of rainwater is often taken to be pH 5.6, however, in the absence of common basic compounds such as NH_3 and $CaCO_3$ may be expected to range from 4.5 to 5.6 due to natural sulfur compounds alone. The pH of the precipitation is expected to be lower than 5.6 for the areas which are exposed to strong influence of SO_2 and NO_x gases (Gülsoy *et al.*, 1999).

2.3 Major inorganic components of acidic aerosols

Ammonia, sulfate, nitrate, sodium, and chloride are the dominant reactive inorganic aerosol components in the atmosphere. Aerosols can exist in the form of solids such as NH_4NO_3 or $(NH_4)_2SO_4$ and aqueous solutions of electrolytes such as NH_4^+, SO_4^{2-}, and NO_3^- (Asif *et al.*, 1999). Inorganic salts constitute 50% or more of total fine particulate matter in the atmosphere, and generally consist of combinations of ammonium, nitrate, sulfate and small amounts of sodium and chloride. In the coarse fraction of aerosols (particles with $d_p > 2.5$ μm) where dust is a significant source of particulate matter, other inorganic species such as Ca, Mg, and K are abundant (Asif *et al.*, 2000). General speaking, the concentrations of $PM_{2.5}$ measured in urban area are highly related to the formation of secondary pollutants and photochemical smog, and are not related to TSP and PM_{10} apparently (Chen *et al.*, 1999). In the atmosphere the primary pollutant sulfur dioxide (SO_2) and the mainly secondary pollutant nitrogen dioxide (NO_2) are readily oxidized to sulfate (SO_4^{2-}) and nitrate (NO_3^-). Whereas NO_3^- may be present in the gas phase as nitric acid vapor, SO_4^{2-} is nearly exclusively found in the aerosol phase (Wyers, 1997). Sulfate constitutes a substantial fraction of the total suspended particulate (TSP) and an even larger

fraction of inhalable particles and fine particulate matter (Tripathi *et al.*, 1996). Many investigator have suggested that particulate sulfate formed in the atmosphere through homogeneous and heterogeneous reaction. Heterogeneous reactions occur in the aqueous surface layer of pre-existing particles where SO_2 react with O_3 or H_2O_2 to produce sulfate. Heterogeneous conversion is sensitive to humidity and its efficiency decrease of humidity. Experiments in a smog chamber suggested the conversion when relative humidity (R.H.) 30% was slower by two times than that when relative humidity 80%. Another possible mechanism of sulfate formation is the homogeneous reactions of SO_2, OH^-, O_2, H_2O, etc. Such reactions should not be sensitive to humidity (Zhang *et al.*, 1999). Ammonia tends to remain in the gas phase if the fine particle is cation rich, But, by the time the fine mode becomes sulfate rich, it begins to capture ammonia from the gas phase in order to neutralize the fine mode (Chul *et al.*, 1999). The heterogeneous formation of nitrate on pre-existing particles is much more efficient than homogeneous formation in the atmosphere. H_2O is needed on particle surface as reactant in the heterogeneous reaction and atmospheric water vapor also condenses onto particle surface during nitrate formation. The disproportionation reaction with surface water, as the most likely reaction (R1), have been discussed by many investigators. The $[H_2O]$ denotes water adsorbed on the surface (Zellweger *et al.*, 1999).

$$2NO_2 + [H_2O] \rightarrow HONO + HNO_3 \qquad \text{(R1)}$$

Photochemical formation of nitrate becomes active under the summer condition with high temperature and sufficient solar radiation, leading to high concentration of total nitrate.

Nitrate particles represent an important removal pathway for nitrogen oxide reaction products. A general tendency is found from these results that the particulate nitrate fraction increases with increasing concentration of cations. The particulate nitrate fraction is found to be sensitive to the sea-salt concentration and to increase as the sea-salt mass increase (Hayami *et al.*, 1998). Nitrate is found in both coarse and fine particles but as different chemical compounds indicating different formation pathways (Stephen *et al.*, 1988).

The formation of nitrate and sulfate on coarse particles is an important removal path of gaseous pollutants of SO_2 and NOx and their reaction products in the atmosphere. When secondary nitrate and sulfate are accumulated in the coarse mode, they can be removed more rapidly by dry or wet deposition because of the larger particle size. The composition of primary coarse particles is related to the formation of secondary species in this mode. Sulfuric acid and water can associate to form sulfate. A previous study used a sulfuric acid/water system to simulate the formation of sulfate in a laboratory chamber. This simulation showed that aerosol particles in the size range between 100nm and 1000nm are generated by dispersing a 20 wt.% sulfuric acid solution (Bunz *et al.*, 1998). Sulfuric acid (H_2SO_4), which is formed in the gas phase from the reaction of SO_2 with OH radicals, can nucleate with water vapor forming H_2SO_4-H_2O droplet or condense on the aerosol particles (Vignati, 1998).

Various researches concluded that coarse mode nitrate is mainly formed by the reaction of HNO_3 with sea-salt particles, especially when maritime and polluted urban air masses are mixed together. This reaction has been suggested to be the major path for the formation of coarse mode nitrate at many coastal areas. NOx transforms into gaseous nitrous and nitric acids, which later react with NaCl in sea-salt aerosols to form $NaNO_3$ and HCl in the so called chloride

depletion reaction.

$$HNO_{3(aq)}+NaCl_{(aq,\ s)} \Rightarrow NaNO_{3(aq,\ s)}+HCl_{(g)} \quad \text{(R2)}$$

$$H_2SO_{4(aq)}+2NaCl_{(aq,\ s)} \Rightarrow Na_2SO_{4(aq,\ s)}+2HCl_{(g)} \quad \text{(R3)}$$

SO_2 oxidation and to a lesser extent H_2SO_4 vapor condensation on sea-salt aerosols can also lead to chloride depletion. This process has been suggested to be the major path for formation of coarse mode non-sea-salt sulfate (nss-sulfate) in the marine boundary layer.

H_2SO_4 gas can condense on sea-salt particles and react with NaCl to form coarse mode non-sea-salt sulfate. But the contribution to nss-sulfate formation by this reaction is less important because the concentration of gas-phase H_2SO_4 is low in both clean and polluted environments. HNO_3, SO_2 or H_2SO_4 can also react with aqueous carbonates such as dissolved $CaCO_3$ and $MgCO_3$ on soil particles to form coarse mode nitrate and sulfate (Zhuang *et al.*, 1999).

$$2HNO_{3(g)}+CaCO_{3(s)} \Rightarrow Ca(NO_3)_{2(s)}+H_2O+CO_{2(g)} \quad \text{(R4)}$$

$$H_2SO_{4(aq,\ g)}+CaCO_{3(s)} \Rightarrow CaSO_{4(s)}+H_2O+CO_{2(g)} \quad . \quad \text{(R5)}$$

3. Experiment

3.1 Sampling Sites

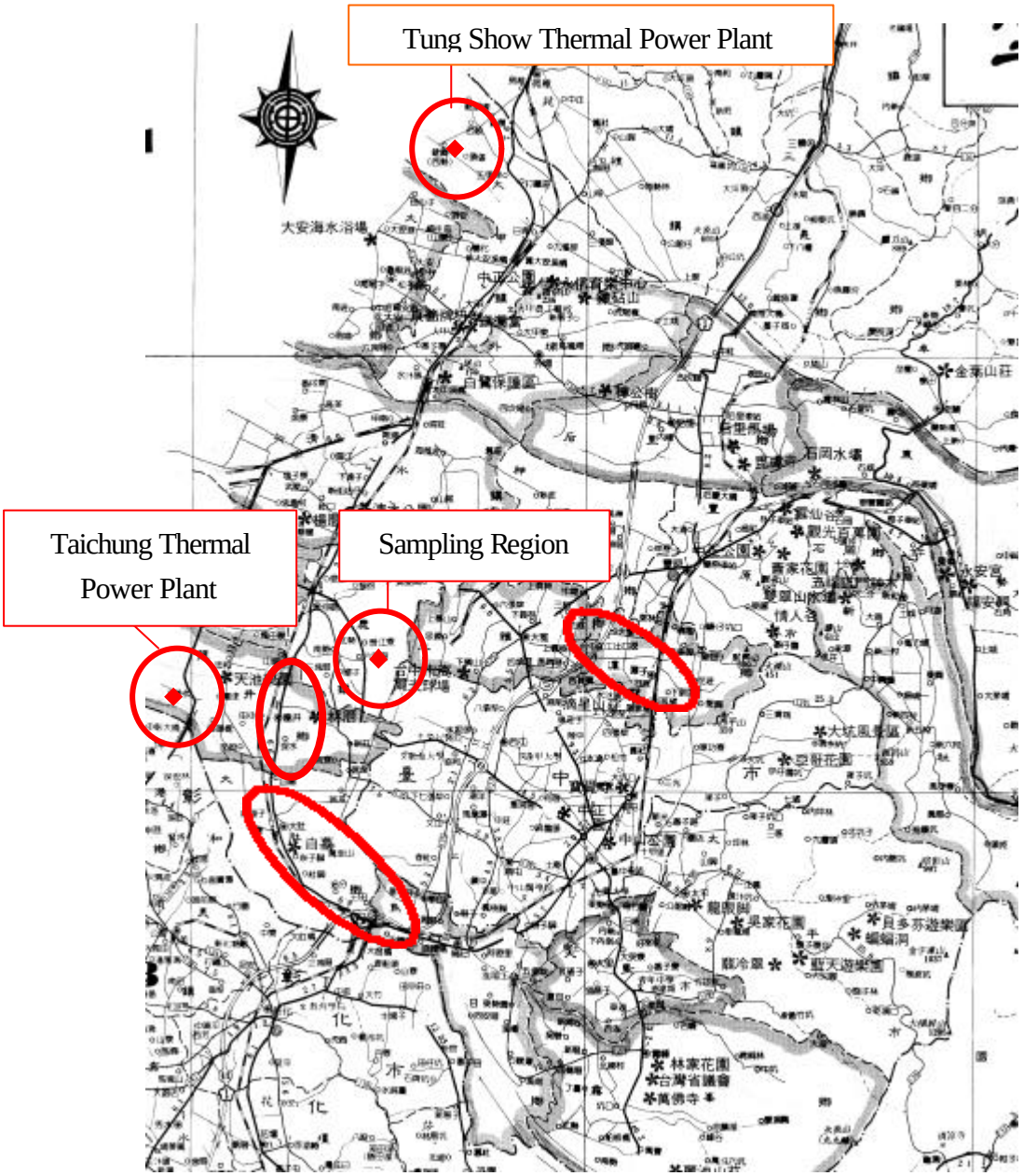

Figure 3.1-1. A map including the sampling region and nearby areas. Circles spread near the sampling regions point out the locations and scope

of industrial areas.

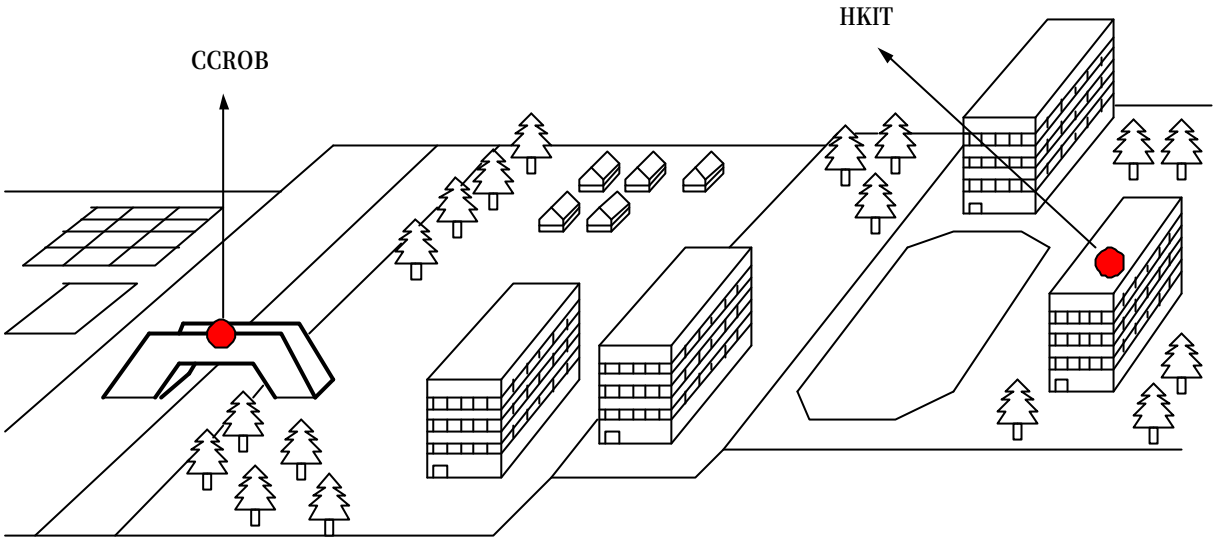

Figure 3.1-2. Locations of two sampling sites (HKIT and CCROB) of this study at Hung-Kuang Institute of Technology.

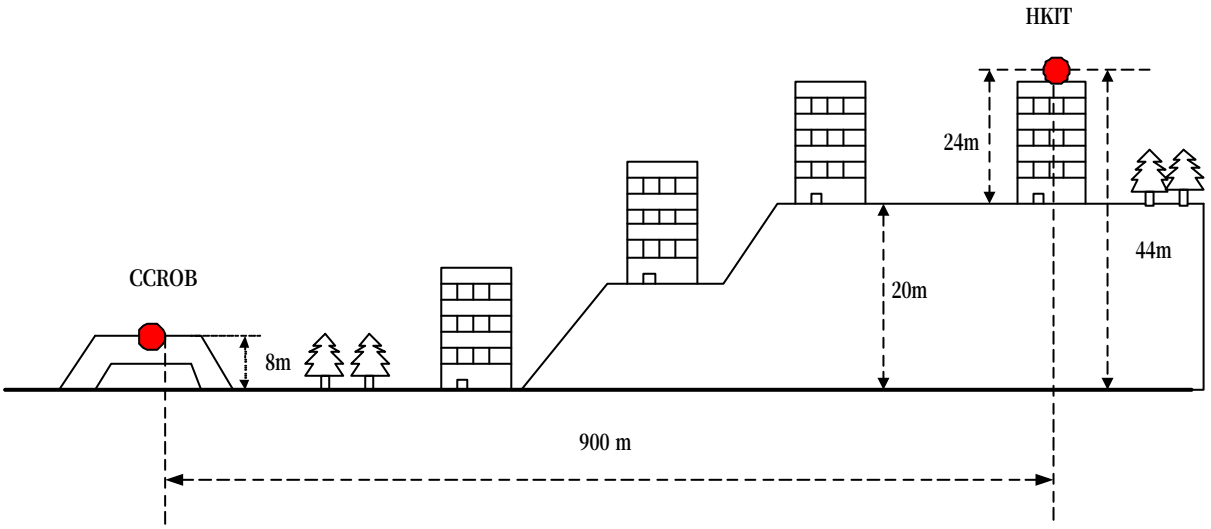

Figure 3.1-3. The section draw of the sampling region.

The sampling region is located in the west side of Taichung City. Two sampling sites characterized as a traffic site and a non-traffic site were set in this sampling region. One sampling site was located at the Chung-Chi Road over

bridge (CCROB), and this site was characterized as a traffic site in the study. Chung-Chi Road is the major passageway which connect Taichung harbor and Taichung City. It' s is one of the busiest traffic road in Taichung City, the traffic flow rate is about 160 cars/min in the daytime. Another sampling site was set on the roof of a eight story building in the campus of Hung-Kuang Institute of Techonology, this site was characterized as a non-traffic site in this study. There were quite some agricultural activities near the two sampling sites. Taiwan Strait is about 15km in the west side of CCROB. The Measurement sites and the experimental region is showed in Figure 3.1-1. Sampling was taken during the period of June 1999 to January 2,000, for a total of 21 sets of sample. Each Sampling was performed continuously for 24hr. Major activities near the sampling site are agriculture and a few small industries. Some small industries which used the coal-fired or oil-fired boiler as their power source are in Da-Du, southern-west of the sampling region. The Taichung thermal power plant, which is the biggest fire power station in the southeast Asia, located in the west side of the sampling region, should be the major sulfur dioxide emission source in the ambient area. There is another thermal power plant, Tung-Show thermal power plant, located in the north side of the sampling region. The straight distance from the sampling site to Taichung thermal power plant is about 15km, and to Tung-Show thermal power plant is about 35km.

Figures 3.1-2 and 3.1-3 displayed the locations of the two sampling sites (CCROB and HKIT) in the sampling region. The horizontal distance of two sampling sites (CCROB and HKIT) was about 900m, and the straight height difference of these two sites were about 44m. The height of the overbridge on Chung-Chi Road was 8m.

3.2 Sampling Program (June 1999 ~ January 2000)

Table 3.2-1 The sampling informations

Date	Sampling No.	Sampling Location	Temperature (℃)	Aeverage R.H. (%)	Wind Speed (m/s)	Prevailing wind
6/12-6/13/1999	1	H	26.8	80.56	6.2	W
6/16-6/17/1999	2	H	25.4	76.79	3.1	SW
7/1-7/2/1999	3	H	27.4	83.19	5.8	WSW
7/13-7/14/1999	4	H	28.9	79.65	5.2	SW
7/26-7/27/1999	5	H	29.9	80.72	4.9	SSW
8/3-8/4/1999	6	H	25.8	79.33	6.9	S
8/16-8/17/1999	7	H	26.2	80.45	5.7	WSW
8/20-8/21/1999	8	H	26.3	87.84	8	SW
9/10-9/11/1999	9	H+C	27.4	91.92	4.2	WSW
9/20-9/21/1999	10	H+C	26	89.79	4	SW
9/28-9/29/1999	11	H+C	26.7	84.33	5.6	NNE
10/3-10/4/1999	12	H+C	25.8	80.82	5.7	NNE
10/15-10/16/1999	13	H+C	23.6	80.64	6	NE
10/25-10/26/1999	14	H+C	21.1	77.46	4.3	NNE
10/28-10/29/1999	15	H+C	22.6	76.76	3.8	NNE
11/1-11/2/1999	16	H+C	20.5	78.33	4.1	NNE
11/10-11/11/1999	17	H+C	21.6	77.15	3.5	NNE
11/21-11/22/1999	18	H+C	19.4	76.37	4.3	NE
12/15-12/16/1999	19	H+C	16.2	73.88	3.6	NE
12/18-12/29/1999	20	H+C	15.3	73.68	5.2	NNE
1/9-1/10/2000	21	H+C	13.5	72.04	2.9	N

※ H : HKIT, Hung-Kuang Institute of Technology. This site was located on the roof of an eight-storie building.

※ C : CCROB, Chung-Chi Road OverBridge. This site was located on a overbridge which comes across Chung-Chi Road.

The sampling period started from June 1999 to January 2000. Meteorological factors such as temperature, relative humidity, wind speed and wind direction were routinely monitored by a meteorological measurements

system (Model 034, Meteorology recorder). The sampling period could be divided into two section : before and after school (Hung-Kuang Institute of Technology) opening. Sampling time were carried out at HKIT for Sampling No. 1 to 8. And for Sampling No. 9 to 21, the sampling were carried out in HKIT and CCROB simultaneously.

3.3 Instruments

3.3.1 Annular Denuder System (ADS)

In recent years, annular denuders have become the most widely employed instruments for sampling and collecting reactive gases such as SO_2, NH_3, HNO_3 and organic vapors in the atmosphere. They have advantages of allowing higher sampling velocities as well as having larger sampling capacities as compared to hollow tube denuders and parallel plate denuders (Lu *et al.*, 1995). Figure 3.3-1 showed standard configuration of the annular denduer system. The outward appearance of ADS was showed in Figure 3.3-2 (right). The performance of diffusion denuders take advantage of the noticeable difference existing between the diffusion coefficients of gases and particles (several orders of magnitude.) When gaseous pollutants are drawn through a denuder, they diffuse towards the denuder walls, which are coated with a chemical suitable for the retention of a specific pollutant or group of pollutants. A normal ADS consisting of denuder tubes, a filter pack and a cyclone (Lee *et al.*, 1993). There are two coaxial glass tubes in each denuder tube, the inner one closed at both sides, which forms two annular channel, the walls of the channel are coated with the chemical able to act as a sink for the pollutants to be collected (Perrino *et al.*, 1999).

The cyclone is used to remove the particles whose size larger than $PM_{2.5}$. Only the particle size equal or smaller than $PM_{2.5}$ can enter four denuder tubes. Each denuder consists of two concentric glass tubes. The inner walls of the concentric glass are coated with gas collection media. A filter pack was connected after to four denuder tubes. Because of the main usage of ADS in this study is gaseous species collection, there were no filters set inside the filter pack. When ADS is in operation, a laminar air stream is pumped through denuder

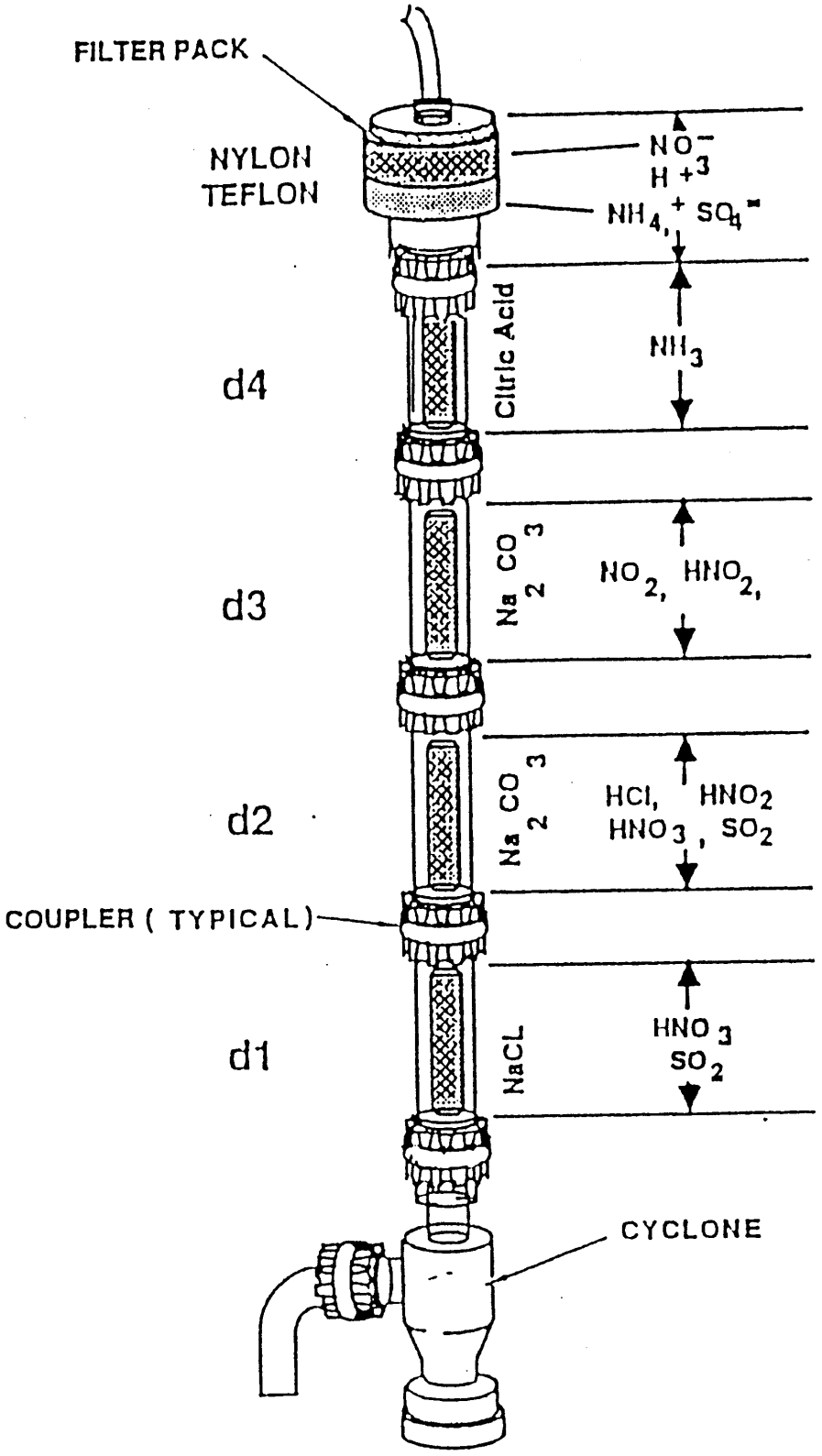

Figure 3.3-1. The standard configuration of annular denuder system (ADS).

(USEPA, 1989)

tubes that were coated with different absorbents suitable for special gas. The gas diffuses from inlet cyclone to the tube wall and is absorbed while the particles are carried on by the laminar air flow and impacted on the filter (Andersen *et al.*, 1994). The air flow rate for ADS is 15 lpm (Liter/min).

3.3.2 Universal Sampler

The Model 310 Universal Air SamplerTM (UASTM) (Figure 3.3-1) is a general purpose air sampler for atmospheric aerosol sampling and for mass concentration, and organic or inorganic analysis. The sampler has a design inlet sampling flow rate of 300 lpm. Fully equipped, it includes two virtual impactors for size fractionation of airborne particles and a Poly-Urethane Filter (PUF) sampler for analysis of volatile organic compounds (VOCs) in the air sample.

Figure 3.3-2. The outward appearance of the Universal sampler (left) and ADS (right).

The sampler is provided with an omni-directional inlet, a PM_{10} (10 μm cut)

virtual impactor classifier, either a $PM_{2.5}$ or PM_{10} virtual impactor classifier, a fine particle filter and a PUF sampler. This allows operation as a high volume dichotomous sampler for size fractionation of airborne particles in the 0-2.5 μm and 2.5-10 μm aerodynamic size ranges. When only one virtual impactor is installed, it can be operated as a PM_{10} or $PM_{2.5}$ sampler, depending on the cut point diameter of the classifier used.

Air is sampled at 300 lpm from the ambient atmosphere through an omni-directional, cylindrical inlet. Particles greater than 10 μm aerodynamic equivalent diameter are removed from the sampled air stream by the PM_{10} classifier and discarded. Particles less than 10 μm flow to the $PM_{2.5}$ classifier loaded downstream. Particles in the 2.5-10 μm range are collected on a 62 mm×165 mm filter and those smaller than 2.5 μm are collected on a 200 mm×250 mm final filter. The filtered air stream is then directed through the PUF sampler to collect the volatile organic compounds in the filtered air stream (Manual of universal sampler, 1996). The main usage of Universal sampler in this study is the $PM_{2.5}$ and PM_{10} collection.

Filters used in this study were Teflon filters for its low chemical interference in sampling and analysis process. The glass fiber filters and quartz filters were avoided due to possible sampling error, even if they were much cheaper than Teflon filters. Previous study (Robert, 1977) indicated some types of filters absorb acidic gases from the ambient air easily, this phenomena results in the sampling error. The principal error involved in sampling of ambient air for total sulfate particulate content is caused by the absorption and subsequent oxidation of ambient SO_2 in the presence of basic components of the filter medium.

3.3.3 Sensitivity of Weighting

Weighting is done on a Shimadzu semi-micro electronic balance, AEL-40SM. The minimum detectable mass for the balance is 0.01 mg, and the maximum detectable is 42 g. Shimadzu electronic printer Model EP-50 is used to connect with Shimadzu electronic balances.

3.4 Experiment Method

3.4.1 Treatment of filters and denuder tubes before sampling

a. Filter for Universal sampler

The 62 mm×165 mm and 200 mm×250 mm with 0.2 μm pores Teflon filters (XP38, 1.0 μm pore size, Geleman Sciences) were used to collect the coarse (2.5-10 μm) and fine (< 2.5μm) particulate concentration respectively. Teflon filters were chosen because of their low weight and low blank levels for ionic species. The Teflon filters were previously dried in a desiccator for a 48-h period and weighed to a precision of ± 10 μg in an analytical balance. Then they were sealed in the filter holder with a cover during transportation to the sampling site or back to the laboratory to prevent contamination.

b. Denuder tubes

Before coating process, each denuder tube was washed by neutral detergents, then rinse by 30 min ultrasonication using deionized water(DI water). The same process was employed to cyclone and filter pack. After drying, denuder tubes were coated by appropriate coating solution. The first denuder tube was coated by 10ml solution of 0.1% W/V NaCl in 1:9 methanol/water to

collect SO_2 and HNO_3. The second and third denuder tubes were coated by 10ml solution of 1% W/V Na_2CO_3 and 1% glycerol in 1:1 methanol/water each. The second denuder tube is used to collect SO_2, HNO_2 and HNO_3. The third denuder tube is used to absorb the interfering gas such as O_3, NO_2 which will result in positive error in the measurement of concentration of HNO_2. The real concentration of HNO_2 is the positive difference between the concentration of HNO_2 measured by secondary and third denuder tube. Fourth denuder tube was coated by 10ml solution of 1% W/V citric acid in methanol to collect NH_3. Another purpose of the fourth denuder tube is to prevent the pH change of aerosols. (If NH_3 gas did not absorb by the fourth denuder tube, NH_3 would easily associate with sulfate particle to form ammonium sulfate, and the pH of the aerosol will be change.) When SO_2 is collected in an aqueous alkaline medium (e.g., the Na_2CO_3 coating of the second and third denuders), it likely exists as SO_3^{2-}. Any NO_2 also captured on the surface can subsequently react with the SO_3^{2-} to produce NO_2^-, resulting the positive error of HNO_2 gas (Sickles *et al.*, 1999). Therefore, the measured concentration of HNO_2 in third denuder tube was used to be a blank value, true concentration of HNO_2 is that the HNO_2 concentration measured in second tube subtract it measured in third tube.

After coating, the denuder tubes were blown to dry by pure nitrogen gas in a gloved box to prevent from the absorption of ammonia gas. The four denuder tubes were connected to the manifold and nitrogen gas blew into the gloved box at 2.5 kg/cm^2. After the tubes were dried, they were immediately capped and sealed with parafilm to isolate them from ambient air until sampling. After all the coating and drying process, the ADS would be brought to the sampling site with good care to prevent smashing and oscillation.

3.4.2 Sampling

After the transportation of denuder tubes, filter pack, cyclone(for ADS) and filters (for Universal sampler) from laboratory to the sampling site, the denuder tubes and filter pack were uncapped and assembled in a house case, and the Teflon filters were set in the right position on Universal sampler. The air flow rate for ADS was 10 lpm, and for Universal sampler was 300 lpm.

3.4.3 Extraction and Analysis

a. Filters for Universal sampler

After sampling, the filters were placed in the desiccator dried for another 48-h period and weighed again in the same analytical balance. From the final weight determination the mass of the sample on each surface was calculated by subtracting the initial weight from the final weight.

The 200mm × 250mm Teflon filter was cut into one-sixteen pieces, and the 62mm × 165mm Teflon filter was cut into one-eight pieces for the analysis for ion species. The one-sixteen and one-eight samples were put into 15ml bottles, 15ml deionized water was added into each bottle. Then all the bottles were sent to ultrasonic process for about 40 minutes. Ion Chromatography (DIONEX DX-100) was used to analyze for the anions.

b. Denuder tubes

Sodium chloride denuder extracts were analyzed for nitrate and sulfate, In some case NaCl coating was replaced with a NaF coating, allowing also the determination of hydrochloric acid and particulate chloride (Perrino *et al.*, 1999). Sodium carbonate denuder extracts were analyzed for nitrite, nitrate and sulfate.

Citric acid-coated denuder extracts were analyzed for ammonium. Anion concentrations were determined by ion chromatography (DIONEX DX-100).

3.4.4 Quality control

The results of quality assurance and quality control include calibration of IC analysis using standard solutions, blank test, recovery efficiency test, reproducibility test and detection limit**.**

a. Blank test

The blank test can be used to determine the background contamination from the sampling and analysis processes. Background contamination was determined by using operational blanks (unexposed filter and denuder). The treatment for blank samples was completely the same as the field samples, but blank samples were not be put into sampler. The background contamination is insignificant and can be ignored. The results of the blank test are shown in Table 3.3-1.

b. Recovery efficiency test

At least 10% of the samples are analyzed in spiking with a known amount of standard chemicals. The recovery efficiency should be inside the range of 75% to 125%. The analysis procedure for the recovery test is the same as that described for the field sample. The results of recovery test were showed in Table 3.3-2

Table 3.3-1. Results of blank analysis.

Analysis item : filters and denuder which were proceeded by whole pretreatment procedures, but not put into sampling.

Analysis Method : Ion Chromatography technique

Date	Type	Species	Blank Conc. (mg/l)	Type	Species	Blank Conc. (mg/l)
5/30/1999	Filter	SO_4^{2-}	0.060	Denuder	HNO_2	N.D.
		NO_2^-	0.021		HNO_3	N.D.
		NO_3^-	0.022		SO_2	N.D.
		Cl^-	0.062		NH_3	N.D.
		NH_4^+	0.051		HCl	N.D.
		Mg^{2+}	N.D.			
		Ca^{2+}	N.D.			
		K^+	N.D.			
		Na^+	N.D.			
9/12/1999	Filter	SO_4^{2-}	0.044	Denuder	HNO_2	N.D.
		NO_2^-	N.D.		HNO_3	N.D.
		NO_3^-	0.048		SO_2	N.D.
		Cl^-	0.074		NH_3	N.D.
		NH_4^+	0.050		HCl	N.D.
		Mg^{2+}	N.D.			
		Ca^{2+}	N.D.			
		K^+	N.D.			
		Na^+	N.D.			
12/23/1999	Filter	SO_4^{2-}	0.035	Denuder	HNO_2	N.D.
		NO_2^-	0.026		HNO_3	N.D.
		NO_3^-	N.D.		SO_2	N.D.
		Cl^-	0.078		NH_3	N.D.
		NH_4^+	0.082		HCl	N.D.
		Mg^{2+}	N.D.			
		Ca^{2+}	N.D.			
		K^+	N.D.			
		Na^+	N.D.			

c. Reproducibility test

The reproducibility test can display the stability of instruments. The procedure is to repeat the analysis of the same sample for seven times. The value of three times standard deviation for repeating analysis should not exceed the upper control limit (+10%) and lower control limit (-10%). If the value of (3 × S.D.) exceed upper and lower control limit, the experiments should be paused to examine the procedures of analysis and instruments.

d. Detection limit

Detection limit was used to determine the lowest concentration level that can be detected to be statistically different from a blank. The detection limit of the chemical species in this study were showed in Table 3.3-3. Method detection limit (MDL) was determined from selected the concentration slightly higher than the low concentration of the standard line, repeated this concentration for seven times to estimate the standard deviation(s). The MDL was equally to be (3×S).

e. Sample storage

Samples were analyzed as soon as possible after sampling. If samples could not be analyzed by inevitable reasons, all of the samples should be put into a refrigerator under 4℃ for storage. In order to avoiding the occurrence of unexpectedly chemical reactions, the storage time should not exceed one week.

Table 3.3-2. Results of recovery tests (n = 7).

Date	Species	Sample amount (mg/l)	Amount added (mg/l)	Amount Found (mg/l)	Recovery efficiency (%)
7/30	SO_4^{2-}	2.00	2.00	4.30	115
	NO_2^-	2.00	2.00	4.02	101
	NO_3^-	2.00	2.00	3.94	97
	Cl^-	1.00	2.00	2.84	92
	NH_4^+	2.00	2.00	3.68	84
	Mg^{2+}	1.00	2.00	3.26	113
	Ca^{2+}	1.00	2.00	3.10	105
	K^+	1.00	2.00	3.34	117
	Na^+	1.00	2.00	3.16	108
11/27	SO_4^{2-}	2.00	2.00	3.78	89
	NO_2^-	2.00	2.00	3.68	84
	NO_3^-	2.00	2.00	3.88	94
	Cl^-	2.00	2.00	3.92	96
	NH_4^+	2.00	2.00	4.30	115
	Mg^{2+}	2.00	2.00	4.02	101
	Ca^{2+}	2.00	2.00	4.40	120
	K^+	2.00	2.00	4.14	107
	Na^+	2.00	2.00	4.24	112

Table 3.3-3. Results of detection limit for chemical species (n = 7).

Species	Detection Limit (mg/l)
SO_4^{2-}	0.010
NO_2^-	0.015
NO_3^-	0.015
Cl^-	0.025
NH_4^+	0.025
Mg^{2+}	0.020
Ca^{2+}	0.024
K^+	0.026
Na^+	0.030

※ Test date : 1999/6/3

4. Results and Discussions

4.1 Results of HKIT

4.1.1 The fine and coarse particles in HKIT

Table 4.1-1 Concentrations of fine and coarse particles before and after school opening in HKIT (Unit : μg/m^3).

Date	No.	Fine	Coarse	Fine/Coarse	Fine/PM_{10}
Before school opening					
6/12-6/13/99	1	34.99	32.65	1.07	0.52
6/16-6/17/99	2	14.18	13.62	1.04	0.51
7/1-7/2/99	3	42.86	24.21	1.77	0.64
7/13-7/14/99	4	24.51	22.60	1.08	0.52
7/26-7/27/99	5	37.44	15.88	2.36	0.70
8/3-8/4/99	6	54.36	33.70	1.61	0.62
8/16-8/17/99	7	45.34	25.71	1.76	0.64
8/20-8/21/99	8	45.47	36.21	1.26	0.56
Average		37.39	25.57	1.49	0.59
RSD		34 %	32 %	44%	7%
After school opening					
9/10-9/11/99	9	36.15	16.62	2.18	0.69
9/20-9/21/99	10	29.97	14.70	2.04	0.67
9/28-9/29/99	11	58.24	27.63	2.11	0.68
10/3-10/4/99	12	32.16	18.82	1.71	0.63
10/15-10/16/99	13	51.35	31.44	1.63	0.62
10/25-10/26/99	14	23.96	18.65	1.28	0.56
10/28-10/29/99	15	49.48	23.80	2.08	0.68
11/1-11/2/99	16	39.21	21.22	1.85	0.65
11/10-11/11/99	17	65.8	42.38	1.55	0.61
11/21-11/22/99	18	58.47	39.62	1.48	0.60
12/15-12/16/99	19	56.81	33.45	1.70	0.63
12/28-12/29/99	20	59.12	39.30	1.50	0.60
1/9-1/10/00	21	60.73	48.66	1.25	0.56
Average		47.80	28.95	1.79	0.64
RSD		29 %	23 %	31%	4.3%
Total					
Average		43.84	27.66	1.64	0.61
RSD		32 %	36 %	38%	5.7%

※ RSD : Relative Standard Deviation (n = 21).

For the sampling of fine ($PM_{2.5}$) and coarse ($PM_{2.5-10}$) particles, the average concentration of fine and coarse particles before school sampling were 37.39 and 25.57 $\mu g/m^3$, respectively; and the average concentration of fine and coarse particle after school opening were 47.80 and 28.95 $\mu g/m^3$, respectively. The fine particles concentrations after school opening were higher than before school opening (one sided p-value < 0.05, T-test). The coarse particle concentrations showed no significant difference before and after school opening (two sided p-value < 0.05, T-test). Increasing traffic inside the campus of Hung-Kuang Institute of Technology could be the reason of the fine particles concentrations increment. Fine particle fractions in PM_{10} were varied from 0.51 to 0.70, the average value was 0.61 during the whole sampling period. Relative standard deviation of Fine/PM_{10} value was 5.7 %, meant that the fine particles occupied a stable fraction of PM_{10} concentrations in the ambient air of Sha-Lu area. The average ratio of fine particle concentration to coarse particle concentration before school opening was 1.49 before school opening, and were 1.79 after school opening. The ratios of fine particle concentration to PM_{10} concentration (Fine/PM_{10}) were 0.59 before school opening and 0.64 after school opening. These ratios mean that the fine particles are the major contributor to PM_{10} at HKIT sampling site. The ratios of fine particles concentrations to coarse particles concentrations after school opening was slightly higher than that before school opening. The variations of coarse particles concentration (RSD = 36 %) were higher than fine particles concentrations (RSD = 32 %) across the whole sampling period. The details of fine and coarse particles concentrations were displayed in Table 4.4-1.

4.1.2 The gas species in HKIT

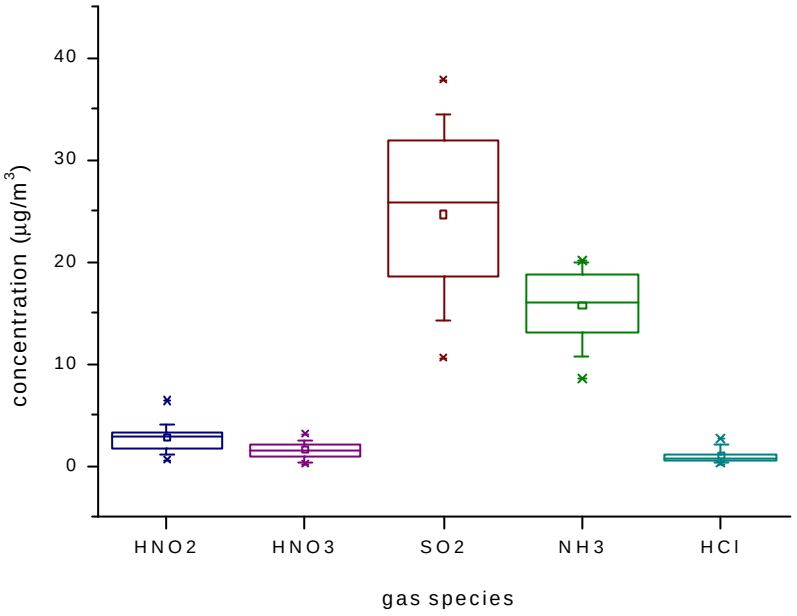

Figure 4.1-1. Comparison of the distribution of gas species across the whole sampling period. The box plots indicate the minimum, 25th percentile, median, 75th percentile, maximum, average and ± S.D. values (n=21).

The gas species HNO_2, HNO_3, SO_2, NH_3 and HCl were measured in HKIT site. Figure 4.1-1 showed the average values and distribution range of the concentration of gaseous HNO_2, HNO_3, SO_2 NH_3 and HCl. The average concentration of HNO_2, HNO_3, SO_2 NH_3 and HCl in the whole sampling period were 2.81, 1.63, 24.69, 15.75, 1.08 μg/m^3, respectively. The standard deviations of HNO_2, HNO_3, SO_2 NH_3 and HCl were 1.34, 0.85, 8.20, 3.72, 0.72 μg/m^3, respectively. The variations of SO_2 and NH_3 concentrations were apparently larger than HNO_2, HNO_3 and HCl. This result is similar to the previous study done in Hsing-Chu (Yang, 1997).

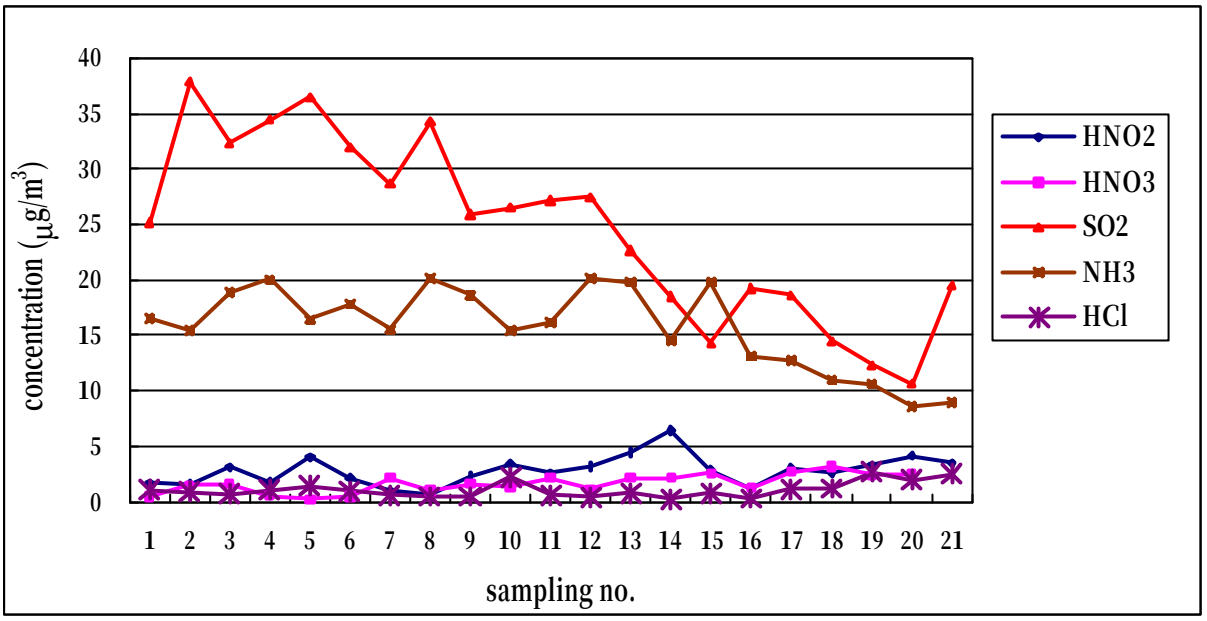

Figure 4.1-2. The concentration of gas phase of HNO_2, HNO_3, SO_2, NH_3 and HCl measured at HKIT site across the whole sampling period (m g/m^3).

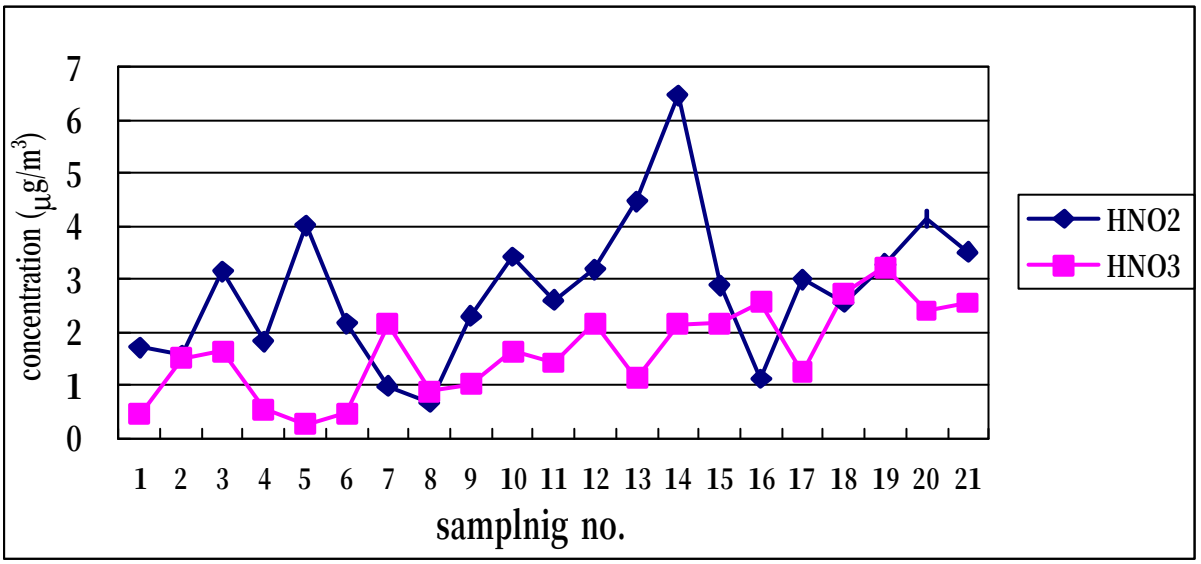

Figure 4.1-3. The variation of the acidic gas HNO_2 and HNO_3 concentration measured at HKIT site across the whole sampling period (m g/m^3).

Figure 4.1-2 showed that the sulfur dioxide had higher concentration in summer (From Sampling No. 2~8, June to August) and then decrease gradually in fall and winter (From sampling No. 9~20, September to December) except the

Sampling No. 21. The ammonium concentration was not varied very much compared to sulfur dioxide, the maximum value was 20.15 $\mu g/m^3$, and the minimum value was 8.60 $\mu g/m^3$. From June to October (Sampling No. 1 to 14), the concentration of ammonia changed between 15 and 20 $\mu g/m^3$, but decreased sharply after Sampling No. 15. A possible reason for the variation trend of ammonia was the decrease agricultural activities around the fall season in the nearby areas. The concentration of HCl was relatively low than other chemical species measured in this study. Figure 4.1-3 showed the more clear variation curve of HNO_2 and HNO_3. It seemed that the two gas species have contrary variation trend.

Comparison of the gas species concentrations before and after school opening

The average concentration of HNO_2, HNO_3, SO_2, NH_3, HCl and NH_3 before school opening were 2.01, 0.88,32.65, 17.62 and 0.91 $\mu g/m^3$, respectively, and after school opening were 3.30, 2.03, 19.80, 14.59 and 1.19 $\mu g/m^3$, respectively. The concentration of HNO_2 and HNO_3 increased apparently after school opening. The concentration of HNO_2 after school opening was 1.64 times higher than before school opening, and the concentration of HNO_3 after school opening was 2.31 times higher than before school opening. The concentration of SO_2 and NH_3 decreased after school opening, and the concentration of HCl increased after school opening.

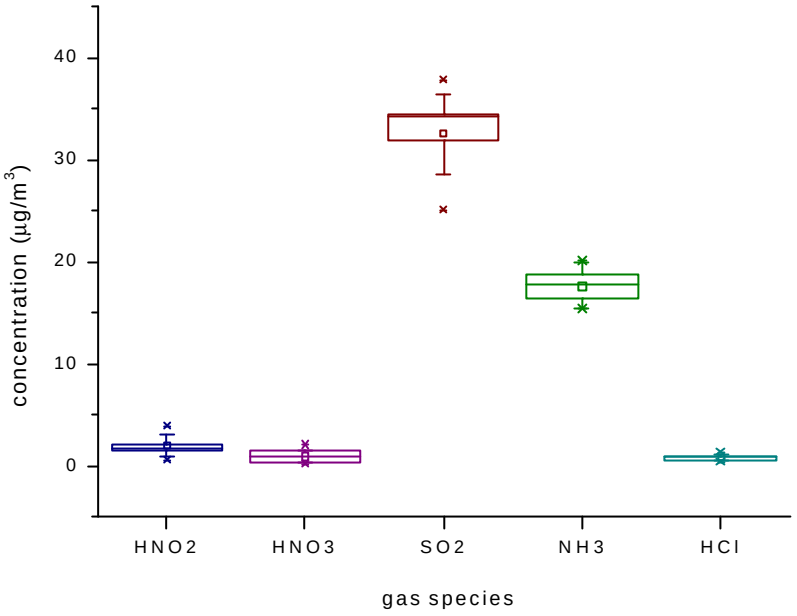

Figure 4.1-4. Comparison of the distribution of gas species before school opening. The box plots indicate the minimum, 25th percentile, median, 75th percentile, maximum, average and ±S.D. values (n = 8).

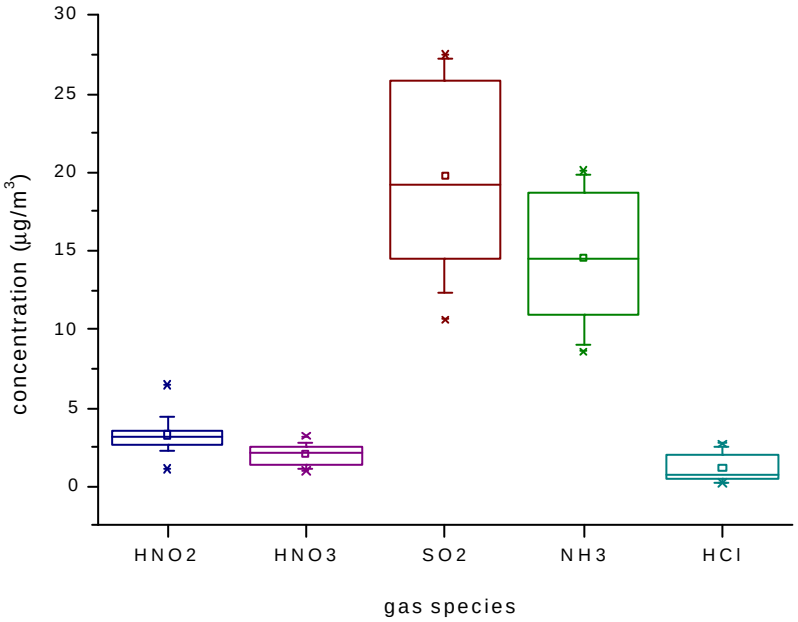

Figure 4.1-5. Comparison of the distribution of gas species after school opening. The box plots indicate the minimum, 25th percentile, median, 75th percentile, maximum, average and ±S.D. values (n = 21).

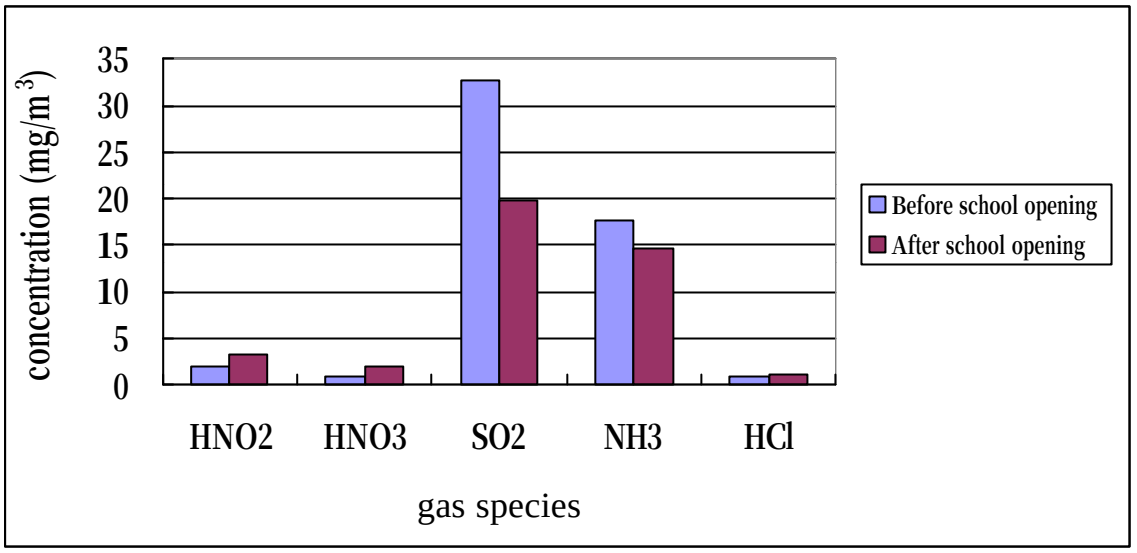

Figure 4.1-6. The comparison of gas species before and after school opening.

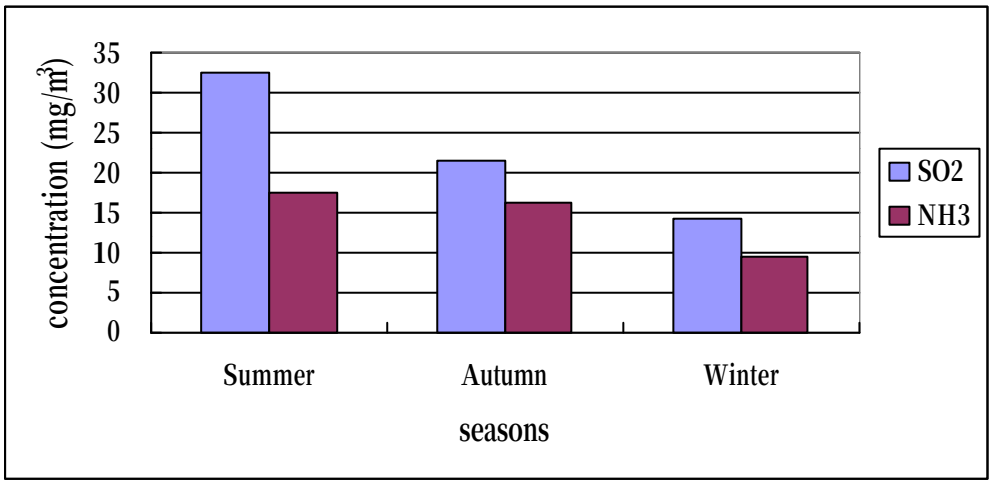

Figure 4.1-7. The average concentrations of HNO_2, HNO_3 and HCl in summer, autumn and winter.

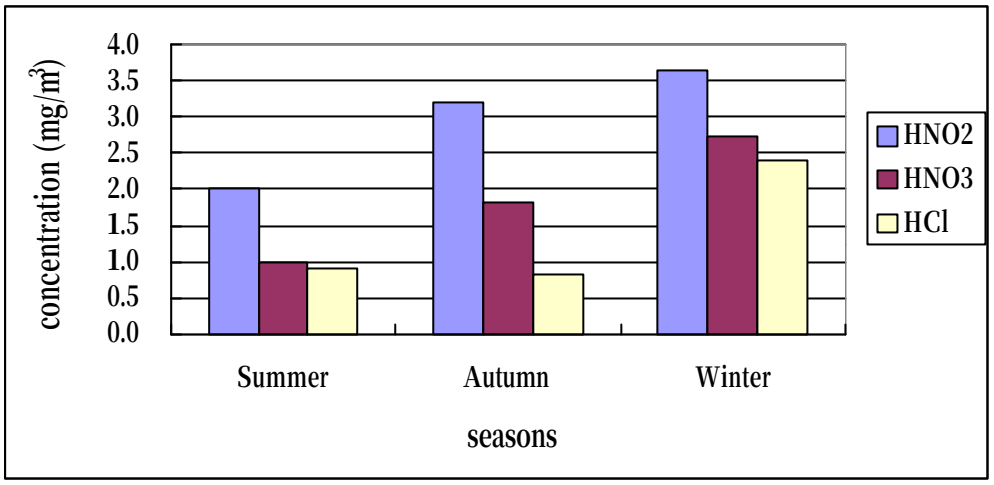

Figure 4.1-8. The concentrations of SO_2 and NH_3 in summer, autumn and winter.

Figure 4.1-6 showed the comparison of gas species concentrations measured at HKIT before and after school opening. The SO_2 and NH_3 concentration before school opening were higher than after school opening showed. However, the HNO_2, HNO_3 and HCl concentration before school opening were lower than after school opening.

A previous measurement in Nara, Japan (Matsumoto *et al.*, 1998) showed that the HNO_2 concentration was higher in winter and lower in summer. The HNO_3 concentration was, on the other hand, higher in summer than in winter. In this study, the average concentration of HNO_2 was 2.01 $\mu g/m^3$ in summer (June, July and August), 3.20 $\mu g/m^3$ in autumn (September, October and December), and 3.64 $\mu g/m^3$ in winter (November and February) at HKIT. The variation trend of HNO_2 concentrations measured in this research was similar to Masumoto's study. However, the concentration of HNO_3 measured at HKIT was higher in summer than in winter, this result was just opposite to the Matsumoto's study. The average HNO_3 concentration at HKIT site was 0.99 $\mu g/m^3$ in summer (June, July and August), 1.82 $\mu g/m^3$ in autumn (September, October and December),

and 2.72 μg/m^3 in winter (November and February). Another study which was done in Japan (Kaneyasu *et al.*, 1995) indicated that high nitrate aerosol concentrations found in the winter were favored by the high concentration of NO_x and by the reaction : NH_4NO_3 (particle) ↔ NH_3 (gas) + HNO_3 (gas). The concentration of $HCl_{(g)}$ was not displayed a season-relative variation. Both SO_2 and NH_3 concentrations were higher in summer and lower in winter.

4.1.3 The inorganic components in particulate phase at HKIT

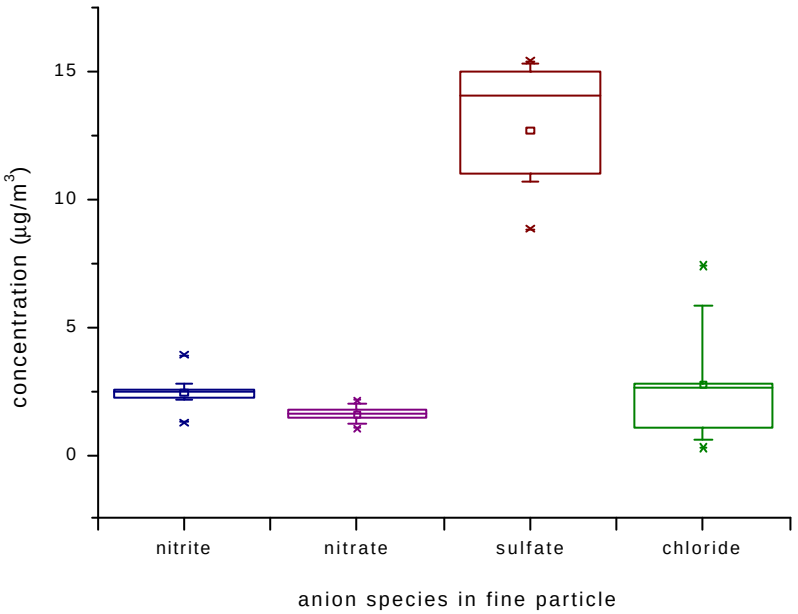

Figure 4.1-9. Comparison of the distribution of anion species in fine particle before school opening. The box plots indicate the minimum, 25th percentile, median, 75th percentile, maximum, average and ±S.D. values (n = 8).

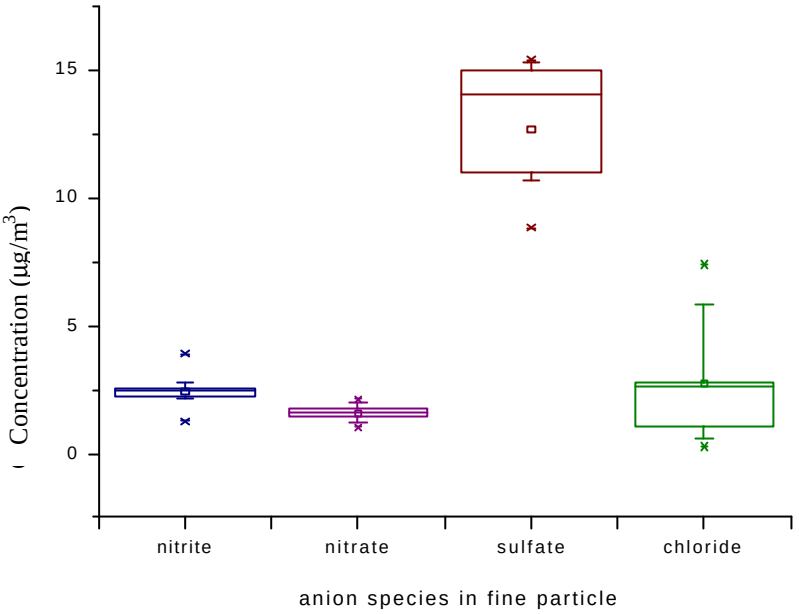

Figure 4.1-10. Comparison of the distribution of anion species in fine particle after school opening. The box plots indicate the minimum, 25th percentile, median, 75th percentile, maximum, average and ±S.D. values (n=13).

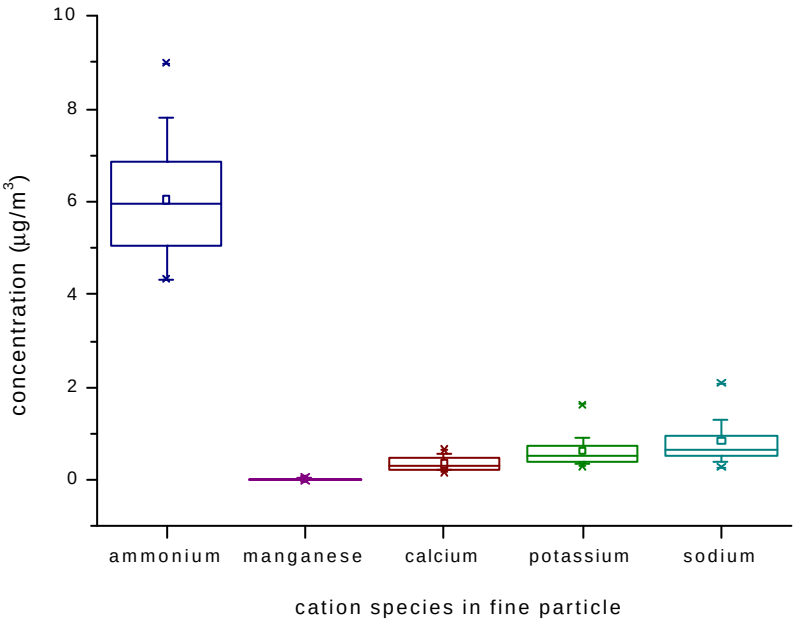

Figure 4.1-11. Comparison of the distribution of cation species in fine particle before school opening. The box plots indicate the minimum, 25th percentile, median, 75th percentile, maximum, average and ±S.D. values (n = 8).

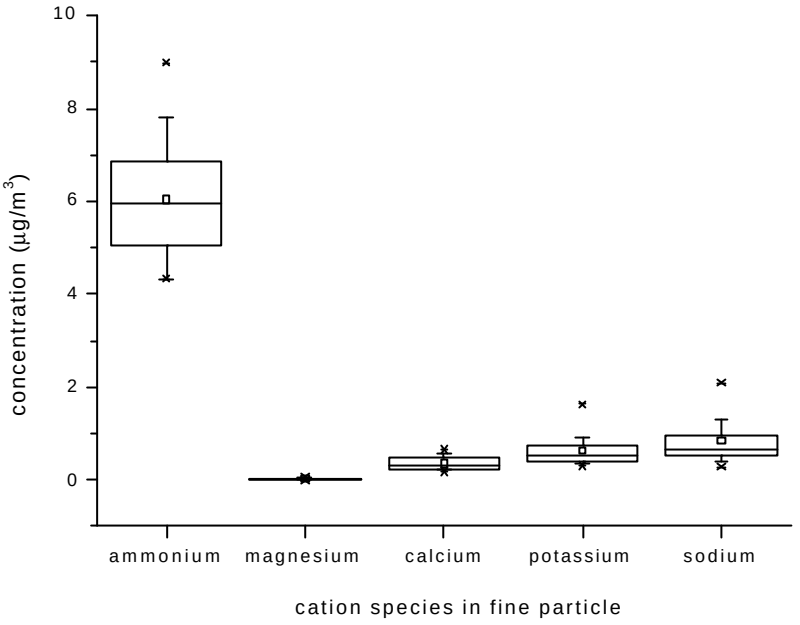

Figure 4.1-12. Comparison of the distribution of cation species in fine particle after school opening. The box plots indicate the minimum, 25th percentile, median, 75th percentile, maximum, average and ±S.D. values (n = 13).

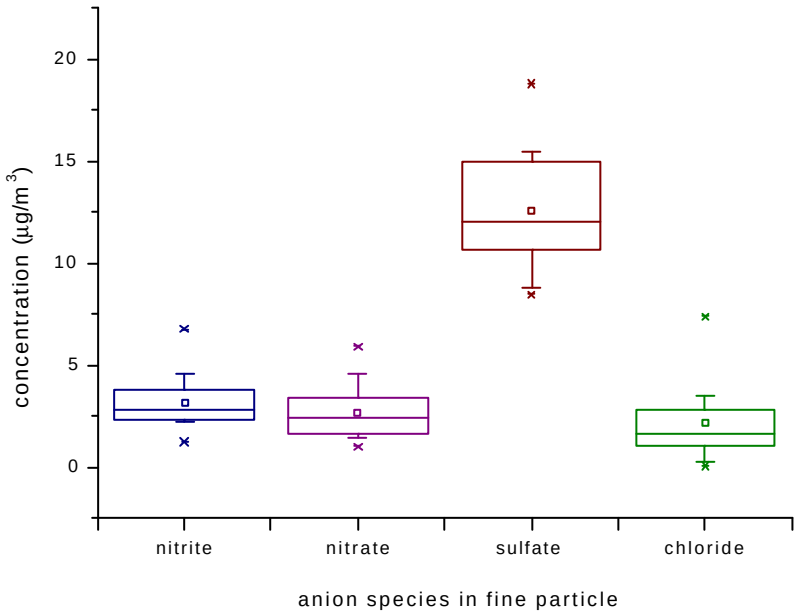

Figure 4.1-13. Comparison of the distribution of anion species in fine particles across the whole sampling period. The box plots indicate the minimum, 25th percentile, median, 75th percentile, maximum, average and ±S.D. values (n = 21).

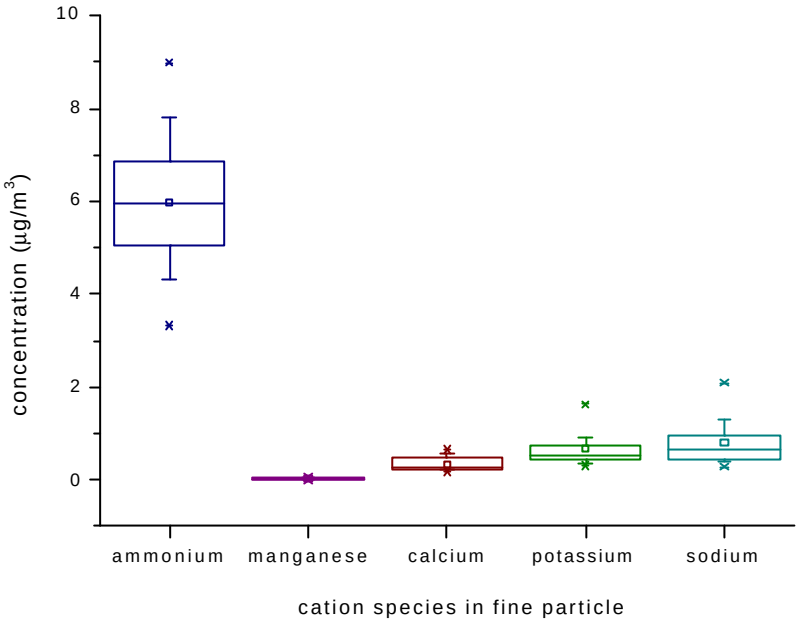

Figure 4.1-14. Comparison of the distribution of cation species in fine particles across the whole sampling period. The box plots indicate the minimum, 25th percentile, median, 75th percentile, maximum, average and ±S.D. values (n = 21).

Concentrations of the anions (NO_2^-, NO_3^-. SO_4^{2-} and Cl^-) and cations (NH_4^+, Mg^{2+}, Ca^{2+}, K^+ and Na^+) in fine particles were displayed in Figure 4.1-9 to Figure 4.1-14. Average concentrations of NO_2^-, NO_3^-. SO_4^{2-} and Cl^- in fine particle were 2.47, 1.59, 12.70, 2.70 µg/m^3 before school opening, respectively; and were 3.61, 3.42, 12.50, 1.90 µg/m^3 after school opening, respectively. The average concentrations of NH_4^+, Mg^{2+}, Ca^{2+}, K^+ and Na^+ in fine particle were 5.90, 0.03, 0.33, 0.71 and 0.78 µg/m^3 before school opening, respectively; and were 6.04, 0.02, 0.36, 0.64 and 0.84 µg/m^3 after school opening, respectively. Average concentrations of NO_2^-, NO_3^-. SO_4^{2-}, Cl^-, NH_4^+, Mg^{2+}, Ca^{2+}, K^+ and Na^+ were 3.18, 2.72, 12.58, 2.22, 5.99, 0.02, 0.35, 0.66 and 0.81 µg/m^3 across the whole sampling period, respectively.

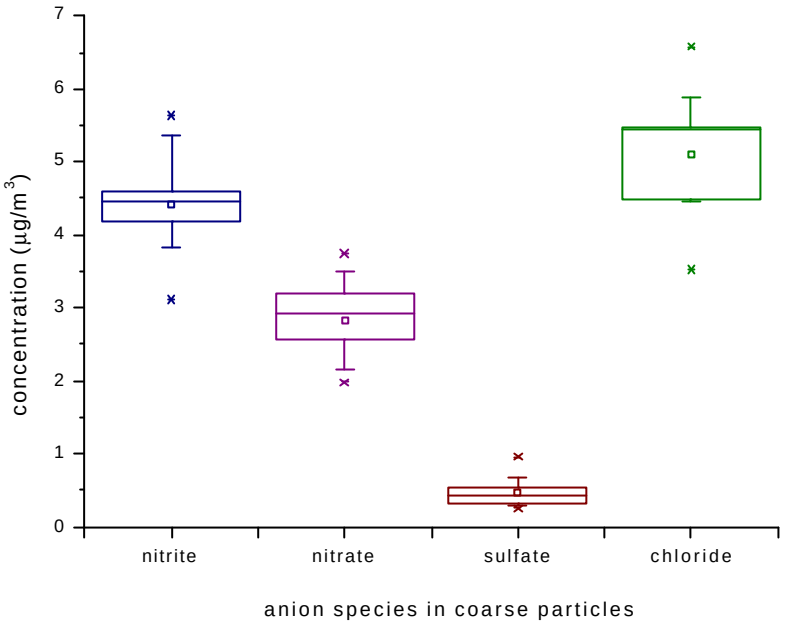

Figure 4.1-15. Comparison of the distribution of anion species in coarse particles before school opening. The box plots indicate the minimum, 25th percentile, median, 75th percentile, maximum, average and ±S.D. values (n = 8).

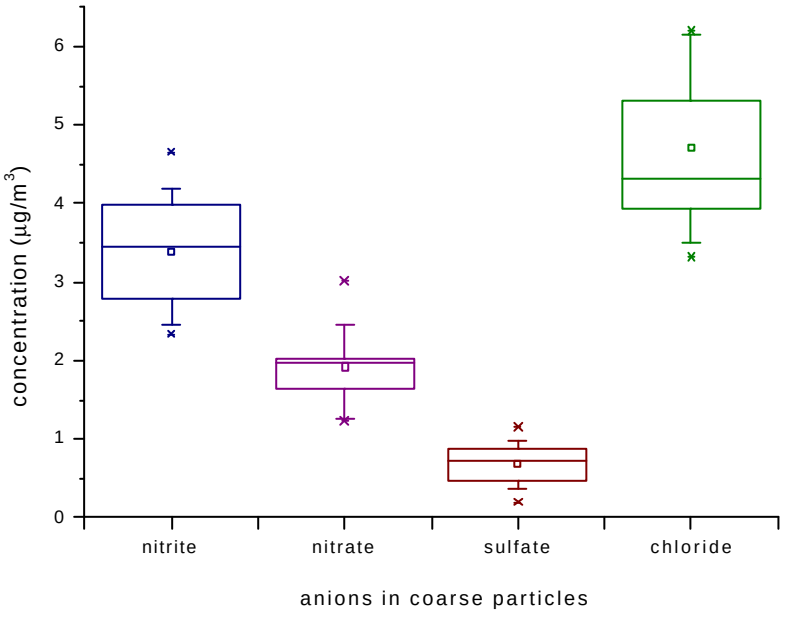

Figure 4.1-16. Comparison of the distribution of anion species in coarse particle after school opening. The box plots indicate the minimum, 25th percentile, median, 75th percentile, maximum, average and ±S.D. values (n = 13).

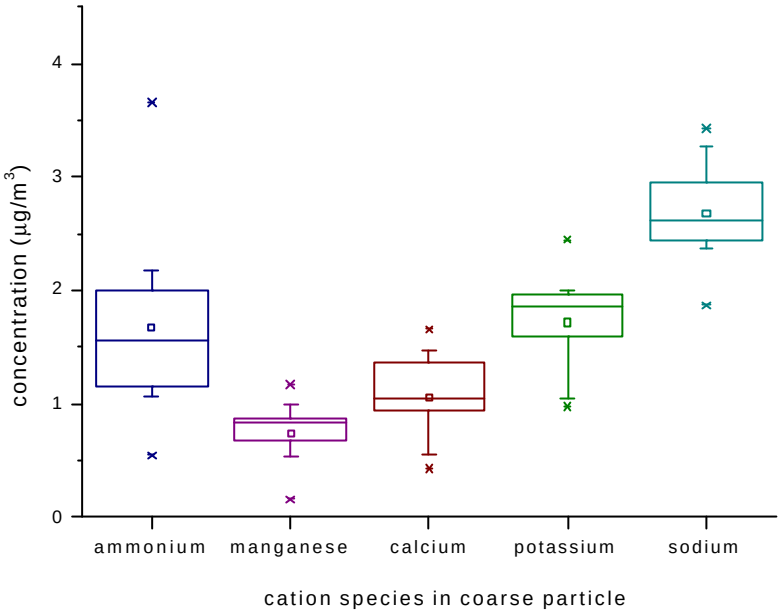

Figure 4.1-17. Comparison of the distribution of cation species in coarse particle before school opening. The box plots indicate the minimum, 25th percentile, median, 75th percentile, maximum, average and ±S.D. values (n = 8).

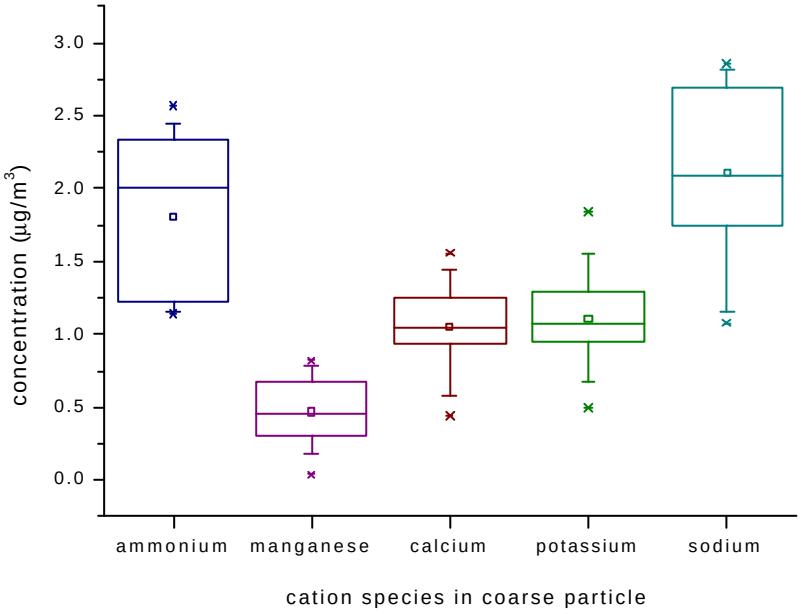

Figure 4.1-18. Comparison of the distribution of cation species in coarse particle after school opening. The box plots indicate the minimum, 25th percentile, median, 75th percentile, maximum, average and ±S.D. values (n = 13).

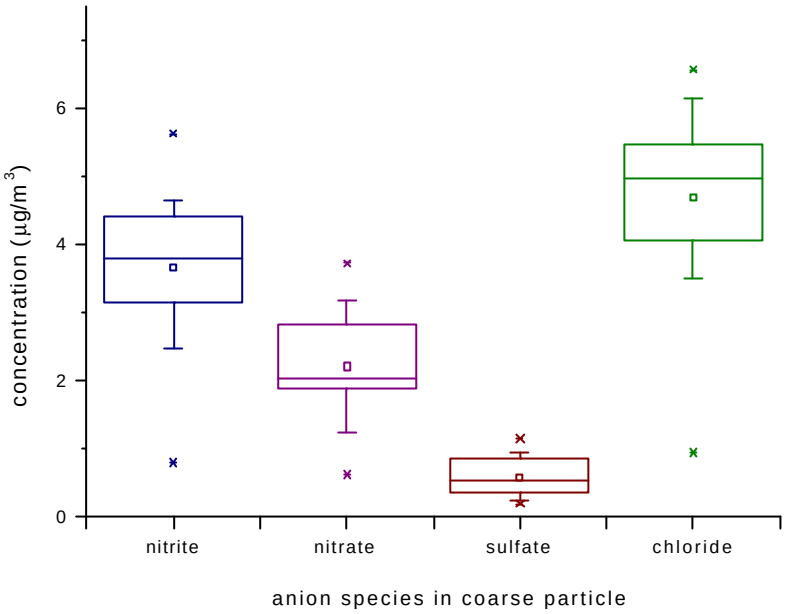

Figure 4.1-19. Comparison of the distribution of anion species in coarse particles across the whole sampling period. The box plots indicate the minimum, 25th percentile, median, 75th percentile, maximum, average and ±S.D. values (n = 21).

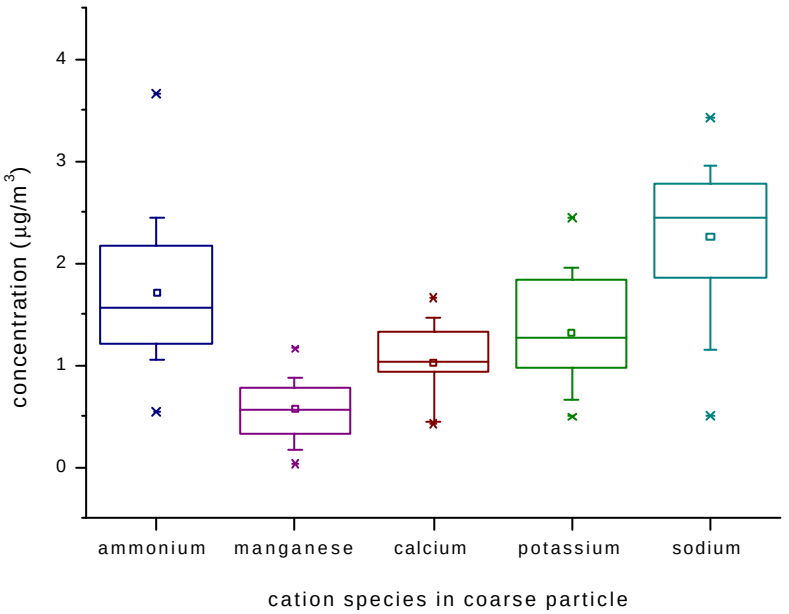

Figure 4.1-20. Comparison of the distribution of cation species in coarse particles across the whole sampling period. The box plots indicate the minimum, 25th percentile, median, 75th percentile, maximum, average and ±S.D. values (n = 21).

Concentrations of the anions (NO_2^-, NO_3^-. SO_4^{2-} and Cl^-) and cations (NH_4^+, Mg^{2+}, Ca^{2+}, K^+ and Na^+) in fine particles were displayed in Figure 4.1-15 to 4.1-20. Average concentrations of NO_2^-, NO_3^-. SO_4^{2-} and Cl^- in coarse particle were 4.42, 2.83, 0.48 and 5.10 μg/m^3 before school opening, respectively; and were 3.39, 1.92, 0.69 and 4.71 μg/m^3 after school opening, respectively. The average concentrations of NH_4^+, Mg^{2+}, Ca^{2+}, K^+ and Na^+ in fine particle were 1.68, 0.75, 1.05, 1.72 and 2.69 μg/m^3 before school opening, respectively; and were 1.80, 0.47, 1.05, 1.11 and 2.11 μg/m^3 after school opening, respectively. Average concentrations of NO_2^-, NO_3^-. SO_4^{2-}, Cl^-, NH_4^+, Mg^{2+}, Ca^{2+}, K^+ and Na^+ were 3.78, 2.27, 0.61, 4.86, 1.76, 0.58, 1.05, 1.34 and 2.33 μg/m^3 across the whole sampling period, respectively.

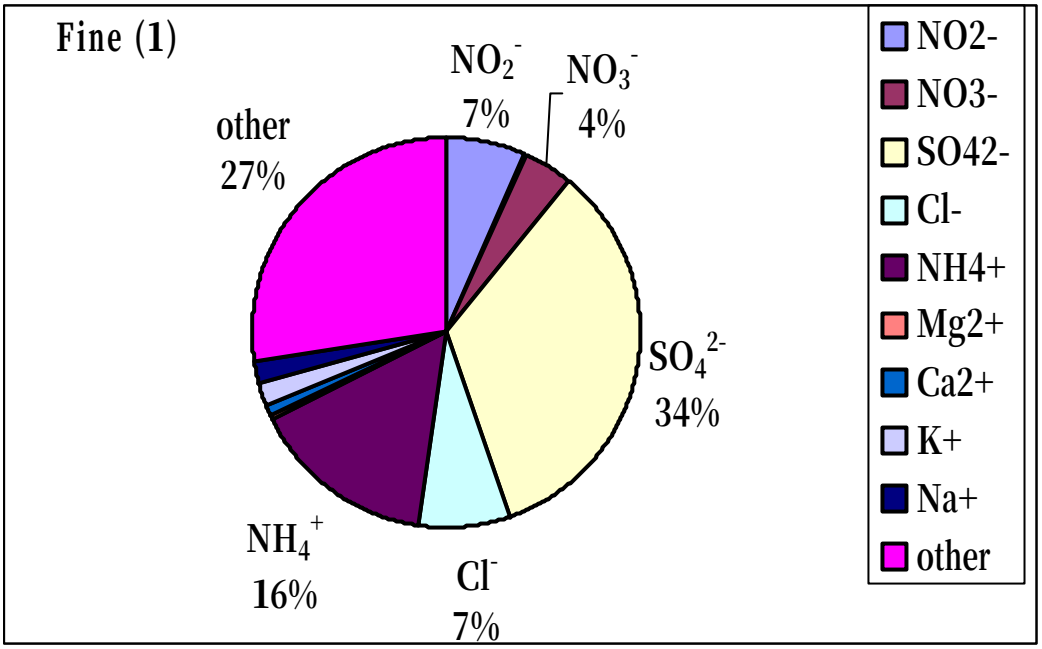

Figure 4.1-21. The chemical composition of fine particle before school opening. The percentages are based on mass concentration fraction (μg/m^3). (1) : before school opening at HKIT sampling site.

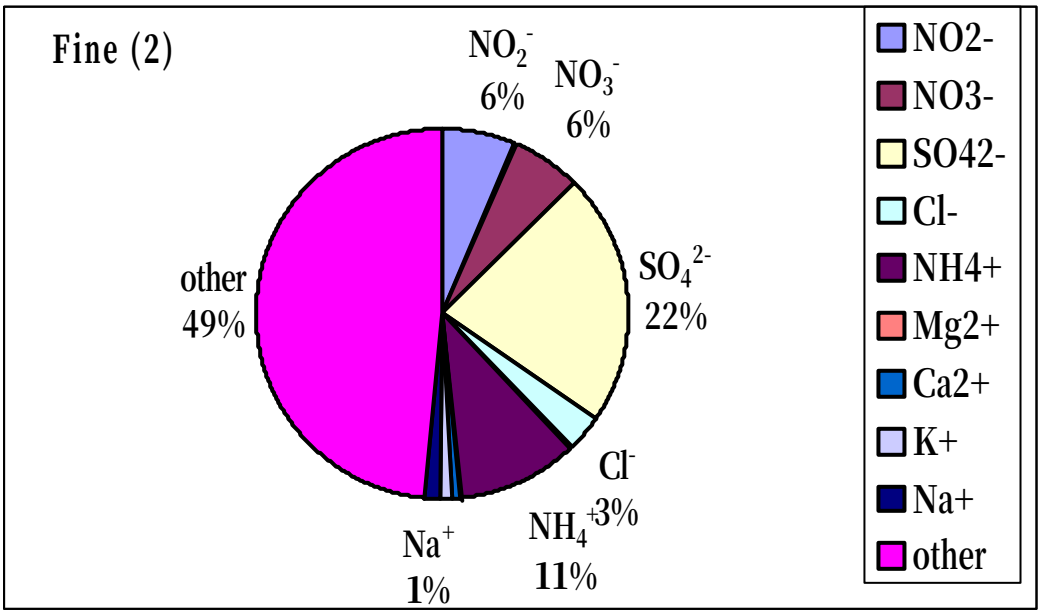

Figure 4.1-22. The chemical composition of fine particle after school opening. The percentages are based on mass concentration fraction (μg/m^3). (2) : after school opening at HKIT sampling site.

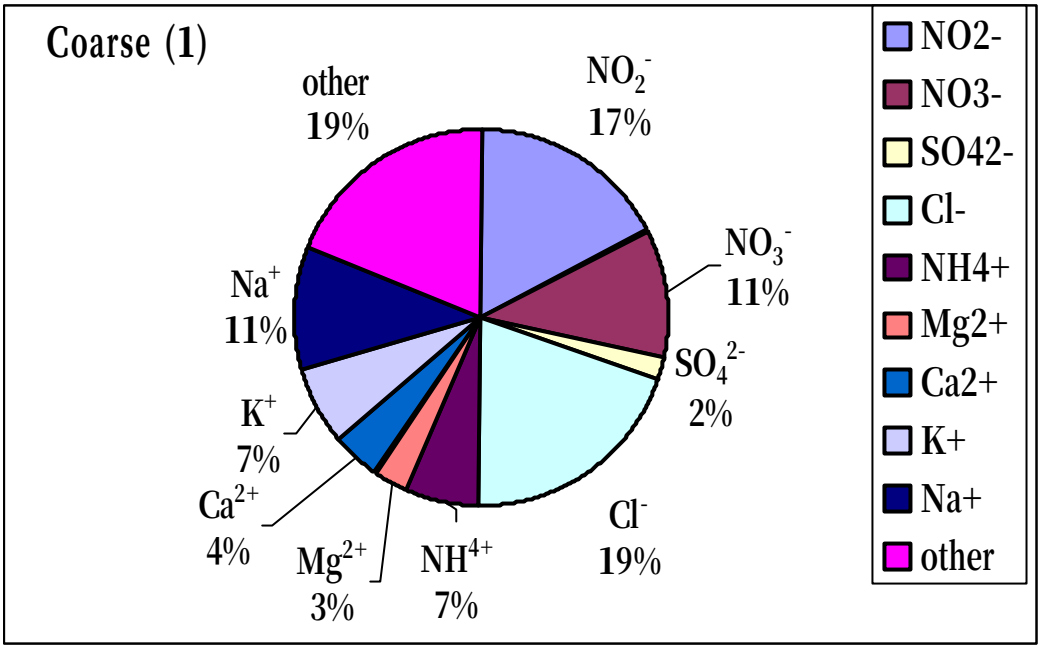

Figure 4.1.23. The chemical composition of coarse particle before school opening. The percentages are based on mass concentration fraction (μg/m^3). (1) : before school opening at HKIT sampling site.

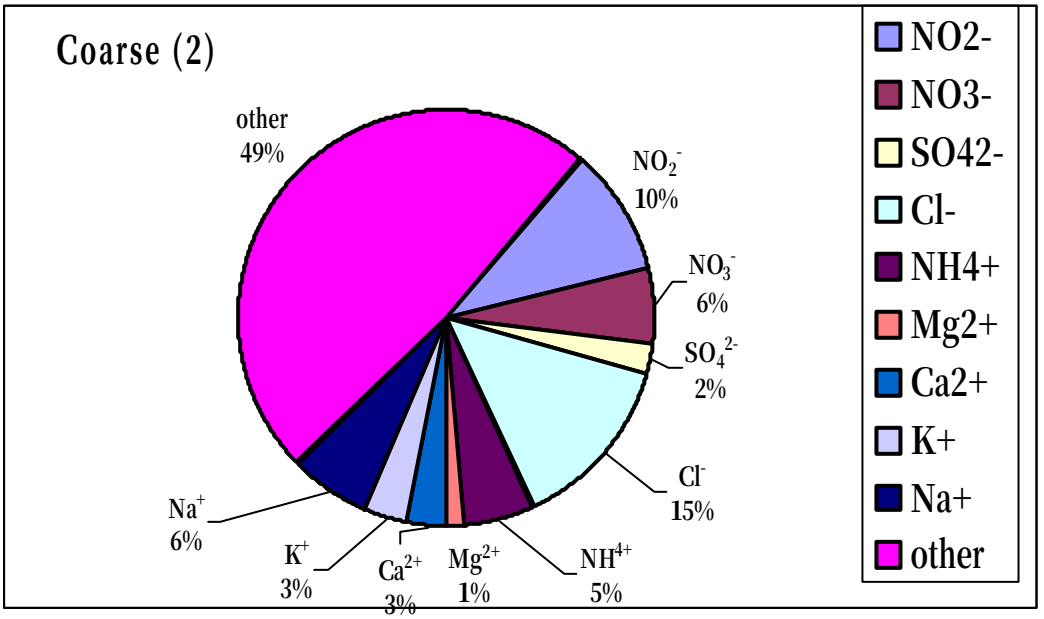

Figure 4.1-24. The chemical composition of coarse particle after school opening. The percentages are based on mass concentration fraction (μg/m^3). (2) : after school opening at HKIT sampling site.

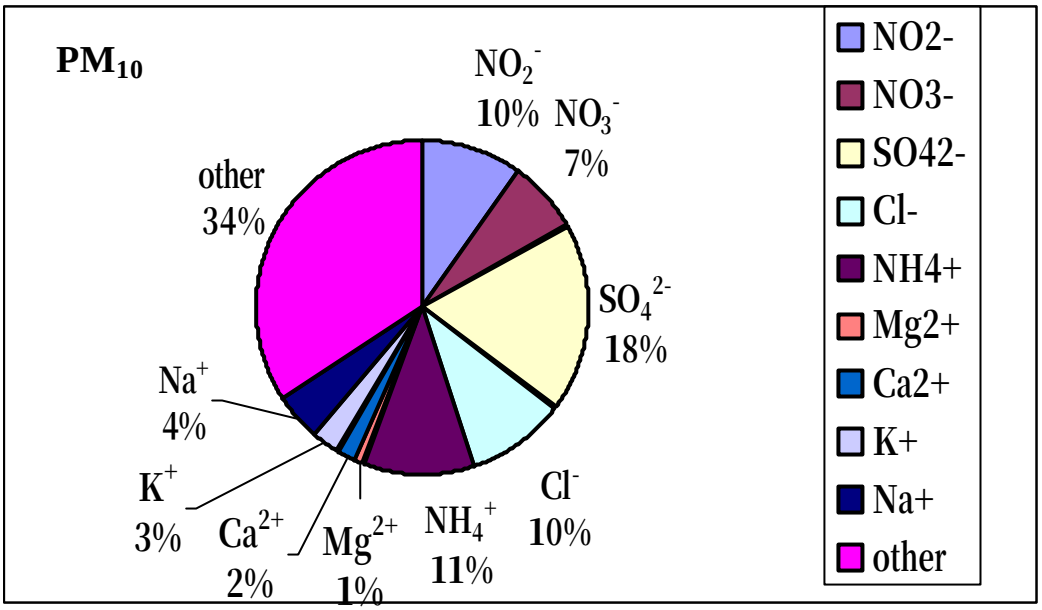

Figure 4.1-25. The chemical composition of PM_{10} across the whole sampling period. The percentages are based on mass concentration fraction (μg/m^3).

Figures 4.1-21 and 4.1-22 showed the chemical composition of fine particle before and after school opening. Sulfate was obviously the major inorganic component of fine particle, both before and after school opening the sulfate fraction exceed twenty percent. The fraction of sulfate after school opening was smaller than that before school opening. Ammonium also occupied a large fraction of the fine particle mass. The fraction of ammonium also decreased after school opening. The metal elements of Mg, Ca, K and Na occupied few fractions of fine particle mass. The rest of other terms occupied a largest fractions in the fine particles mass mode before and after school opening (27 % and 49 %, respectively) at HKIT sampling sites. The terms could be composed of EC, OC, Si, Al, Fe, Mn, and water. Similar results can also obtain in the previous study (Yuan *et al.*, 1999; Chen, 2000).

Figures 4.1-23 and 4.1-24 showed the chemical composition of coarse particle before and after school opening. The fraction of sulfate and ammonium

in coarse particle mode were much smaller than it was in the fine particle mode. Nitrite and nitrate fractions in coarse mode were larger than it were in the fine particle mode. The nitrite and nitrate fractions decreased after school opening. Metal elements (Mg, Ca, K and Na) fractions in coarse particle mode were larger than that in fine particle mode. All metal element fractions decreased after school opening in this study.

It was remarkable that the "other" term fraction increased greatly after school opening. This phenomena appeared both in the fine and coarse particles, implying that increased human activities after school opening made a quite change of the chemical compositions of suspended particles.

Figure 4.1-25 showed the average chemical compositions of PM_{10}. The major inorganic soluble anions (sulfate, nitrate, nitrite and chloride) occupied a fraction of 45 % of the total PM_{10} mass. And the cations measured in this study (Mg^{2+}, Ca^{2+}, K^{+}, Na^{+} and NH_4^{+}) occupied a fraction of 23 % of the total PM_{10} mass.

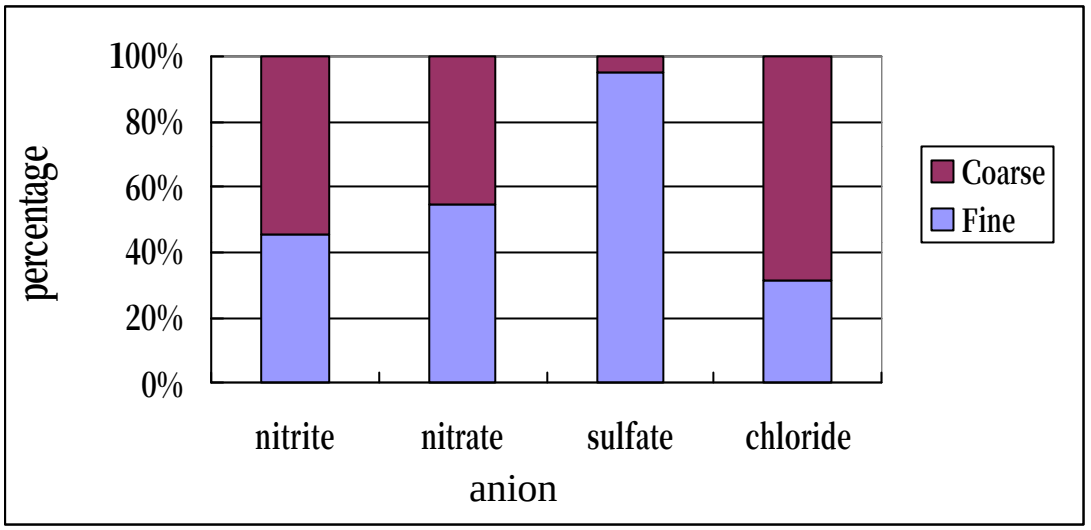

Figure 4.1-26. The distribution of nitrite, nitrate, sulfate and chloride in fine and coarse particles.

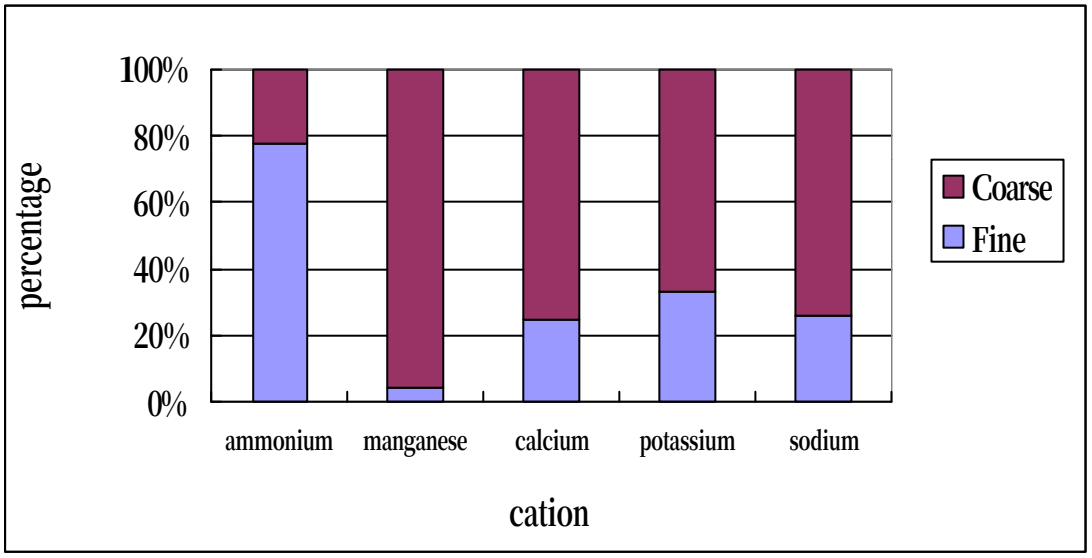

Figure 4.1-27. The distribution of ammonium, magnesium, calcium, potassium and sodium in fine and coarse particles.

Figures 4.1-26 and 4.1-27 displayed the distribution of anions and cations in the fine and coarse particles mode. Sulfate and ammonium were distributed over fine particles mainly. Nitrite and nitrate were distributed almost equally in fine and coarse particles. Chloride and metal elements were distributed mainly in coarse particles.

Table 4.1-2. Correlation matrix of fine particulate chemical species at HKIT sampling site.

Fine	NO_2^-	NO_3^-	SO_4^{2-}	Cl^-	NH_4^+	Mg^{2+}	Ca^{2+}	K^+	Na^+
NO_2^-	1.0000								
NO_3^-	0.0120	1.0000							
SO_4^{2-}	0.0056	0.1055	1.0000						
Cl^-	0.0087	0.1055	0.0987	1.0000					
NH_4^+	0.1553	0.0626	0.8451	0.1298	1.0000				
Mg^{2+}	0.1228	0.0006	0.1528	0.4502	0.0711	1.0000			
Ca^{2+}	0.0357	0.0877	0.1697	0.0867	0.0699	0.0693	1.0000		
K^+	0.0268	0.0877	0.1528	0.0387	0.1975	0.0107	0.0370	1.0000	
Na^+	0.0696	0.0212	0.1161	0.0867	0.1259	0.4064	0.0180	0.0071	1.0000

Table 4.1-3. Correlation matrix of coarse particulate chemical species at HKIT sampling site.

Coarse	NO_2^-	NO_3^-	SO_4^{2-}	Cl^-	NH_4^+	Mg^{2+}	Ca^{2+}	K^+	Na^+
NO_2^-	1.0000								
NO_3^-	0.1137	1.0000							
SO_4^{2-}	0.0001	0.0106	1.0000						
Cl^-	0.0881	0.0002	0.0921	1.0000					
NH_4^+	0.0082	0.0120	0.0095	0.0084	1.0000				
Mg^{2+}	0.0349	0.0574	0.0176	0.0636	0.0014	1.0000			
Ca^{2+}	0.0076	0.0934	0.0884	0.1827	0.0693	0.0015	1.0000		
K^+	0.2164	0.0434	0.1200	0.0342	0.0301	0.1645	0.0086	1.0000	
Na^+	0.1864	0.0764	0.0180	0.7961	0.0208	0.1040	0.0086	0.0644	1.0000

Table 4.1-2 and 4.1-3 displayed the correlation between chemical species measured in this study of fine and coarse particles at HKIT sampling site. For the chemical species of fine particles, the concentrations of SO_4^{2-} have high R-square value of 0.845 with NH_4^+, which means SO_4^{2-} concentration is highly related to NH_4^+. There are moderately correlation between concentrations of Cl^-

and Mg^{2+} (R-square = 0.450), the concentrations of Mg^{2+} and Na^{+} also have moderately correlation (R-square = 0.406). For the chemical species of coarse particles, the concentrations of Cl^{-} have high correlation (R-square = 0.796) with Na^{+}. The high correlation between Cl^{-} and Na^{+} indicate that sea-salt aerosols were the major contributor of coarse particle mass. The Mg concentrations have a moderate correlation with Cl^{-} and Na^{+} concentrations, indicating that some Mg^{2+} measured at Sha-Lu were provided by sea-salt aerosols.

Table 4.1-4. Ratios of anions and cations of fine and coarse particles at HKIT sampling site.

Ratios	Fine	Coarse
NH_4^+ / SO_4^{2-}	2.539	19.449
Na^+ / Cl^-	1.590	0.732
$NH_4^+ / (SO_4^{2-}) + (NO_3^-) + (NO_2^-) + (Cl^-)$	1.109	0.018
$(NH_4^+) + (Na^+) + (K^+) + (Mg^{2+}) + (Ca^{2+}) / (SO_4^{2-}) + (NO_3^-) + (NO_2^-) + (Cl^-)$	1.089	0.550

Table 4.1-4 shows the ratios of cations to anions measured at HKIT sampling site. All ratios displayed in Table 4.1-4 are based on average concentrations in the whole sampling period. These ratios provide an information of the configurations of inorganic chemical species for fine and coarse particles.

Ammonium sulfate is the most stable inorganic salt in aerosols. There are several configurations of ammonium sulfate existing in solid aerosols phase, such as $(NH_4)_2SO_4$ (NH_4^+/SO_4^{2-} = 2), $(NH_4)_3H(SO_4)_2$ (NH_4^+/SO_4^{2-} = 1.5) and NH_4HSO_4 (NH_4^+/SO_4^{2-} = 1). Figure 4.1-28 shows that all ratios of ammonium to

sulfate in this study (21 data points) are located between 1 to 2. In Table 4.1-4, the average ratio of ammonium to sulfate was 2.539 in fine particles, suggest that the major configuration of ammonium sulfate should be $(NH_4)_2SO_4$. The value of $(NH_4^+) / (SO_4^{2-} + NO_3^- + NO_2^- + Cl^-)$ was 1.109, which is very close to 1, proves that the surplus NH_4^+ are associated with NO_3^-, NO_2^- and Cl^-. The value of $(NH_4^+) / (SO_4^{2-} + NO_3^- + NO_2^- + Cl^-)$ is 0.018 in the coarse particles mode, which means that the NH_4^+ is not the major cations associate with SO_4^{2-}, NO_3^-, NO_2^- and Cl^- in coarse particle. Because of the quite low concentrations of sulfate and ammonium in coarse particle, the major inorganic salts in coarse particles should not be ammonium sulfate, the salts of nitrite, nitrate and chloride should be the major inorganic salts in coarse particles instead. When all cations and anions are taken into account, the ratios of $(NH_4^+ + Na^+ + K^+ + Mg^{2+} + Ca^{2+})/(SO_4^{2-} + NO_3^- + NO_2^- + Cl^-)$ in fine and coarse particle are 1.089 and 0.550, respectively. These results show that the cations and anions in fine particles are at equilibrium, but the cations are lack in coarse particles. The reasonable explanation is that some cations which exist in coarse particle are still not detected in this study, such as Fe, Mn and Al.

The ratio of Na^+ to Cl^- in sea-salt aerosols is close to 1. And the ratios of Na^+ to Cl^- is 0.732 in coarse particles. The results indicating that sea-salt aerosols occupy an important fraction of coarse particle mass.

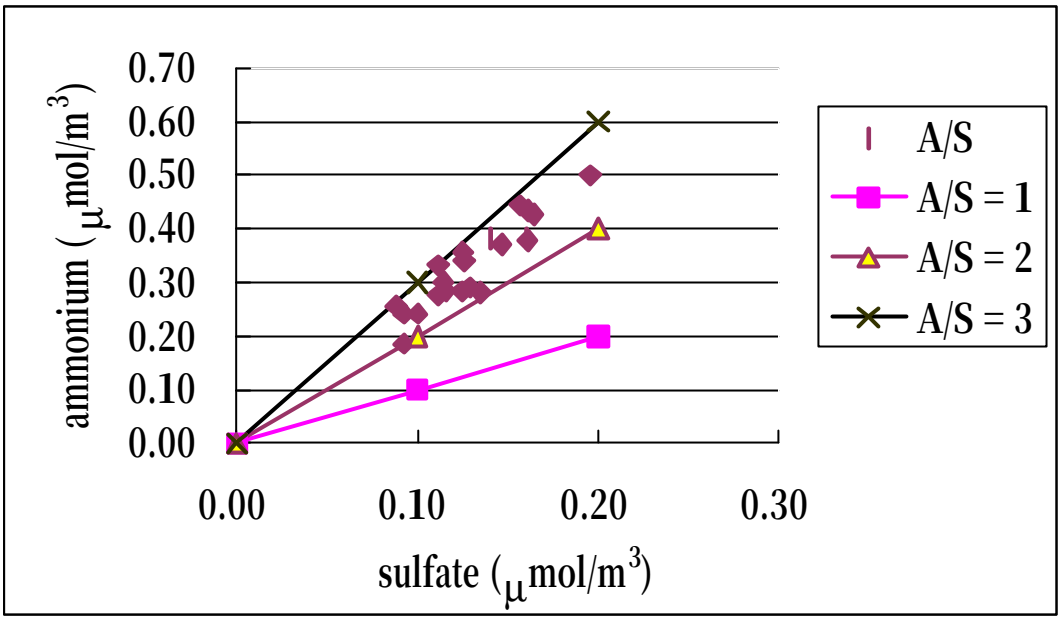

Figure 4.1-28. The distribution of ratios of ammonium to sulfate in the fine particles mode (21 data points) measured at HKIT sampling site. A/S : (ammonium concentration / sulfate concentration)

4.2 Results of CCROB

4.2.1 The fine and coarse particles at CCROB.

Table 4.2-1 The concentrations of fine and coarse particles measured at CCROB. (Unit : μg/m^3)

Date	No.	Fine	Coarse	Fine/Coarse	Fine/PM_{10}
9/10-9/11/1999	9	27.17	16.40	1.66	0.62
9/20-9/21/1999	10	30.61	18.63	1.64	0.62
9/28-9/29/1999	11	41.34	17.45	2.37	0.70
10/3-10/4/1999	12	32.72	14.79	2.21	0.69
10/15-10/16/1999	13	44.84	20.85	2.15	0.68
10/25-10/26/1999	14	53.86	24.16	2.23	0.69
10/28-10/29/1999	15	44.51	22.12	2.01	0.67
11/1-11/2/1999	16	58.16	27.59	2.11	0.68
11/10-11/11/1999	17	63.59	32.94	1.93	0.66
11/21-11/22/1999	18	62.20	37.41	1.66	0.62
12/15-12/16/1999	19	60.65	32.32	1.88	0.65
12/18-12/29/1999	20	56.86	21.16	2.69	0.73
1/9-1/10/2000	21	49.34	23.18	2.13	0.68
Average		48.14	23.77	2.05	0.67
RSD		26 %	14 %	30 %	3 %

※ RSD : standard deviation (n = 13).

For the sampling of fine ($PM_{2.5}$) and coarse ($PM_{2.5-10}$) particles, the average concentration of fine and coarse particles were 48.14 and 23.77 μg/m^3, respectively. The concentration of fine particles is 2.05 times to coarse particles in average. The variations of fine particles concentration (RSD = 26 %) were higher than coarse particles (RSD = 14 %) concentration. Fine particle fraction in PM_{10} varied from 0.62 to 0.73, and the average value is 0.67.

4.2.1 The gas species in CCROB

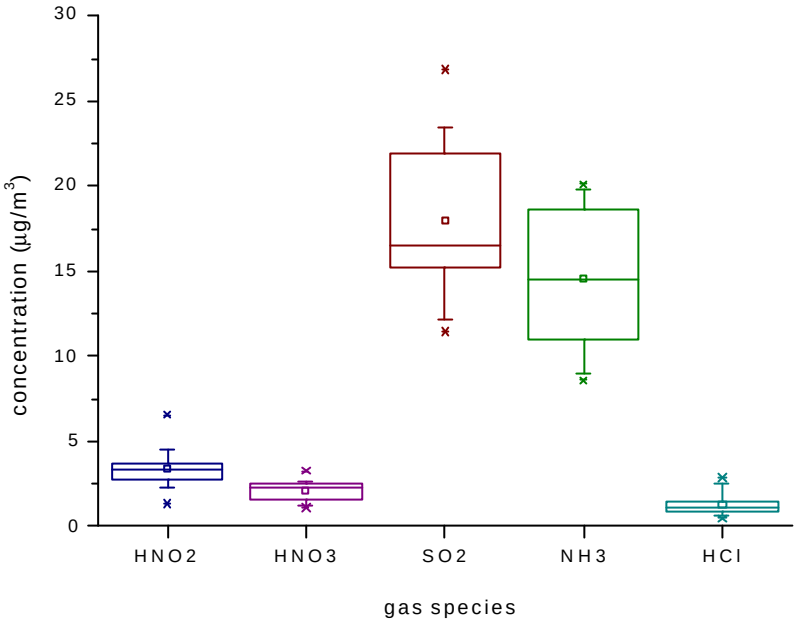

Figure 4.2-1. Comparison of the distribution of gas species. The box plots indicate the minimum, 25th percentile, median, 75th percentile, maximum, average and ± S.D. values (n = 13).

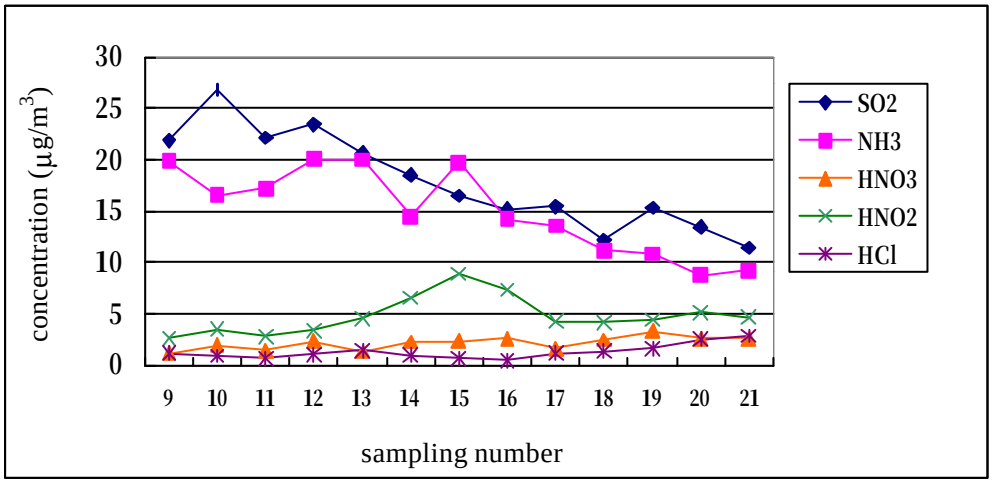

Figure 4.2-2. The concentration of gas phase of HNO_2, HNO_3, SO_2, NH_3 and HCl measured at CCROB site across the whole sampling period (μg/m^3).

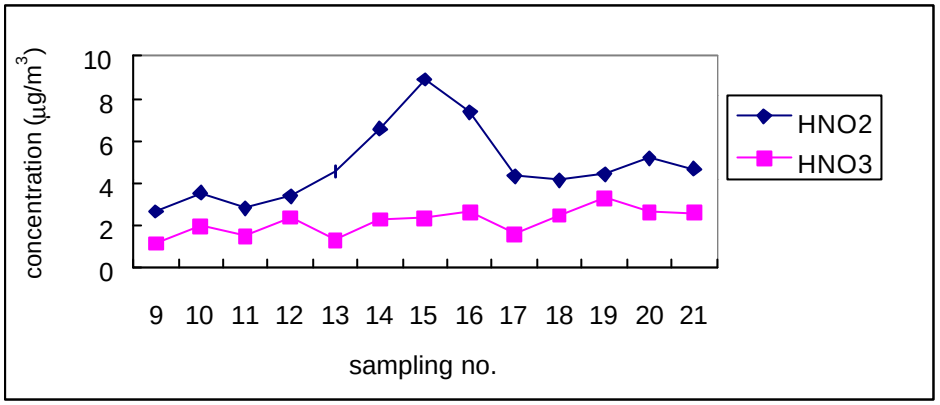

Figure 4.2-3. The variation of acidic gas HNO_2 and HNO_3 concentration measured at CCROB site across the whole sampling period (μg/m^3).

The average concentrations of HNO_2, HNO_3, SO_2, NH_3, HCl and NH_3 measured at CCROB site were 3.41, 2.14, 17.94, 14.59 and 1.29 μg/m^3, respectively. The standard deviations were 1.25, 0.63, 4.74, 4.14 and 0.71, respectively. Similar to the situation in HKIT site, the SO_2 concentrations decreased and were lower in winter. From June to October (Sampling No. 1 to 14), the concentration of ammonia changed between 15 and 20 μg/m^3, but decreased sharply after Sampling No. 15. A possible reason for the variation trend of ammonia was the decrease agricultural activities around the fall season in the nearby areas. The concentrations of HCl were apparently low compared to other gas species measured in CCROB. Figure 4.2-3 showed the variation trend of concentrations of HNO_2 and HNO_3. The average concentration of HNO_2 in winter was higher than it was in autumn, similarly to the results measured in HKIT site. The HNO_3 concentrations in CCROB showed no seasonal variation.

4.2.3 The inorganic components in particulate phase in CCROB.

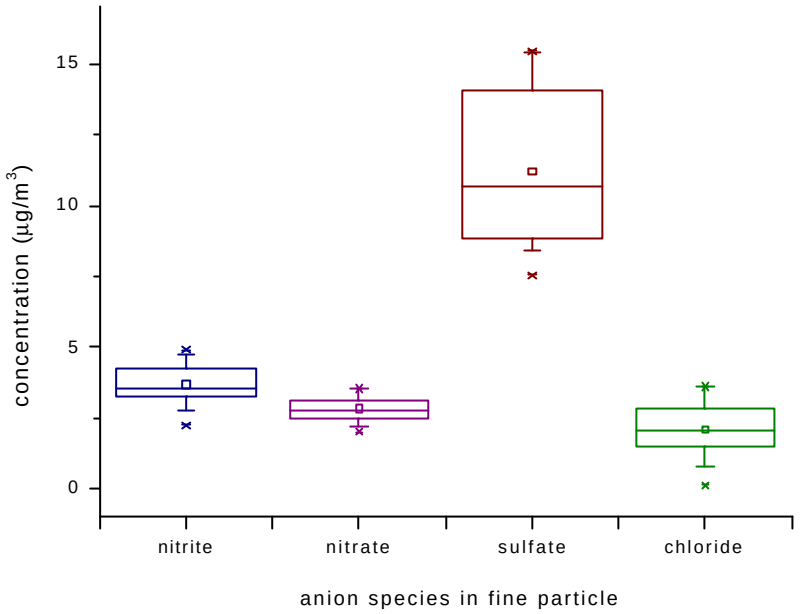

Figure 4.2-4. Comparison of the distribution of anion species in fine particles. The box plots indicate the minimum, 25th percentile, median, 75th percentile, maximum, average and ± S.D. values (n = 13).

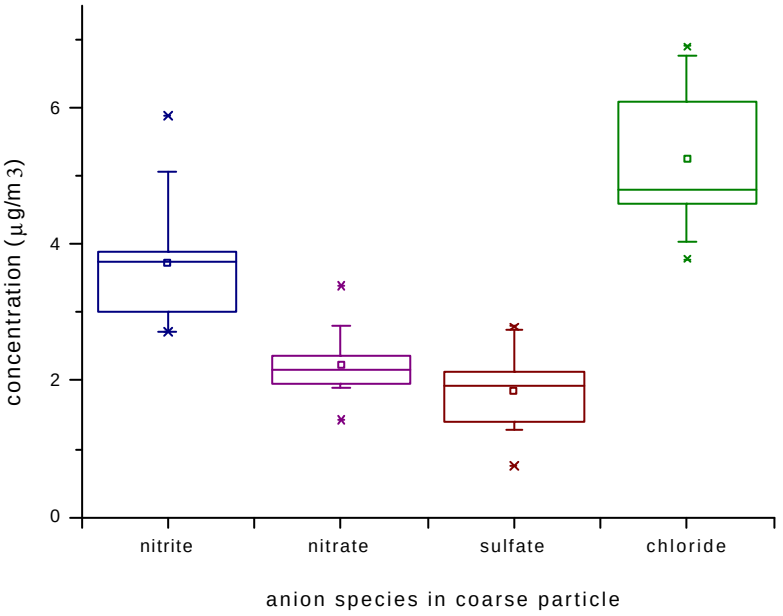

Figure 4.2-5. Comparison of the distribution of anion species in coarse particles. The box plots indicate the minimum, 25th percentile, median, 75th percentile, maximum, average and ± S.D. values (n = 13).

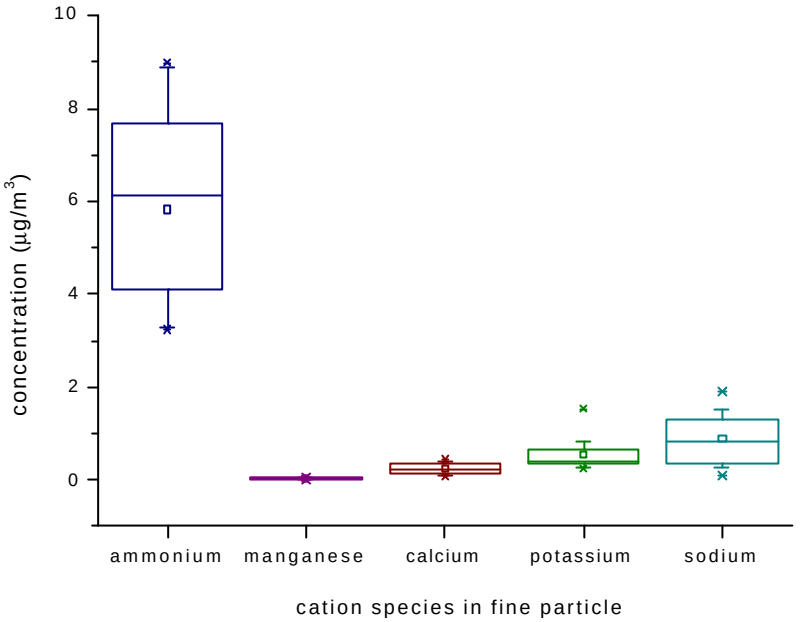

Figure 4.2-6. Comparison of the distribution of cation species in fine particles. The box plots indicate the minimum, 25th percentile, median, 75th percentile, maximum, average and ± S.D. values (n = 13).

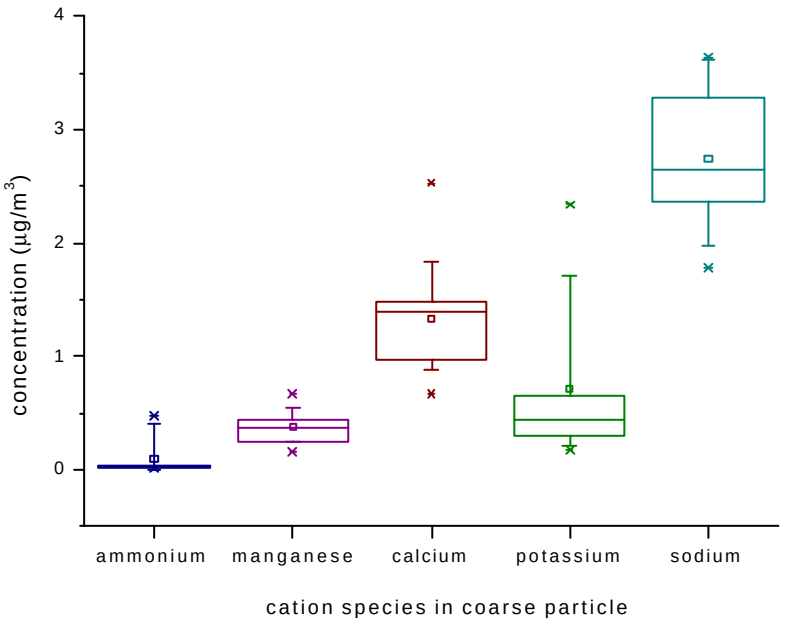

Figure 4.2-7. Comparison of the distribution of cation species in coarse particles. The box plots indicate the minimum, 25th percentile, median, 75th percentile, maximum, average and ± S.D. values (n = 13).

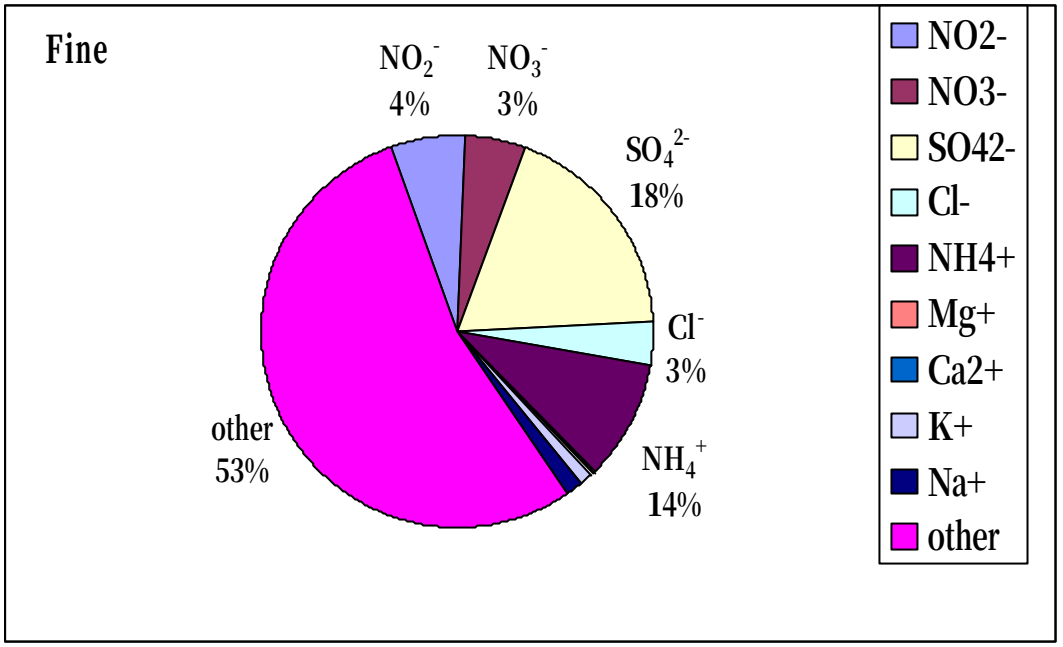

Figure 4.2-8. The chemical composition of fine particle at CCROB. The percentages are based on mass concentration fraction (μg/m^3).

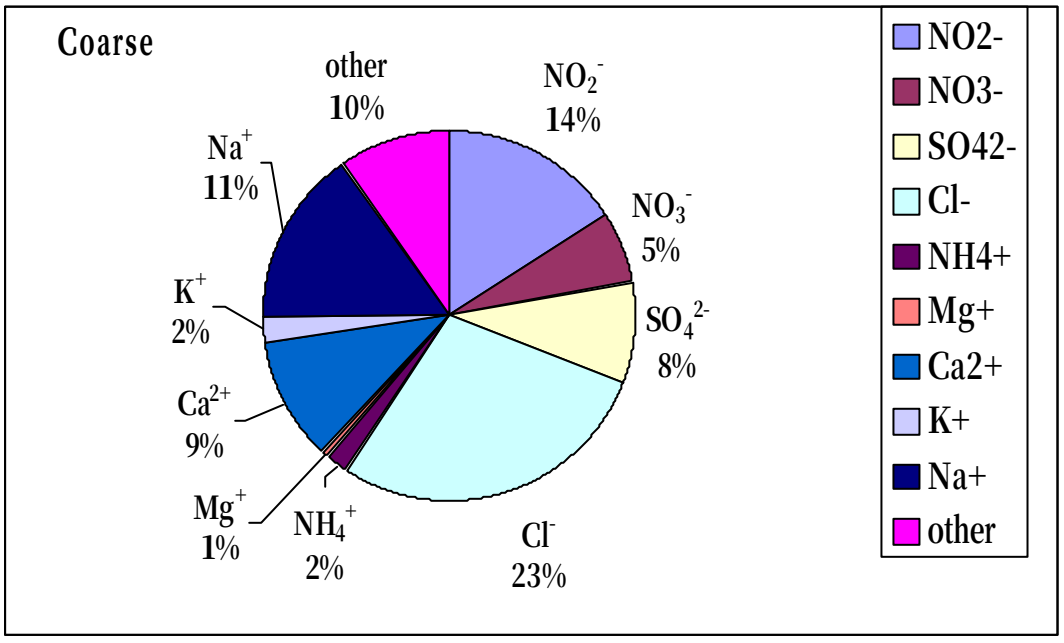

Figure 4.2-9. The chemical composition of coarse particle at CCROB. The percentages are based on mass concentration (μg/m^3) fraction.

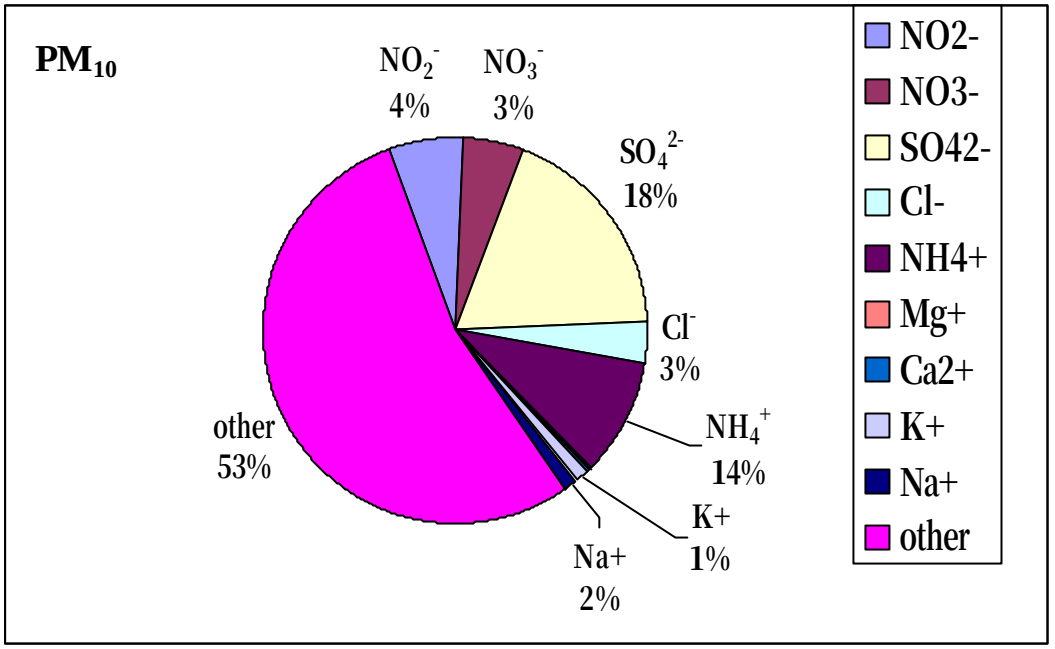

Figure 4.2-10. The chemical composition of PM_{10} at CCROB. The percentages are based on mass concentration (μg/m^3) fraction.

Concentrations of the anions (NO_2^-, NO_3^-. SO_4^{2-} and Cl^-) and cations (NH_4^+, Mg^{2+}, Ca^{2+}, K^+ and Na^+) in fine particles and coarse particles in CCROB were displayed in Figure 4.2-4 to Figure 4.2-7. Average concentrations of NO_2^-, NO_3^-. SO_4^{2-} and Cl^- in fine particle were 3.69, 2.84, 11.18, 2.12 μg/m^3, respectively; and were 3.74, 1.57, 1.38, 3.94 μg/m^3 in coarse particles, respectively. Average concentrations of NH_4^+, Mg^{2+}, Ca^{2+}, K^+ and Na^+ were 5.83, 0.03, 0.24, 0.54, 0.89 μg/m^3 in fine particles, respectively; and were 0.10, 0.28, 0.95, 0.61, 2.08 μg/m^3 in coarse particles, respectively.

Figures 4.2-8 to 4.2-9 show the chemical compositions of fine and coarse particles. In fine particles, the sulfate and ammonium are the major inorganic components, the fraction occupied by sulfate and ammonium are 18% and 14%, respectively. But in coarse particles, sulfate and ammonium occupy a very small fraction of 8% and 2%, respectively. The fractions of metal elements such as

magnesium, calcium, potassium and sodium in the fine particles are very small. However, metal elements occupy a larger fraction in coarse particles than that in fine particles, the fractions of magnesium, calcium, potassium and sodium are 1 %, 9 %, 2 % and 11 %, respectively. The rest of other terms occupied a largest fractions in the fine particles mass mode before and after school opening (53 % and 11 %, respectively) at HKIT sampling sites. The terms could be composed of EC, OC, Si, Al, Fe, Mn, and water. Similar results can also obtain in the previous study (Yuan *et al.*, 1999; Chen, 2000).

Figure 4.2-10 showed the chemical compositions of PM_{10} at CCROB across the whole sampling period. Sulfate was obviously the major inorganic soluble components of PM_{10}, and the ammonium was the major cation which could neutralize sulfate in PM_{10}. Metal elements measured in this study (Mg, Ca, K and Na) occupied very low fraction in PM_{10} mass. The reason for the extra low fraction of metal elements in PM_{10} was that more than half of PM_{10} were fine particles, and the metal elements concentrations distributed in fine particles were very low in this study.

Previous measurements (Tsai *et al.*, 1997) in central Taiwan showed that sulfate concentrations were generally higher than nitrate concentrations ine particles, sulfate was the major inorganic component of suspended particles in central Taiwan. Ahmed's study (Ahmed *et al.*, 1995) indicated that sodium, magnesium and chloride arises from marine sources, calcium is mainly soil derived. The major source of nitrate is the atmospheric oxidation of NO_x to HNO_3, and its total or partial neutralization by natural atmospheric ammonia. The distribution of semivolatile compounds (such as nitrate and chloride) between the gas and particle phases varies with the amount of available particulate matter on which they can accumulate (McMurry, 2000).

Table 4.2-2 Comparison of the chemical compositions of $PM_{2.5}$ and PM_{10} with other measurements. (Unit :%)

Species / Location	Type	SO_4^{2-}	NO_3^-	Cl^-	NH_4^+	Mg^{2+}	Ca^{2+}	K^+	Na^+	Other
Lu-Gang[1]	PM_{10}	23	19	5	5	---	1	---	16	47
Shen-Gang[1]	PM_{10}	27	17	6	5	--	1	---	0	44
Wu-Qi[1]	PM_{10}	26	18	6	3	---	1	---	1	45
Zhang-Hua[1]	PM_{10}	23	19	6	3	---	1	---	1	47
Cao-Tun[1]	PM_{10}	21	21	3	4	---	1	---	1	49
Qian-Zhen[2]	$PM_{2.5}$	21	10	2	8	0	1	1	1	18
	$PM_{2.5-10}$	6	10	4	0	1	4	1	3	48
CCROB[3]	$PM_{2.5}$	18	3	3	14	0	1	1	2	53
	$PM_{2.5-10}$	8	5	23	2	1	9	2	11	10
	PM_{10}	18	3	3	14	0	0	1	2	53
HKIT[3]	$PM_{2.5}$	22	6	3	11	0	1	1	1	48
	$PM_{2.5-10}$	2	6	14	5	1	3	3	6	48
	PM_{10}	22	6	3	11	1	2	3	1	34

[1]: Central Taiwan (Cheng *et al.*, 1999); [2]: Gao-Xiong (Yuan *et al.*, 1999); [3]: Sha-Lu, Taichung (Chen 2000).

Table 4.2-2 displayed the comparison of the chemical composition of $PM_{2.5}$, $PM_{2.5-10}$ and PM_{10} with other studies. The results reflect the SO_4^{2-} and NH_4^+ are dominant in fine particle mode for Qian-Zhen, CCROB and HKIT. However, Cl^-, Mg^{2+}, Ca^{2+}, K^+ and Na^+ were distributed in $PM_{2.5-10}$ mainly for Qian-Zhen, CCROB and HKIT. The NO_2^- and NO_3^- were distributed evenly in $PM_{2.5}$ and $PM_{2.5-10}$ for Qian-Zhen, CCROB and HKIT.

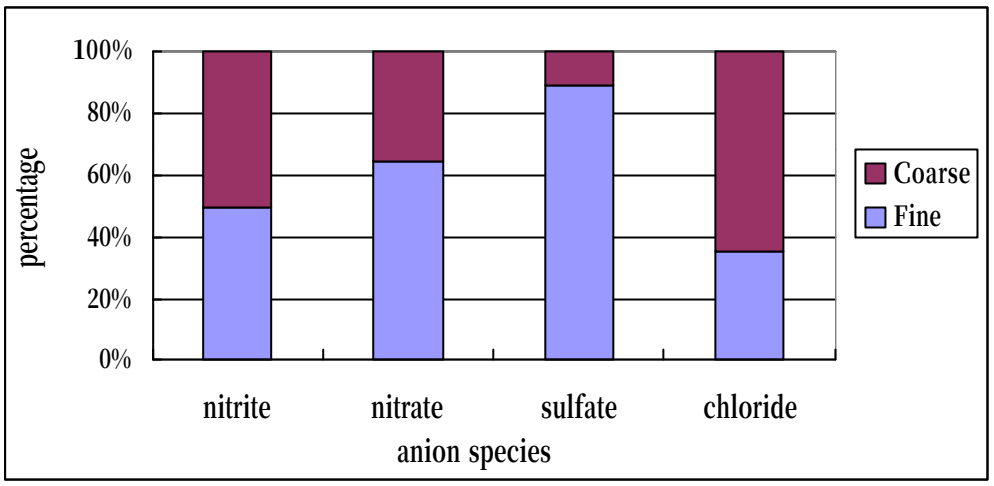

Figure 4.2-11. The distribution of nitrite, nitrate, sulfate and chloride in fine and coarse particles.

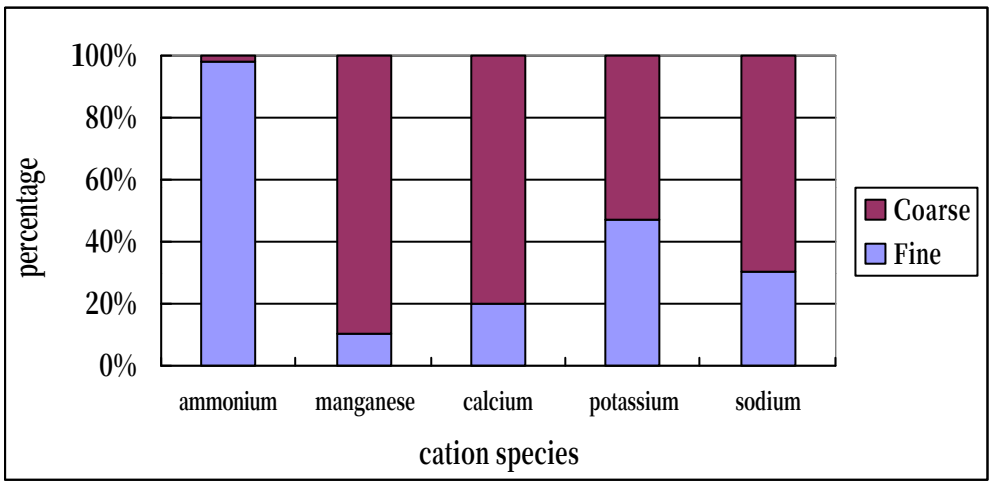

Figure 4.2-12. The distribution of ammonium, magnesium, calcium, potassium and sodium in fine and coarse particles.

Figures 4.2-11 and 4.2-12 displayed the distribution of anions and cations in fine and coarse particles. Sulfate was distributed over fine particles mainly. Ammonium was almost completely distributed over fine particles in CCROB. Nitrite was distributed equally in both fine and coarse particles. Concentration of nitrate distributed in fine particles was a little higher than it was in coarse

particles. Chloride and metal elements were distributed mainly in coarse particles.

Table 4.2-2. Correlation matrix of fine particulate chemical species at CCROB sampling site.

Fine	NO_2^-	NO_3^-	SO_4^{2-}	Cl^-	NH_4^+	Mg^+	Ca^{2+}	K^+	Na^+
NO^{2-}	1.0000								
NO^{3-}	0.0973	1.0000							
SO_4^{2-}	0.0000	0.1212	1.0000						
Cl^-	0.0084	0.1369	0.1459	1.0000					
NH_4^+	0.0017	0.1239	0.8811	0.1338	1.0000				
Mg^+	0.0000	0.0012	0.1637	0.0005	0.0295	1.0000			
Ca^{2+}	0.3911	0.2578	0.0144	0.0019	0.0007	0.0254	1.0000		
K^+	0.1639	0.0037	0.1305	0.0053	0.1723	0.0827	0.0000	1.0000	
Na^+	0.0011	0.0031	0.1781	0.7716	0.1024	0.0886	0.0433	0.2811	1.0000

Table 4.2-3. Correlation matrix of coarse particulate chemical species at CCROB sampling site.

Coarse	NO_2^-	NO_3^-	SO_4^{2-}	Cl^-	NH_4^+	Mg^+	Ca^{2+}	K^+	Na^+
NO^{2-}	1.0000								
NO^{3-}	0.3838	1.0000							
SO_4^{2-}	0.0663	0.1397	1.0000						
Cl^-	0.3495	0.0083	0.0118	1.0000					
NH_4^+	0.0934	0.1730	0.0132	0.5060	1.0000				
Mg^+	0.1050	0.0223	0.1510	0.0269	0.3044	1.0000			
Ca^{2+}	0.0446	0.0423	0.0058	0.1644	0.2594	0.1745	1.0000		
K^+	0.4532	0.1244	0.0058	0.1740	0.0021	0.0067	0.0007	1.0000	
Na^+	0.1512	0.0481	0.0118	0.8159	0.3380	0.0001	0.0754	0.2147	1.0000

Tables 4.2-2 and 4.2-3 display the correlation between chemical species measured in this study for fine and coarse particles at CCROB site. For the chemical species of fine particles, the concentrations of SO_4^{2-} have high r-square value of 0.881 with NH_4^+. There are moderately correlation between concentrations of Ca^{2+} and NO_2^- (R-square = 0.391). The concentrations of Ca^{2+} and NO_3^- also have slightly correlation (R-square = 0.258). For the chemical

species of coarse particles, the concentrations of Cl^- have high correlation (R-square = 0.816) with Na^+. A moderate correlation exist between NH_4^+ and Cl- with R-square = 0.506. The concentration of K and NO_2^- have moderately correlation (R-square = 0.453).

Table 4.2-13. Ratios of anions and cations of fine and coarse particles at CCROB site.

Ratios	Fine	Coarse
NH_4^+ / SO_4^{2-}	3.268	0.406
Na^+ / Cl^-	0.524	0.805
$NH_4^+ / (SO_4^{2-}) + (NO_3^-) + (NO_2^-) + (Cl^-)$	1.291	0.022
$(NH_4^+) + (Na^+) + (K^+) + (Mg^{2+}) + (Ca^{2+})/ (SO_4^{2-}) + (NO_3^-) + (NO_2^-) + (Cl^-)$	1.489	0.676

From Table 4.2-4, it shows that the ratios of ammonium to sulfate are 3.268 in fine particles, means that there are quite a few amounts of ammonium nitrite, ammonium nitrate or ammonium chloride exists in fine particle at CCROB. Figure 4.2-13 shows the more than half of the A/S (Ammonium/sulfate) ratios are larger than 3. Because there is few ammonium distributed in coarse particles, the value of ($NH_4^+ / SO_4^{2-} + NO_3^- + NO_2^- + Cl^-$) in fine particles is 0.022. This result hint that most of nitrite, nitrate and chloride were distributed in the coarse particles associate with metal ions or H^+, not ammonium. The value of ($NH_4^+ + Na^+ + K^+ + Mg^{2+} + Ca^{2+}$)/($SO_4^{2-} + NO_3^- + NO_2^- + Cl^-$) in coarse particle is 0.676, indicating that the cations measured in this study do not balance the anions in coarse particle. There are still some cations not detected existing in the coarse particles. The cations and anions should reach to balance state if sufficient

cations in coarse particle are taken into account. The ratio of sodium to chloride in coarse particle is 0.805, indicating that the sea-salt aerosols are the major contributor of coarse particles.

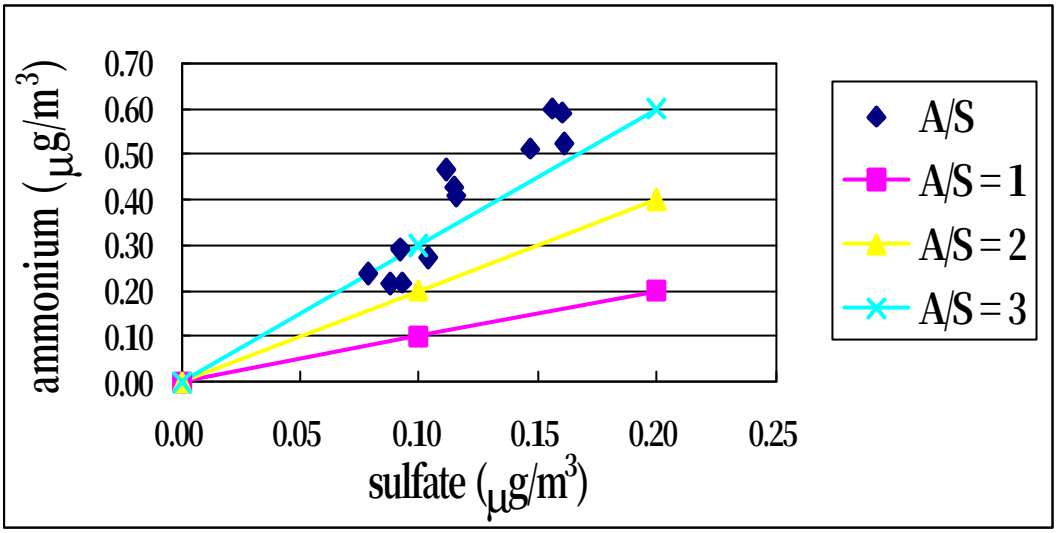

Figure 4.2-13. The distribution of ratios of ammonium to sulfate in the fine particles mode (21 data points) measured at CCROB sampling site. A/S : (ammonium concentration / sulfate concentration).

4.3 Comparison of the results between HKIT and CCROB

4.3.1 Comparison of gas concentrations

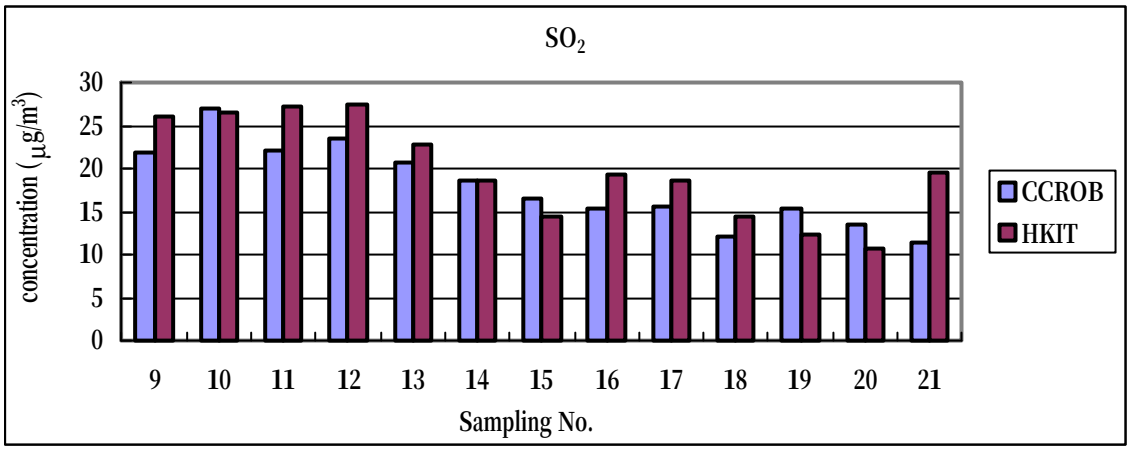

Figure 4.3-1. Comparison of the SO_2 concentrations measured at HKIT and CCROB across the whole sampling period.

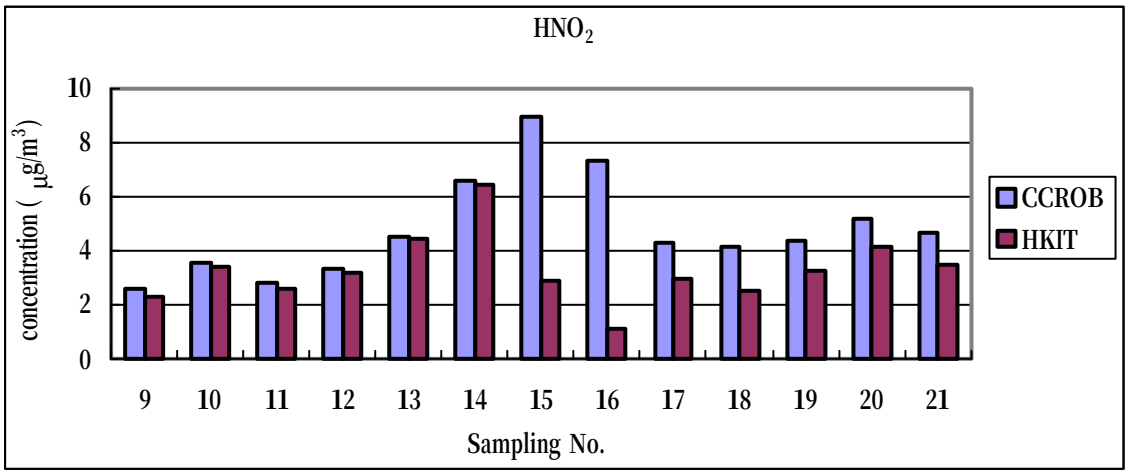

Figure 4.3-2. Comparison of the HNO_2 concentrations measured at HKIT and CCROB across the whole sampling period.

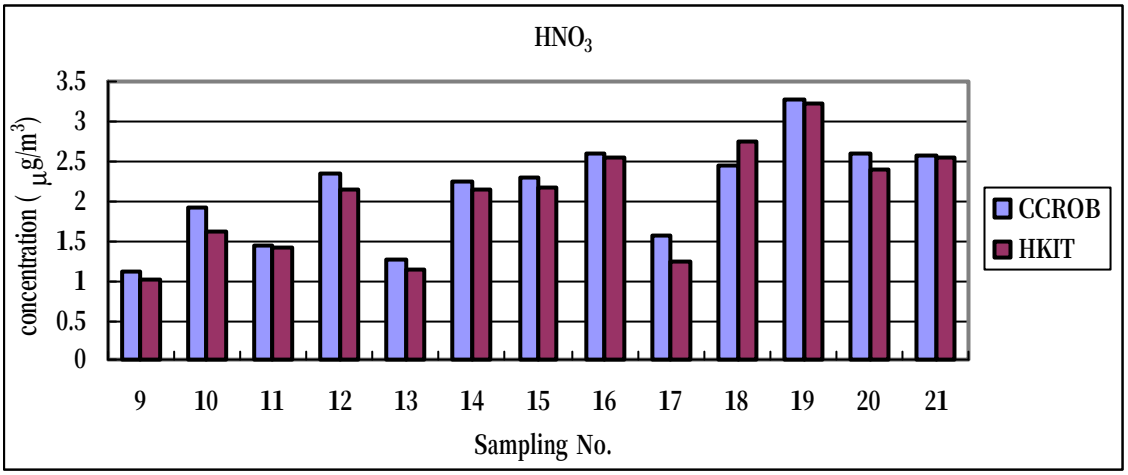

Figure 4.3-3. Comparison of the HNO_3 concentrations measured at HKIT and CCROB across the whole sampling period.

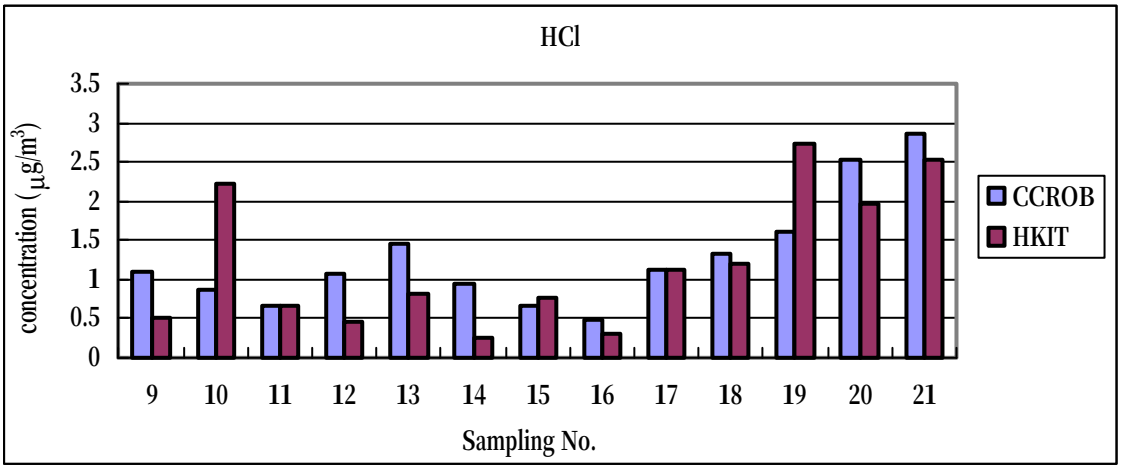

Figure 4.3-4. Comparison of the HCl concentrations measured at HKIT and CCROB across the whole sampling period.

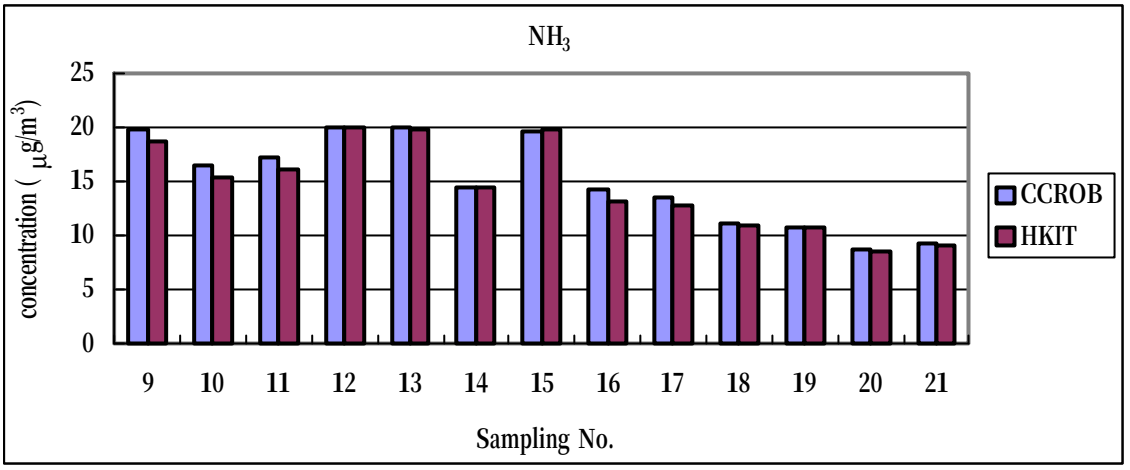

Figure 4.3-5. Comparison of the NH_3 concentrations measured at HKIT and CCROB across the whole sampling period.

The average concentrations of SO_2 in HKIT and CCROB were 19.80 and 17.94 μg/m^3, respectively. Average concentrations of HNO_2 in HKIT and CCROB were 3.30 and 4.80 μg/m^3, respectively. Average concentrations of HNO_3 in HKIT and CCROB were 2.03 and 2.14 μg/m^3, respectively. Average concentrations of NH_3 in HKIT and CCROB were 14.59 and 15.07 μg/m^3, respectively. Average concentrations of HCl in HKIT and CCROB were 1.19 and 1.29 μg/m^3, respectively. Only the SO_2 concentrations in HKIT were higher than in CCROB. All other gas concentrations measured in this study were higher in CCROB than in HKIT.

4.3.2 Comparison of the concentrations of particulate mass and inorganic components of fine and coarse particles at HKIT and CCROB.

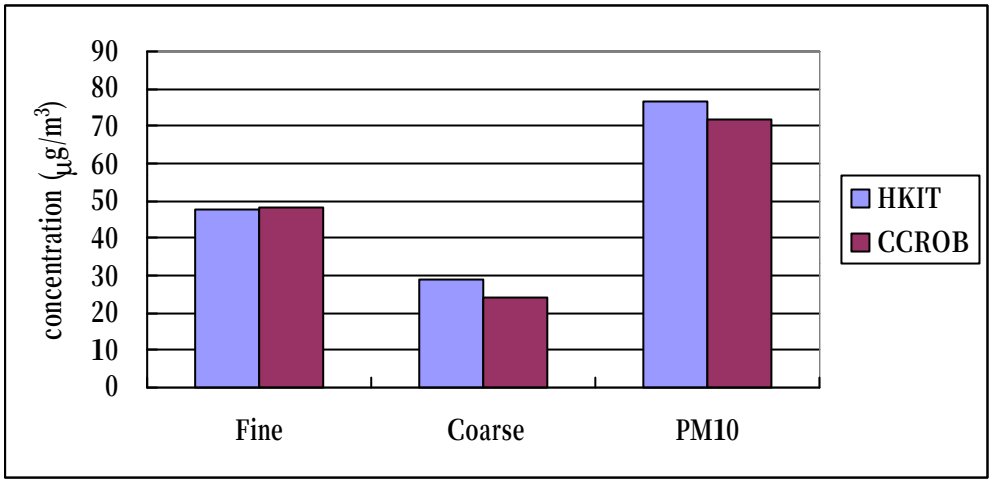

Figure 4.3-6 The comparison of average particulate mass concentration at HKIT and CCROB.

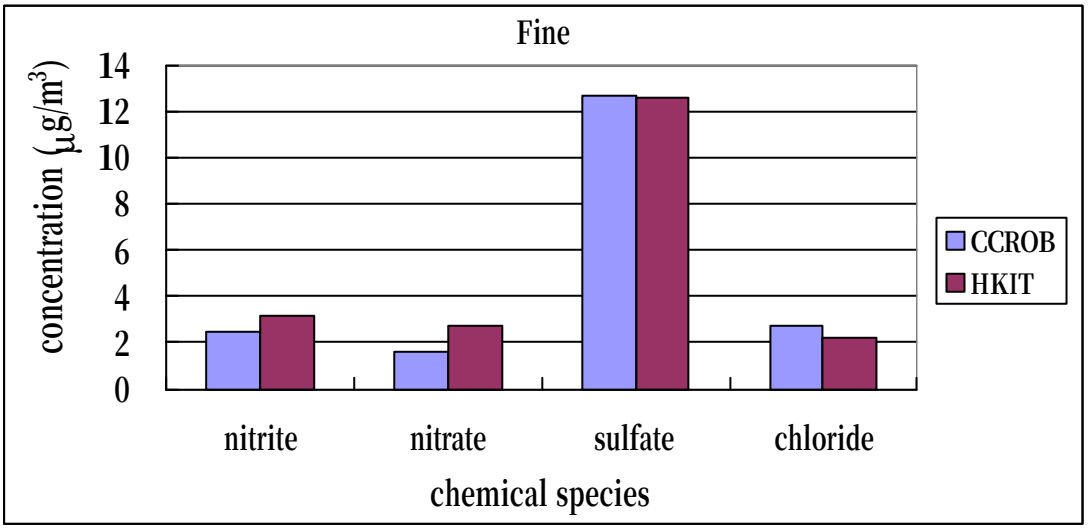

Figure 4.3-7 Comparison of the average anions concentrations at fine particles measured at CCROB and HKIT.

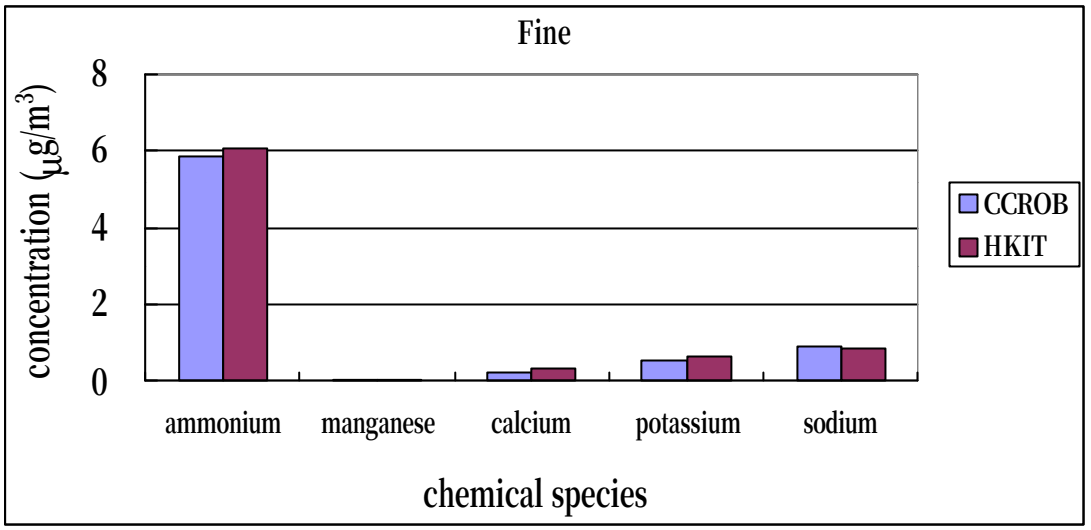

Figure 4.3-8. Comparison of the average cations concentrations at fine particles measured at CCROB and HKIT.

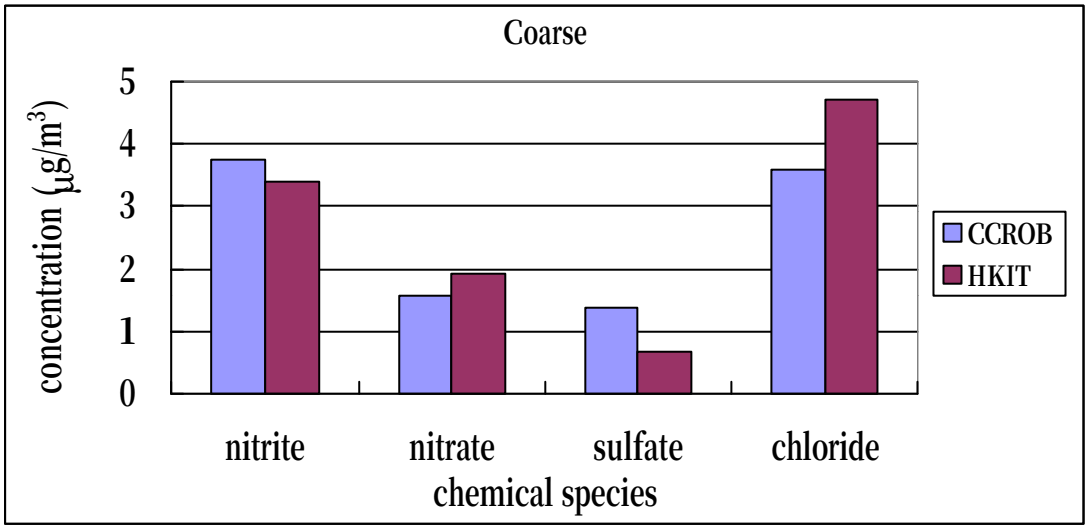

Figure 4.3-9. Comparison of the average anions concentrations measured in coarse particles at CCROB and HKIT.

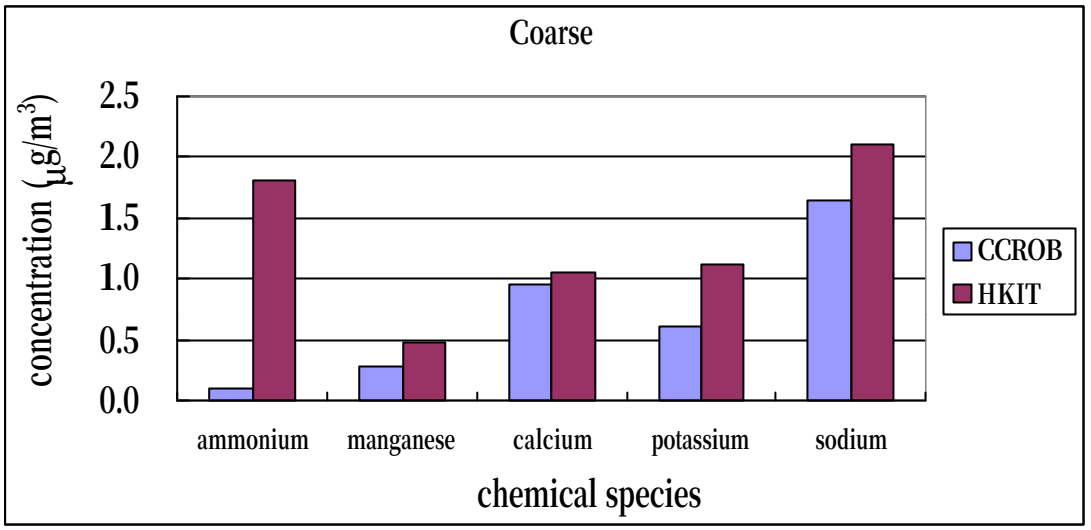

Figure 4.3-10. Comparison of the average cations concentrations measured in coarse particles at CCROB and HKIT.

The average concentrations of fine particles ($PM_{2.5}$) and PM_{10} measured at CCROB were higher than HKIT. The result of T-test showed no significant difference between the fine particles concentrations measured at CCROB and HKIT (two sided p-value < 0.05, T-test). Concentrations of coarse measured at HKIT were significantly higher than CCROB (one sided p-value < 0.05, T-test). The reason for the higher coarse particles concentrations at HKIT highway construction just right behind HKIT sampling site. The highway construction near HKIT sampling site proceeded continuously across the whole sampling period, which produced many naked grounds and suspended soil particles. A previous measurement near the construction sites showed that there were 50~70 % of the suspended particles near the construction ground were coarse (2.5-10μm) or larger (>10μm) particles (Zheng, 1992), this results indicated that construction activities were able to rise the coarse particles concentrations in the ambient air. In the fine particles, the concentrations of SO_4^{2}, Cl^-, Na^+ and Mg^{2+} at CCROB were higher than at HKIT. In the coarse particles, only the

concentrations of NO_2^- and SO_4^{2-} at CCROB were higher than that were at HKIT. The higher concentrations of calcium, manganese and potassium in HKIT (compared to CCROB) was caused by more soil particles existing in the ambient air at HKIT sampling site. Previous study indicated that the coarse particles produced from construction or natural soil resuspension were abundant of Si, Al, K, Ca, Mg and Fe (Chow, 1995).

To sum up, the construction activities were the HKIT sampling site raised the coarse particles concentrations, and led to the increase of the metal elements concentrations which existed in the coarse particle mode.

Table 4.3-1 Comparison of the ratios of inorganic components concentrations in fine particle mode to that in coarse particle mode measured at HKIT and CCROB sampling site.

	NO_2^-	NO_3^-	SO_4^{2-}	Cl^-	NH_4^+	Mg^{2+}	Ca^{2+}	K^+	Na^+
HKIT									
F (mg/m^3)	3.18	2.72	12.58	2.22	5.99	0.02	0.35	0.66	0.81
C (mg/m^3)	3.78	2.27	0.61	4.86	1.76	0.58	1.05	1.34	2.33
F/C	0.84	1.20	20.71	0.46	3.41	0.04	0.33	0.49	0.35
CCROB									
F (mg/m^3)	3.69	2.84	11.18	2.12	5.83	0.03	0.24	0.54	0.89
C (mg/m^3)	3.74	1.57	1.38	3.94	0.10	0.28	0.95	0.61	2.08
F/C	0.99	1.81	8.12	0.54	59.79	0.11	0.25	0.89	0.43

※ F : The average concentration of an inorganic component in fine particle mode.

※ C : The average concentration of an inorganic component in coarse particle mode.

※ F/C : The ratio of average inorganic component concentrations in fine particle mode to that in coarse particle mode.

※ Each value listed in this table was the average value of 21 data points.

Table 4.3-1 showed the comparison of ratios of inorganic components concentrations in fine particle mode to coarse particle mode for two different sampling sites in this study. The F/C values of sulfate, ammonium, magnesium, and potassium showed great variations. The F/C values for SO_4^{2-}, NH_4^+ and Mg^{2+} were varied between 8.12-20.71, 3.41-59.79 and 0.04-0.11, respectively.

4.3.3 Comparison of the chemical compositions of $PM_{2.5}$, $PM_{2.5-10}$ and PM_{10} at HKIT and CCROB.

Table 4.3-2 Comparison of chemical compositions of fine particles, coarse particles and PM_{10} at HKIT and CCROB. (%)

Chemical Species	NO_2^-	NO_3^-	SO_4^{2-}	Cl^-	NH_4^+	Mg^{2+}	Ca^{2+}	K^+	Na^+	other
Fine particles ($PM_{2.5}$)										
HKIT	6	6	22	3	11	0	1	1	1	49
CCROB	4	3	18	3	14	0	0	1	2	53
Coarse particles ($PM_{2.5-10}$)										
HKIT	10	6	2	15	5	1	3	3	6	49
CCROB	14	5	8	23	2	1	9	2	11	10
PM_{10}										
HKIT	6	6	22	3	11	1	2	3	1	34
CCROB	4	3	18	3	14	0	2	2	4	43

Table 4.3-2 displayed the comparison of chemical compositions measured at HKIT and CCROB sampling sites. For $PM_{2.5}$, the fractions of nitrite, nitrate and sulfate at HKIT were higher than CCROB, but the fractions of ammonium and sodium at HKIT were lower than CCROB. For $PM_{2.5-10}$, the fractions of nitrate, ammonium and potassium at HKIT were higher than CCROB, but the fractions of nitrite, sulfate, chloride, calcium and sodium at HKIT were lower than CCROB. For PM_{10}, the fractions of nitrite, nitrate, sulfate and potassium at HKIT were higher than CCROB, but the fractions of ammonium and sodium at HKIT were lower than CCROB.

4.4 Meteorological factors

The concentration, composition, and particle size of suspended particulate matter at a given site are determined by such factors as meteorological properties of the atmosphere, topographical influences, emission sources, and by particle parameters such as density, shape, and hygropicity (Loliadima *et al.*, 1998). The liquid water content of ammonium nitrate, ammonium sulfate, sodium chloride, and other soluble species increases with relative humidity. The suspended particles contain these soluble components will be increased the diameter with the relative humidity (Tang *et al.*, 1993). Four meteorological factors are also measured and concerned in this study. Wind direction, wind speed (m/s), relative humidity (%), temperature (℃) were monitored routinely by a meteorological measurements system located in the roof of a building which has eight stories, just in the same building with HKIT site. The data measured at HKIT site were used to associated with the meteorological data monitored by meteorological measurements system.

4.4.1 Correlation to wind speed, relative humidity, temperature

Table 4.4-1 to 4.4-3 displayed the correlation between the concentrations of chemical species and meteorological factors. Table 4.4-1 showed that the concentrations of gas species SO_2, NH_3 and HNO_3 have high relationship with the temperature. Table 4.4-2 showed the correlation between inorganic components in fine particles and meteorological factors, the results displayed that most inorganic chemical species concentrations showed no significant correlation to meteorological factors, except nitrate and sulfate. The nitrate concentrations were moderately related to temperature (R-square = 0.570), and the sulfate concentrations were also moderately related to the relative humidity (R-square = 0.543). Table 4.4-3 showed the correlation between inorganic components in coarse particles and meteorological factors. Results showed that the sodium concentrations had a quite high correlation to temperature (R-square = 0.690), and the chloride concentrations were moderately related to the relative humidity (R-square = 0.527). Figure 4.4-1 displayed the clear data of the relationships between the chemical species concentrations and meteorological factors with highly r-square values. Concentrations of gas species SO_2, HNO_3, NH_3 and particulate species Na were positive related to temperature. However, the concentrations of NO_3^- were negative related to temperature. SO_4^{2-} and Cl^- concentrations were positive related to the relative humidity.

Table 4.4-1. Correlation matrix of gas species concentrations to the meteorological factors across the whole sampling period (n = 21).

Gas	HNO_2	HNO_3	SO_2	NH_3	HCl
Wind speed (m/s)	0.0721	0.2534	0.1757	0.2998	0.1649
Temperature (°C)	0.1031	0.5949	0.6776	0.6678	0.2849
R.H. (%)	0.0617	0.2481	0.2528	0.3752	0.1326

Table 4.4-2. Correlation matrix of particulate species concentrations in fine particle mode to the meteorological factors across the whole sampling period (n = 21).

Fine	NO_2^-	NO_3^-	SO_4^{2-}	Cl^-	NH_4^+	Mg^{2+}	Ca^{2+}	K^+	Na^+
Wind speed	0.0049	0.1058	0.0084	0.0002	0.0167	0.0463	0.2352	0.0015	0.0014
Temperature	0.0051	0.5696	0.1629	0.0034	0.1691	0.0008	0.0800	0.0782	0.0782
R.H.	0.0035	0.2836	0.5435	0.0681	0.4945	0.0278	0.0145	0.1370	0.1541

Table 4.4-3. Correlation matrix of particulate species concentrations in coarse particle mode to the meteorological factors across the whole sampling period (n = 21).

Coarse	NO_2^-	NO_3^-	SO_4^{2-}	Cl^-	NH_4^+	Mg^{2+}	Ca^{2+}	K^+	Na^+
Wind speed	0.0016	0.1316	0.0975	0.1782	0.0012	0.1838	0.0041	0.1782	0.3034
Temperature	0.2728	0.2413	0.0041	0.4288	0.0644	0.1028	0.0838	0.0930	0.6900
R.H.	0.0558	0.0258	0.0758	0.5268	0.0506	0.0461	0.1215	0.0221	0.5162

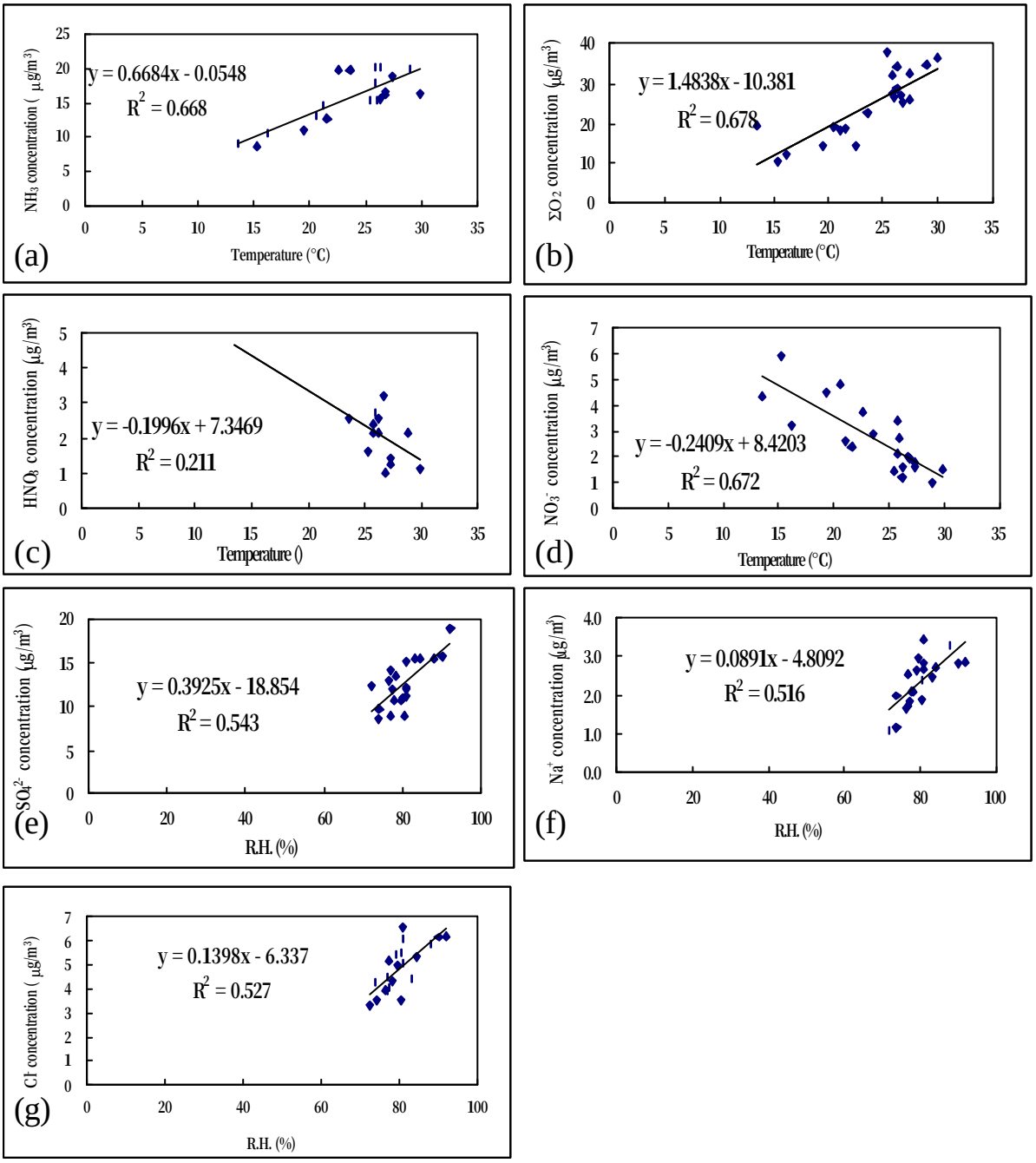

Figure 4.4-1. The correlation between (a) NH_3 Conc . and Temp. (b) SO_2 Conc. and Temp. (c) HNO_3 Conc. and Temp. (d) NO_3^- Conc. and Temp. (e) SO_4^{2-} Conc. and R.H. (f) Na^+ Conc. and R.H. (g) Cl^- Conc. and R.H.

4.4.2 Wind direction effect

Wind directions affect the transport line of air pollutants. The dominant wind directions in Sha-Lu area were southern-west in summer, and northern-east in winter. Figure 4.4-2 to 4.4-4 shows the average concentrations of air pollutants (gaseous pollutants and particulate pollutants) from each wind direction. These data provided a information of the input directions of each air pollutant. Although Taichung thermal power station, the biggest thermal power station in the southern-east Asia, located in the west side of the sampling region, results showed that SO_2 gas came from S, SSW and SW mainly, instead of west. This phenomena suggested that Taichung thermal power station was not the largest SO_2 contributor to the sampling region. The factories surrounded in the directions of southern-west and south should be the major SO_2 contributor of Sha-Lu area. Similar to SO_2, the average concentrations of HNO_2, HNO_3, sulfate, nitrite and nitrate do not appear high values from the direction which thermal power plants located. Because of the lack for hourly data (only 24hr sampling was carried out in this study) of pollutant concentrations, errors may occured when only the prevail wind direction was considered. Results showed in Figures 4.4-2 to 4.4-4 provide a approximate information of the wind direction effect.

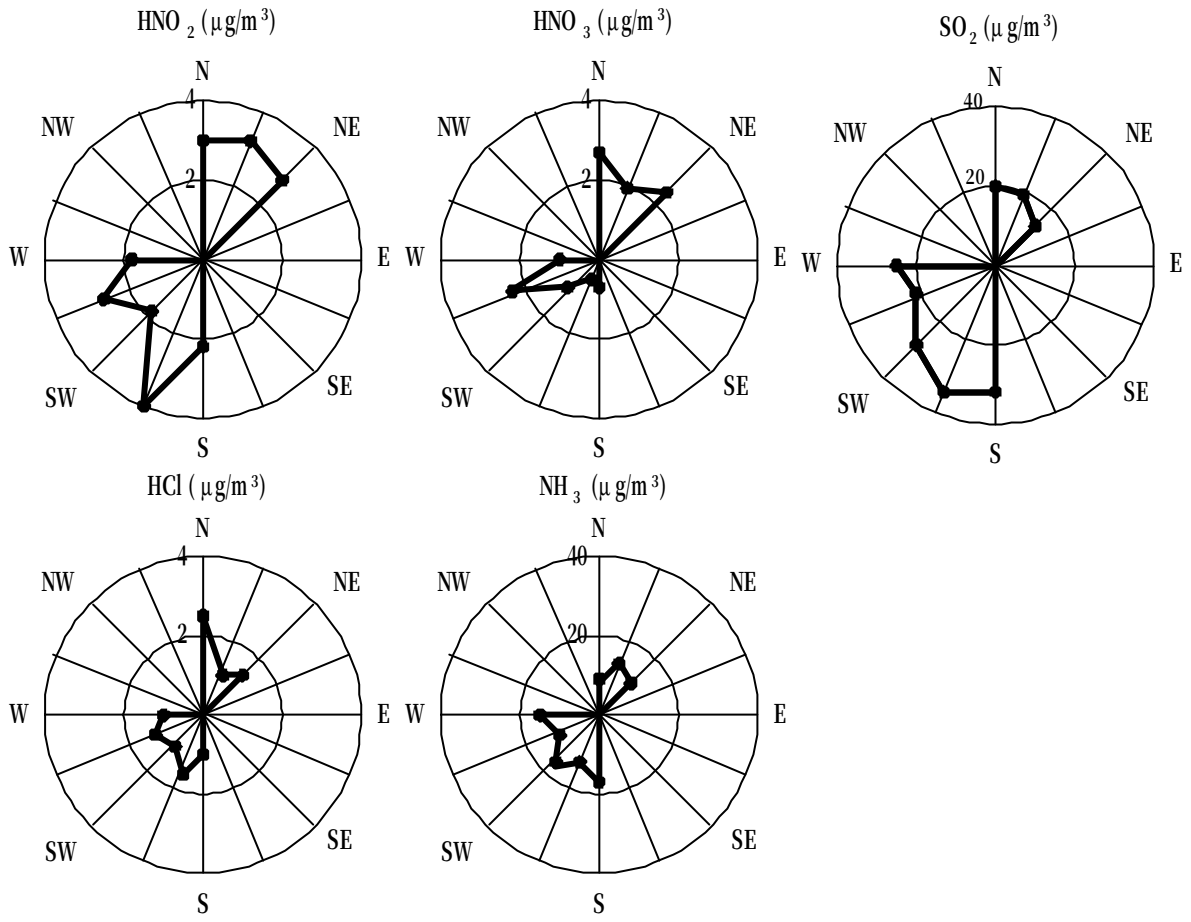

Figure 4.4-2. Average concentrations of air pollutants from each direction.

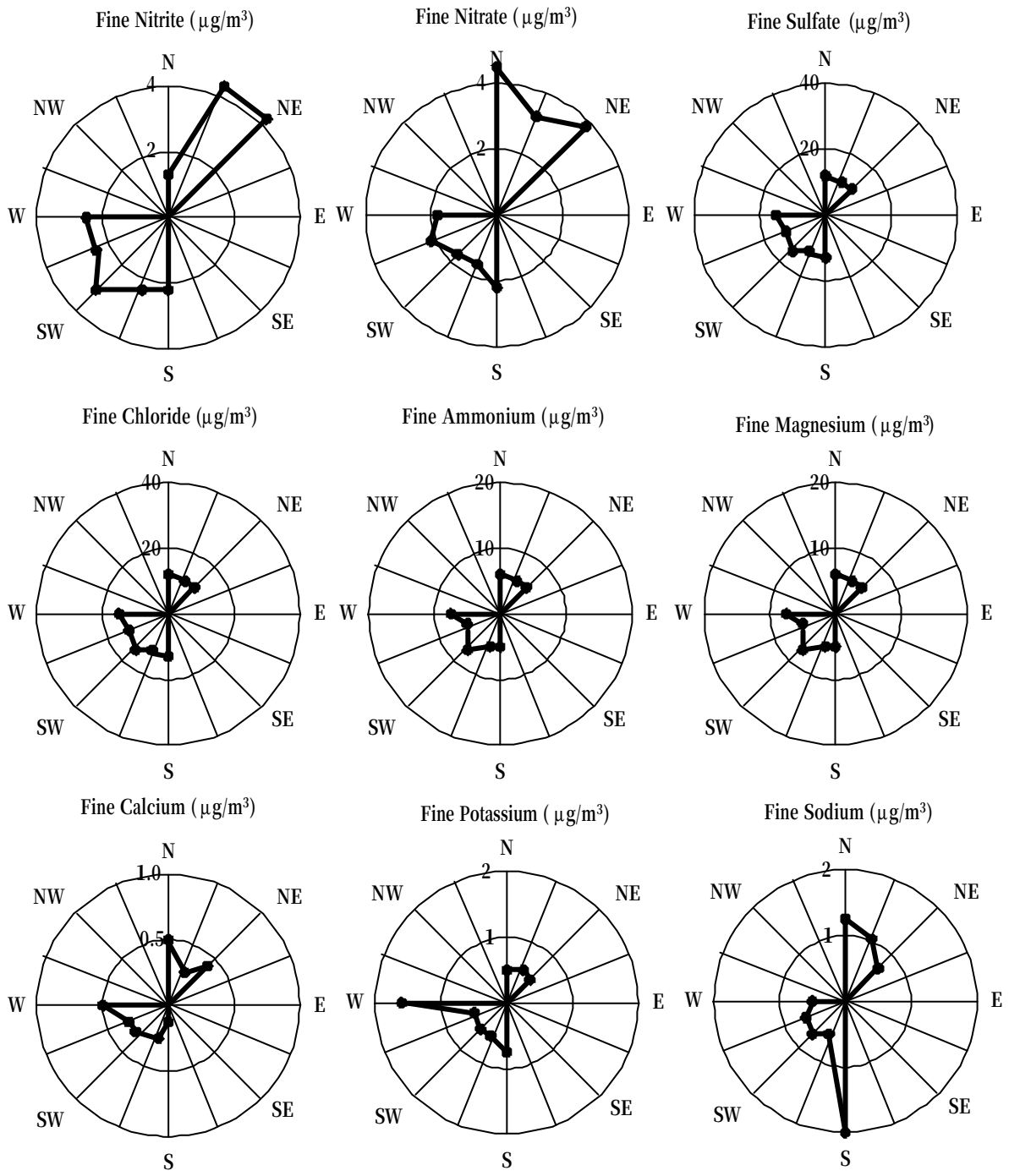

Figure 4.4-2. Average concentrations of air pollutants from each direction.

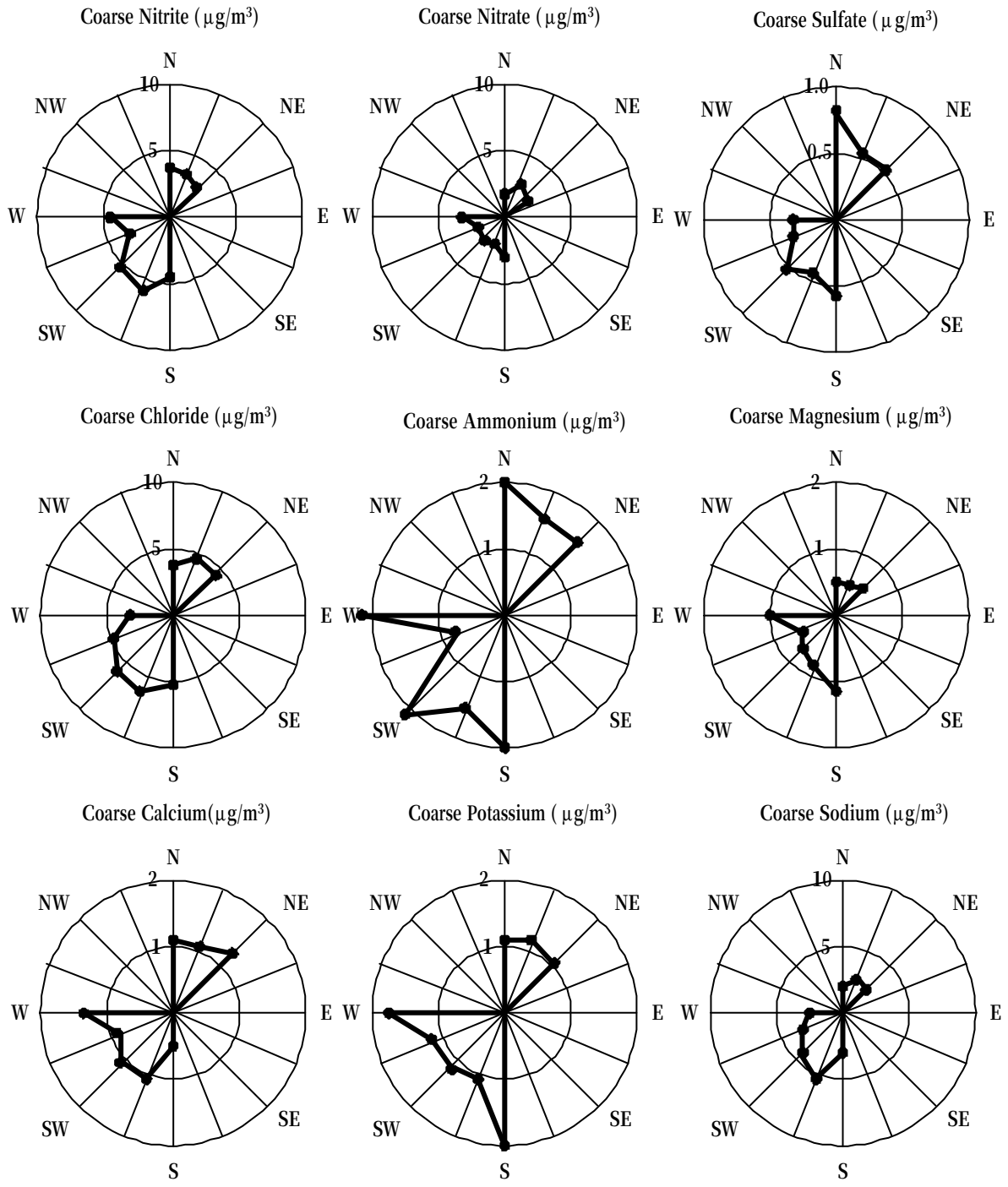

Figure 4.4-2. Average concentrations of air pollutants from each direction.

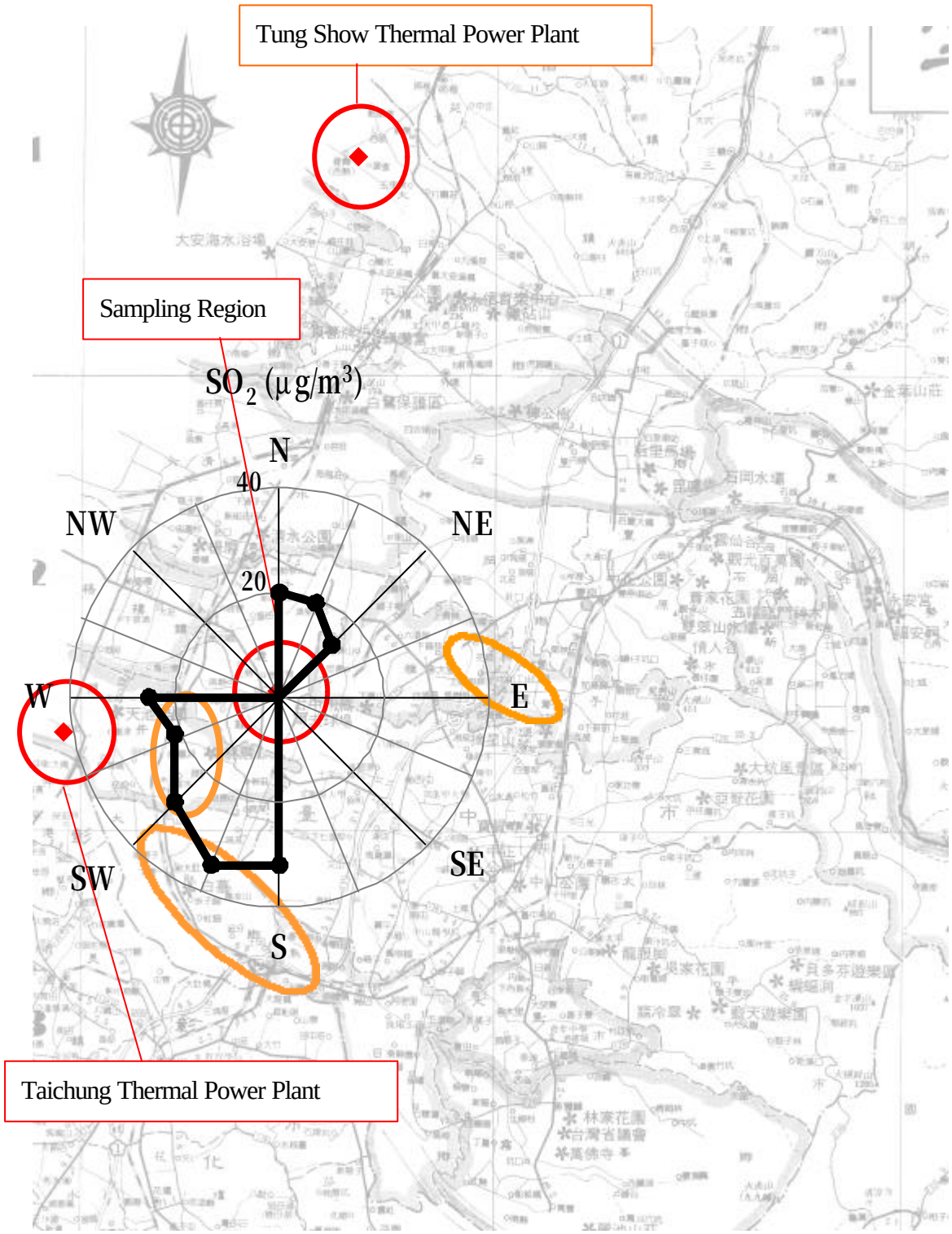

Figure 4.4-3. The average input concentration of SO_2 from each direction on the map. Circles spread near the sampling regions point out the locations and scope of industrial areas.

4.5 Comparison with other studies

Table 4.5-1 Comparison of the concentrations of fine and coarse particles with other studies (unit : μg/m^3).

Sampling condition			Fine particle	Coarse particle
Author	Year	Site		
Thurston	1985	Watertown (Boston)	17.4	8.6
Okamoto *et al.*	1986	Kashima (Japan)	17.7	17.5
Chow *et al.*	1994	Long Beach (California)	48.6	22.5
Gras *et al.*	1991	Footscray (Melbourne)	16.7	----
Yang	1998	CME* (Taichung)	67.15	36.24
Yang	1998	HKIT (Sha-Lu)	25.65	21.61
This study	1999	HKIT (Sha-Lu)	43.84	27.66
This study	1999	CCROB (Sha-Lu)	48.14	23.77

*** : CME : Chung-Ming Elementary school, located beside a crossroad of Taichung City.**

Table 4.5-2 Comparison of the chemical spices concentrations of fine particles with other studies (unit : μg/m^3).

Sampling condition			SO_4^{2}	NO_3^{-}	NH_4^{+}	SO_2	HNO_2	HNO_3	NH_3
Author	Year	Site							
Tanner *et al.*	1982	Brookhaven	8.54	1.74	2.27	21.12	---	3.40	6.61
Lee *et al.*	1993	Chicago	5.55	4.21	2.74	21.2	0.99	0.81	1.63
Chan *et al.*	1993	Taipei	7.38	2.14	2.48	17.53	4.42	0.77	4.66
Chow *et al.*	1994	Long Beach	2.2	21.4	---	---	---	---	---
Matsumoto *et al.*	1998	Nara	4.27	2.09	1.70	4.32	1.46	1.61	2.43
Chung *et al.*	1998	England	4.23	4.74	2.15	---	---	---	---
Yang	1998	CME (Taichung)	11.2	7.36	---	---	---	---	---
This study	1999	HKIT (Sha-Lu)	12.58	2.72	5.99	24.69	2.81	1.63	15.75
This study	1999	CCROB (Sha-Lu)	11.18	1.84	8.75	19.35	3.72	2.05	14.62

Table 4.5-1 showed comparisons of particulate mass and chemical species concentrations with other studies. Generally speaking, the fine and coarse particles concentrations measured at Sha-Lu and Taichung City were higher than other city. For fine particles concentrations, Table 4.5-1 displayed that fine particles concentrations measured in Sha-Lu were 67.15 in 1998 and 43.84 $\mu g/m^3$ in 1999. It was notable that the average fine particle concentration measured at HKIT sampling site in 1999 was obviously higher than it was in 1998, but still lower than the value measure at CME sampling site (urban sampling site, located beside a crossroad in Taichung City). And for average coarse particle concentration, the value measured at HKIT sampling site in 1999 was higher than it was in 1998. The major fine particles emission sources near the HKIT sampling site were motor vehicles. A parking space (max capacity: 125 cars) was set up near the HKIT sampling site during the sampling period, this could be the main factor that caused the great increment of fine particles concentrations in 1999. The average coarse particle concentration measured at HKIT sampling site in 1999 was also higher than it was in 1998. The suggested reason for the higher average coarse particle concentration in 1999 was construction activities executing after the HKIT sampling site.

Table 4.5-2 showed the comparison of gaseous and fine-particulate chemical species concentration with other studies. For particulate chemical species, the sulfate and ammonium concentration were apparently higher than other study. The high ammonium concentration in fine particle mode should be caused by the high NH_3 concentration in the ambient air of Sha-Lu. For gaseous species, the $NH_{3(g)}$ concentration measured in this study was greatly higher than other studies. NH_3 gas often produced by agricultural activities or industrial sources. There were some farmlands and a duck farm near Hung-Kuang Institute of

Technology, but agriculture were not the major human activities in this area. To identify the emission source of NH_3, more data of measurements and investigation of the nearby areas are needed.

Although the sampling area was not an urban area, the average sulfate concentration in fine particle mode was obviously higher than the other urban cities such as Chicago, Long Beach and Taipei. The concentrations of gas species such as SO_2, HNO_2, HNO_3 and NH_3 also were not lower than other urban cities. These meant that the fine particles in the ambient air of Sha-Lu were seriously polluted by the nearby urban and industrial areas. The long-range transport property of fine particles made it easier that the fine particles brought the pollutants produced in urban and industrial area to the rural area. Table 4.5-2 displayed that the sulfate in fine particle mode measured in CME (urban site) have a high concentration of 11.2 $\mu g/m^3$, meant that the fine particles were serious polluted in Tauchung City before them were transported to other places.

5.Conclusions and suggestions

5.1 Conclusions

The concentrations of gaseous species, particulate mass of fine and coarse particles, and inorganic cmponents of fine and coarse particles were measured at two different sites (HKIT and CCROB) in Sha-Lu from June 1999 to January 2000. Annular denuder system (ADS) was used to measure gaseous species, and the Universal sampler was used to measure particulate species. This study provide the data of average gaseous and particulate species concentrations in different seasons, comparison of the results measured at HKIT and CCROB, and the effect of meteorological factor (wind direction, wind speed, temperature and relative humidity). The experiments were hence made the following conclusions.

1. At HKIT site, the concentrations of fine particles after school opening were higher than before school opening (one sided p-value < 0.05, T-test). However, the concentrations of coarse particles showed no significant difference before and after school opening (two sided p-value < 0.05, T-test). Increasing traffic and human activities after school opening caused the increment of fine particle. Although the average concentration of fine particles measured at CCROB sampling site (48.14 $\mu g/m^3$) was slightly higher than that measured at HKIT sampling site (47.80 $\mu g/m^3$) after school opening, the result of T-test showed that there was no significant difference between the fine particles concentrations measured at CCROB and HKIT (two sided p-value < 0.05, T-test). The concentrations of coarse particles measured at HKIT sampling were significant higher than that measured at

CCROB (one sided p-value < 0.05, T-test). The freeway construction behind the HKIT sampling site caused the higher average coarse particle concentration at HKIT sampling site.

2. For the data of gas concentrations, the data of gaseous pollutants measured at HKIT site showed that SO_2 and NH_3 average concentrations were higher in summer and lower in winter. The concentration of NH_3 varied with the agricultural activities period. HNO_2 and HNO_3 average concentrations were both higher in winter and lower in summer. In the comparison of average concentrations of gaseous pollutant before and after school opening, SO_2 and NH_3 average concentrations before school opening were higher than after school opening. However, HNO_2, HNO_3 and HCl concentrations increased after school opening. When compared with the results measured at CCROB, average concentrations of all gaseous pollutants considered in this study (HNO_2, HNO_3, SO_2, NH_3 and HCl) at HKIT were higher than those measured at CCROB sampling sites.
3. The inorganic soluble components such as sulfate, nitrite, nitrate, chloride, ammonium, sodium, potassium, manganese and calcium occupied large fractions (34% at HKIT sampling site, and 53% at CCROB sampling site) of PM_{10} mass concentration. Sulfate and ammonium were mainly distributed in fine particles (32% ~ 50% of fine particles mass). Chloride, sodium, potassium, manganese and calcium were mainly distributed in coarse particles (totally 44~ 72% of coarse particles mass). Nitrite and nitrate were distributed evenly in fine and coarse particles. The unknown composition accounted for 27% ~ 49 % in fine particles, and 8% ~39% in coarse particles. The unknown composition possibly includes EC (elemental carbon), OC (organic carbon), carbonate and water contents.

4. The sulfate fraction in fine particles at HKIT (22 %) was higher than CCROB (18 %), but the ammonium fraction of fine particle mass in HKIT (11 %) was lower than CCROB (14 %). Chloride, sodium and nitrite fractions of coarse particle mass in CCROB were higher than HKIT.
5. Ammonium concentrations were highly positive related to sulfate concentrations (R-square = 0.845) in fine particles. The ratio of ammonium to sulfate was 2.54 in fine particle, and the value of $(NH_4^+) / (SO_4^{2-} + NO_3^- + NO_2^- + Cl^-)$ in fine particles was 1.109, suggested that the major configuration of ammonium sulfate in fine particles was $(NH_4)_2SO_4$, the surplus ammonium would associate with nitrite, nitrate and chloride. In coarse particles, there were few ammonium and sulfate existed. For this reason, most inorganic salts existed in coarse particles were nitrite, nitrate and chloride.
6. The value of $(NH_4^+ + Na^+ + K^+ + Mg^{2+} + Ca^{2+})/(SO_4^{2-} + NO_3^- + NO_2^- + Cl^-)$ in fine particles was 1.089, which is very close to 1.000, means that the cations and anions almost reached to balance, the major anions and cations should be detected by this study in fine particles. However, the value of $(NH_4^+ + Na^+ + K^+ + Mg^{2+} + Ca^{2+})/(SO_4^{2-} + NO_3^- + NO_2^- + Cl^-)$ in coarse particles was 0.550, indicated that the concentrations of cations in coarse particles were not sufficient to equilibrate with anions. The reasonable explanation was that there were some cations which were undetected in this study may exist in the coarse particles, such as Al, Fe, Mn and Si.
7. Na^+ and Cl^- were distributed mainly (about 65% of Cl and Na were distributed in fine particle mode) in coarse particles. The ratio of sodium to chloride was 0.732, and the concentrations of sodium and chloride were positive related with R-square = 0.796. This indicated that the sea-salt aerosols occupy a quite fraction of coarse particles.

8. For the relationship between chemical species concentrations and meteorological factors, the concentrations of HNO_3, SO_2, NH_3 and Na^+ were moderately positive related to temperature (R-square = 0.668, 0.668, 0.668 and 0.690, respectively). NO_3^- concentration was moderately negative related to temperature (R-square = 0.672). SO_4^{2-} and Cl^- concentrations were moderately positive related to relative humidity (R-square = 0.543 and 0.527, respectively).
9. The wind directions determined the input directions of air pollutants to the sampling region. Results showed that SO_2 came from SW, SSW and S mainly. Although Taichung thermal power plant was located in the west side of the sampling region, the average SO_2 concentration were not related proportionally along this direction. Therefore, the thermal power plant was not the largest SO_2 emission source of Sha-Lu area. However, the highest SO_2 concentrations occurred in the direction of SSW. Many factories located in the directions of S, SSW and SW, these factories were the possible major source of SO_2 emission.
10. Although Sha-Lu was not an urban area, the gas and particulate chemical species concentration in fine particle mode measured at Sha-Lu were not lower than other big cities such as Chicago, Long Beach and Taipei. The fine particles which were produced in urban and industrial area were easily transported by wind from emission sources to the rural area, and brought some pollutants which were formed in urban and industrial areas to the rural area.

5.2 Suggestion

1. To get more details of the aerodynamic diameter distributions of air pollutants, the more effective instrument with more cut size, such as MOUDI, is recommended in the future works.
2. SEM is an useful method to understand the surface characters and appearance of suspended particle samples. The data measured from SEM can be used to identify the emission source type of suspended particles.
3. By 24hr sampling, the daily divergence of air pollutants concentrations are ignored, and errors may occur in determination of the input directions of air pollutants. To improve this, automatic sampling instruments which can execute sampling in a short time interval (for example, collect a sample once a hour) are needed. With more detailed data, the daily divergence and input direction of air pollutants concentrations could be correctly identify.
4. Receptor model is an useful method qualify and quantify the emission sources of air pollutants. For the usage of receptor model, accurate measurement of air pollutants, exact investigation of the possible emission sources near the sampling area, and understanding of the index pollutants of each type of emission source are necessary. In order to introduce receptor model method in this study, more detailed measurement and investigation of the emission sources in the ambient area must be carried out in the future.
5. For the air pollution of SO_2, this study indicated that industrial factories contribute more SO_2 than thermal power plant to the sampling area. Many factories spread in Lung-Jin and Da-Du used coal-fired or diesel boilers, were major reasons for contributing high SO_2 concentrations. To decrease SO_2 emission, low sulfur-containing fuel is needed to implement for industries.

6. Reference

Alan W., G., Douglas A., L., and William G. C. (1995) "PM_{10} source apportionment study in Bulhead City, Arizona." Air & Waste Manage. Assoc. 45 : 75-82

Ahmed Y. A., Khalil E. M., Saeed A. A., Asma M. A. and Mahdia I. A. (1995) "Estimation of inorganic particulate matter in atmospheres of villages in Bahrain, by dry fall." Atmos. Environ. 29 : 1519-1529.

Alfred W. and Hansson H. C. (1995) "Formation of ammonium chloride particles from hydrogen chloride and ammonia in the atmosphere." J. Aerosol Sci. 26 : 463-464.

Andersen H.V. and Hovmand M.F. (1994) "Measurements of ammonia and ammonium by denuder and filter pack." Atmos. Environ. 28 : 3495-3512

Asif S. A., Pandis S. N. (1999) "Prediction of multicomponent inorganic atmospheric aerosol behavior.", Atmos. Environ. 33 745-757

Asif S. A., Spyros N. P. (2000) "The effect of metastable equilibrium states on the partitioning of nitrate between the gas and aerosol phases." Atmos. Environ. 34 : 157-168.

B.D. Tripathi, S.S.Chaturavedi and R.D.Tripathi (1996) "Seasonal variation in ambient air concentration of nitrate and sulfate aerosols in a tropical city, Varanasi." Atmos. Environ. 30: 2773-2778

Burkhardt J., Sutton M. A., Milford C., Storeton-west R. L. and Fowler D. (1998) "Ammonia concentrations at a site in southern Scotland from 2 year of contibuous measurements." Atmos. Environ. 32 : 325-331

Chan C. C. and Fu L. F (1993) " The spatial distrubution of acid aerosols around a petrochemical complex areas before comstruction." International Conference on Aerosol Science and Technology, 291-303.

Chan Y. C., Simpson R. W., Mctainsh G. H., Vowles P. D., Cohen D. D., Bailey

G.M. (1999) “Source apportionment of $PM_{2.}5$ and PM_{10} Brisbane (Australia) by receptor modeling”. Atmos. Environ. 33 : 3251-3268.

Charles F. C., Ian J. F. (1999) ”Gas-to-particle conversion in the atmosphere: I. Evidence from empirical atmospheric aerosols.” Atmos. Environ. 33 : 475-487.

Chen K. S., Lin G. F. (1999) “The characteristics and sources of PM2.5 in the ambient air in Kau-Shung.” The International Conference on Aerosol Science and Technology. 76-84

Cheng W. L., Yan Y. L., Lai M. S.(1999) “A study of the characteristics and source analysis of suspended particles in central Taiwan.” 16th Air Pollution Control Technology Conference : 599-604.

Chow J. C., Watson, J. G., Fujita E. M., Lu Z. and Lawson D. R. (1994) “Temporal and spatial variations of PM2.5 and PM10 aerosol in the Southern California Air quality study.” Atmos. Environ. 28 : 2061-2080.

Chow J. C. (1995) “Measurement methods to determine compliance with ambient air quality standards for suspended particles.” Air & Waste Manage. Assoc. 45 : 320-382.

Chul H. S., Gregory R. C., “The aging process of naturally emitted aerosol (sea-salt and mineral aerosol) during long range transport”, Atmos. Environ. 33, 2203-2218.

Fang G. C., Chang C. N., Wu Y. S., Fu P. P., Chang K.F., Yang D.G. (1999) “The characteristic study of TSP, $PM_{2.5\sim10}$ and $PM_{2.5}$ in the rural site of central Taiwan” The Science of the Total Environment 232, 177-184.

Funasaka K., Miyazaki T., Kawaraya T., Tsuruho K., Mizuno T. (1998) ”Characteristics of particulates and gaseous pollutants in a highway tunnel.” Environmental Pollution, 102, 171-176

Gau M. C. and Long S. C. (1999) “A study of PM10 in temples.” The International Conference on Aerosol Science and Technology. 67-75.

Gras J. L., Gillett T. W., Bentley S. T., Ayers G. P. and Firsotne T. (1991) CSIRO-EPA Melbourne Aerosols Study, final report CSIRO, Australia.

Gülsoy G., Tayanç M., Ertürk F. (1999) "Chemival analysis of the major ions in the precipitation of İstanbul, Turkey." Environmental Pollution 1.5 : 273-280.

Harrison R. M., Shi J. P., Jones M. R. (1999) "Continuous measurements of aerosol physical properties in the urban atmosphere", Atmos. Environ. 33 : 1037-1047.

Hayami H. and Gregory R. C., (1998) "Factors influencing the seasonal variation in particulate nitrate at Cheju Island, South Korea. " Atmos. Environ. 32 : 1427-1434.

Hoek G., Mennen M. G., Allen G. A., Hofschreuder P. and Meulen T. V. D. (1996) "Concentration of acidic air pollutants in the Netherlands." Atmos. Environ. 30 : 3141-3150.

Janssen L. H. J. M., Buringh E., Meulen A. V. D., Hout K. D. V. D. (1999) "A method to estimate the distribution of various fractions of OM10 in ambient air in the Netherlands." Atmos. Environ. 33 : 3325-3334.

Kaneyasu N. and Ohta S. and Murao N. (1995) "Seasonal variation in the chemical composition of atmospheric aerosols and gaseous species in Sapporo, Japan." Atmos. Environ. 29 :1559-1568.

Katsanos N. A., De Santis F., Cordoba A., Roubani-Kalantzopoulou, Pasella D. (1999) "Corrosive effects from the deposition of gaseous pollutants on surfaces of cultural and artistic value inside museums." Journal of Hazardous Materials A64 : 21-36.

Koliadima A., Athanasopoulou A. and Karaiskakis G. (1998) "Particulate matter in air of the cities of Athens and Patras (Greece) : Particle-size distribution and elemental concentrations." Aerosol Science and Technology 28 : 292-300.

Lara S. H., Glen R. C., Jec G., Michael A. and Ilhan O. (1998) "Physical and chemical characterization of atmospheric ultrafine particles in the Los Angles

area.” Environ. Sci. & Tech. 32 : 1153-1161.

Lee H. S., Wadden R. A. and Scheff P. A. (1993) “Measurement and evaluation of acid air pollutants in Chicago using an annular denuder system.” Atmos. Environ. 27A : 543-553.

Lee H. S., Wadden R. A. and Scheff P. A. (1996) “Measurement and evaluation of acid air pollutants in Chicago using an annular denuder system.” Atmos. Environ.1993, 27A, 543-553.

Lidia M., Stephen T., Dale G., Chris G., Esther R. (1999) ”A study of horizontal and vertical profile of submicrometer particles in relation to a busy road.” Atmos. Environ. 33 : 1261-1274.

Lu C. S., Bai H. L. and Lin Y. M. (1995) ”A Model for predicting performance of an annular denuder system.”, J. Aerosol Sci. 26 : 1117-1129.

Malderen V. H., Grieken R. V., Bufetov N. V., Koutzenogii K. P. (1996) “ Chemical characterization of individual aerosol particles in central Siberia.” Environ. Sci. Technol. 30 : 312-321.

Mats E.R., Gustafsson L., Franzén G. (2000) "Inland transport of marine aerosols in southern Sweden." Atmos. Environ. 34 : 313-325.

Matsumoto M., Okita T. (1998) “Long term measurements of atmoepheric gaseous and aerosol species using an annular denuder system in NARA, JAPAN.” Atmos. Environ. 32 : 1419-1425.

McMurry P. H. (2000) "A review atmospheric aerosol measurements." Atmos. Environ. 34 : 1959-1999.

Model 310 Universal Air Sampler™ Instruction Manual (USA™), MSP Corporation, 1313 Fifth Street, S. E. Suite 206 Minneapolis, MN, USA, 55414, 1996.

Okamoto S., Kobayashi K. and Yamada T. (1986) “Characterisation of aerosols in the Kashima area and a source apportionment study.” In Sydney clean air congress 1986, 253-262, 1986.

Perrino C., Concetta M., Sciano T., Allegrini I. (1999) ”Use of ion chromatography for monitoring atmospheric pollution in background networks.” Journal of Chromatography A, 846 : 269-275.

Robert W. C. (1977) “Effect of environmental Variable on collection of atmospheric sulfate.” Environ. Sci. & Tech. 11 : 873-878.

Ronald B. McCulloch, Stephen Few G., George C. Murray Jr. and Aneja V. P. (1998) "Analysis of ammonia, ammonium aerosols and acid gases in the atmosphere at a commercial hog farm in eastern North Carolina, USA." Environmental Pollution 102 : 263-268.

Rou C. S., Su H. I., Wen C.Y. (1999) “An application of digital image treatment for atmospheric visibility detection”, The International Conference on Aerosol Science and Technology. 63-66.

Schwartz J., Dockery D. W. and Neas L. M. (1996) “Is daily mortality associated specifically with fine particles?”, Air & Waste Manage Assoc. 46 : 927-939.

Schürch S., Geiser M., Lee M. M., Gehr P. (1999) “ Particles at the airway interfaces of the lung.” Colloids and Surfaces B : Biointerfaces 15 : 339-353.

Sickles J. E., Hodson L. L., Vorburger L. M. (1999) “Evaluation of the filter pack for long-duration sampling of ambient air.” Atmos. Environ. 33 : 2187-2202.

Spengler J. D., Keller G. D., Koutrakis P. and Raizenne M. (1990) "Acid air and health." Environ. Sci. & Tech. 24 : 946-956.

Stephen M. W., Walter J. and Joseph L. O. (1988) ”Measurement of aerosol size distributions for nitrate and major ionic species.” Atmos. Environ. 22 : 1649-1656.

Tanner R.L., Leaderer B. P., Spengler J. D. (1981) “Acidity of atmospheric aerosols.” Environ. Sci. & Tech. 15 : 1150-1153.

Tang I. N. and Munkelwitz H. R. (1993) “Composition and temperature dependence of deliquescence properties of hygroscopic aerosols.” Atmos.

Environ. 27 : 467-473.

Tindale N. W., Pease P.P. (1999) ”Aerosols over the Arabian Sea: Atmospheric transport pathways and concentrations of dust and sea salt.”, Atmos. Environ. 46 : 1577-1595.

Tsai Y. L. and Cheng M. T. (1997) “Relationship between visibility, meteorological factors and aerosol composition in the Taichung near-shore area.” International Conference on Aerosol Technology : 76-84.

Thurston G. D. and Spengler J. D. (1985) “A quantitative assessment of source contributions to inhalable matter pollution in metropolitan Boston.” Atmos. Environ. 19 : 9-25.

Tψseth K., Hanssen J. E., Semb A. (1999) "Temporal and spatial variations of airborne Mg, Cl, Na, Ca and K in rural area of Norway." The Science of the Total Environment 234 : 75-85.

Venkatram A., Fitz D., Bumiller K., Du S., Boeck M., Ganguly Chandragupta (1999) " Using a dispersion model to estimate emission rates of particulate matter form paved roads." Atmos. Environ. 33 : 1093-1102

Vignati E., Raes F. and Berkowicz R. (1998) “Internal and external mixing of aerosols in the H_2O-H_2SO_4 and soot system.” J. Aerosol Sci. 29 : S801-S802.

Wang C. S. and Hung S. Z.(1999) “Characteristics of ultra fine particles in urban atmosphere.” The International Conference on Aerosol Science and Technology. 59-62

Wyers G. P. (1997) "Micrometeorological measurement of the dry deposition flux of sulphate and nitrate aerosols to coniferous forest." Atmos. Environ. 31 : 333-343

Yang D. G. (1999) “The study of particulate mass chemical species in urban, suburban and rural areas during daytime and nighttime period in central Taiwan Taichung.” A Master Thesis of Institute of Environmental Science college, Tung-Hai University.

Yang T. Y. (1997) “A study of the characteristics of acidic aerosols at a monitoring station in Taipei.” A Master Thesis of Institute of Environmental Engineer College of Engineering, National Chiao Tung University.

Yuan C. S., Chang T. Z., Yuan Z., Yang H. Y., Lin V. Y., Li C. H., Li C. D. (1999) “The relationship between visibility of the atmosphere and characteristic of ational Conference on Aerosol Science and Technology. 67-75.

Zellweger C., Ammann M., Hofer P., Baltensperger U. (1999) “NO_y speciation with a combined wet effluent diffusion denuder-aerosol collector coupled to ion chromatography.” Atmos. Environ. 33 : 1131-1140.

Zhang D., Iwasaka Y. (1999) ”Nitrate and sulfate in individual Asian dust-storm particles in Beijing, China in spring of 1995 and 1996”, Atmos. Environ., 33 : 3213-3223

Zheng F. T. (1992) “The study of characteristics of suspended particles in Taipei.” Taipei City Environment Protection Bureau Project.

Zhuang H., Chak K. Chan, Fang M., Wexler A. S. (1999) “Formation of nitrate and non-sea-salt sulfate on coarse particles”, Atmos. Environ. 33 : 4223-4233